A PSEUDO INDIVIDUAL NEAR REAL-TIME MEASUREMENT FOR ASSESSING

AIR POLLUTION EXPOSURE IN SELECTED TEXAS CITIES

DISSERTATION

Presented to the Graduate Council of
Texas State University-San Marcos
in Partial Fulfillment
of the Requirements

for the Degree

Doctor of PHILOSOPHY

by

Tianfang Bernie Fang, B.A., M.S.

San Marcos, Texas
December 2012

A PSEUDO INDIVIDUAL NEAR REAL-TIME MEASUREMENT FOR ASSESSING

AIR POLLUTION EXPOSURE IN SELECTED TEXAS CITIES

Committee Members Approved:

_____
Yongmei Lu, Chair

_____
F. Benjamin Zhan

_____
Richard W. Dixon

_____
Mark A. Fonstad

_____
Ge Lin

Approved:

_____
J. Michael Willoughby
Dean of the Graduate College

FAIR USE AND AUTHOR'S PERMISSION STATEMENT

Fair Use

Duplication Permission

TABLE OF CONTENTS

LIST OF TABLES

LIST OF FIGURES

ABSTRACT

A PSEUDO INDIVIDUAL NEAR REAL-TIME MEASUREMENT FOR ASSESSING

AIR POLLUTION EXPOSURE IN SELECTED TEXAS CITIES

by

Tianfang Bernie Fang, B.A., M.S.

Texas State University-San Marcos

December 2012

SUPERVISING PROFESSOR: YONGMEI LU

Air pollution causes severe health effects and economic loss. Many major air-pollution-related studies focus on place-based measures and simulation. Typical place-based air pollution studies cannot portray individuals' air pollution exposure scenarios. In recent years, individual-based air pollution exposure measures have been developed rapidly.

Based on an extensive literature review of place-based geography and people-based geography, air pollution exposure assessment methods (including place-based and individual-based ones), and health effects of air pollution exposure, this dissertation research aims to investigate an innovative modeling approach for assessing individual

near real-time air pollution exposure. The first part of the model development is to design a series of near real-time space-time air pollution scenario cubes. Originating from time geography, space-time cubes provide an approach to integrate spatial and temporal air pollution information into a 3D space. The base of space-time cubes represents the variation of air pollution in a 2D geographical space while the height represents time. The second part of the model development is to geovisualize volunteers' individual real-time space-time trajectories using 3D space-time path maps. The last part of the model development is to integrate space-time cubes and space-time trajectories to develop the pseudo individual near real-time air pollution monitoring (PIRAM in short) models and the derivative models – the integrated pseudo individual near real-time air quality index (PIRAQI in short) models and the integrated pseudo individual near real-time air pollution dose simulation (PIRADS in short) models. Volunteers' individual diurnal ambient ozone (O_3) pollution exposures in Houston, Austin, and San Antonio are modeled in this dissertation research.

The contributions of this dissertation research are four-fold. First, it can help in understanding air pollution and individual exposure from a people-based geography perspective. Second, it enriches the individual-based air pollution exposure measure study by emphasizing individual travel behaviors in the individual air pollution exposure context. Third, its results can reveal the characteristics of the individual real-time air pollution exposure, which will contribute to local air pollution policy making. Fourth, the PIRAM platform only needs one handheld device terminal, such as a GPS smartphone, which ensure a good end user experience and potential commercial value.

CHAPTER I

INTRODUCTION

Background

Air pollution issues have emerged along with global industrialization since the early twentieth century. The Meuse Valley, Belgium fog disaster of 1930 (Nemery, Hoet and Nemmar 2001), the Donora, PA fluoride smog of 1948 (Helfand, Lazarus and Theerman 2001), the great London smog of 1952 (Bell, Davis and Fletcher 2004a), and the Bhopal, India gas tragedy of 1984 (Cullinan, Acquilla and Dhara 1996) manifest that high air pollution exposure can cause increases in not only the morbidity rate but also mortality rate. Furthermore, recent evidence reveals that the accumulation of low air pollution exposure can also produce severe health effects, such as death, disability, and illness (Somers and Cooper 2009, Sram et al. 2005). According to an environmental risk report of the World Health Organization (WHO), the annual air-pollution-caused-deaths worldwide in 2002 were about 2.36 million, which were well above the deaths caused by other environmental risk factors, such as water, sanitation, and hygiene in the same year (WHO 2007). Another WHO report shows that the worldwide disability-adjusted life years (DALYs) for air pollution in 2004 was about 64.14 million (WHO 2009). Air pollution, especially outdoor air pollution and tobacco smoke, is believed to cause more than 20% of lower respiratory infections, 66% of lung cancer, and 2% of

1

cardiopulmonary diseases (Cohen et al. 2004). Besides health effects, air pollution can cause huge economic loss. In 2002, the gross annual damages (GAD) of air pollution in the U.S. is estimated to be between \$71 billion and \$277 billion (Muller and Mendelsohn 2007).

Geographically, more than half of the counties in the U.S. are located in poor air quality areas (see Figure 1.1). The state of the air 2010 report by the American Lung Association (ALA) (2010) indicates that about 43% of the nation's total population is exposed to high particulate matter (PM) levels and 76% of the nation's total population is exposed to high ozone (O_3) levels during 2006-2008.
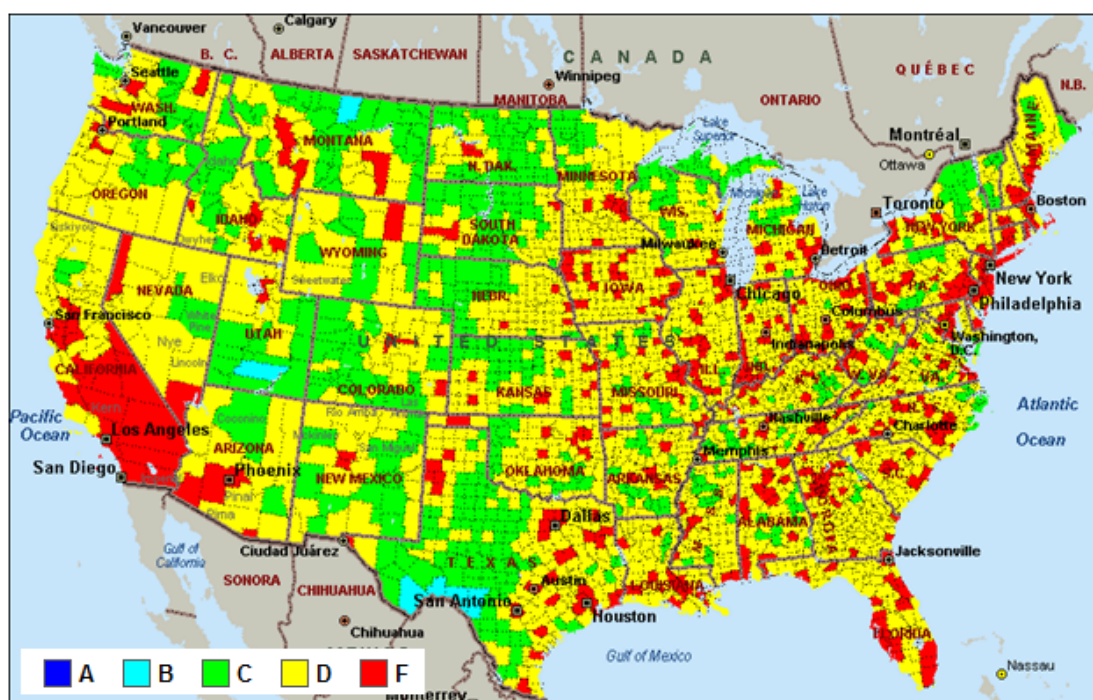
Figure 1.1. County Level Air Quality in the Lower Forty-Eight States of the U.S.

Source: CreativeMethods , 2010.

Note: Grade A means best air quality; Grade B means good air quality; grade C means moderate air quality; grade D means bad air quality; grade F means worst air quality.

Due to air pollution health effects and air pollution related economic loss, air pollution issues have received extensive research interests in recent decades. A number of air pollution exposure related studies emerged. Two major groups of such studies are air pollution exposure assessment studies and air pollution health effect studies – the former group investigates the exposure dose of air pollutant, and the latter group researches adverse health effects of air pollution exposure. This dissertation research focuses on air pollution exposure assessment.

For human air pollution exposure assessment, recent studies take advantage of atmospheric science, geographic science, computer science, and bioscience. In the early periods of research, major air pollution exposure assessment studies took static places as research objects. Proximity models and air dispersion models are typical examples. Based on the evidence that residential proximity to major roads may increase residents' respiratory morbidity, which includes diseases such as asthma and allergy, many proximity models simulate air pollution exposure conditions for those who live near air pollutant emission sources (Barzyk et al. 2009). Air dispersion models are based on air dispersion theories; they are widely used in regional air pollution assessment (e.g., county level). In 2000, the U.S. Environmental Protection Agency (EPA) proposed an air dispersion model named the American Meteorological Society/U.S. Environmental Protection Agency regulatory model (AERMOD). AERMOD has been accepted as a

standard model for steady state air pollution dispersion assessment in many countries (Rosenbaum et al. 2008). These air pollution exposure assessments are called place-based approaches. Place-based assessment methods usually have concise structures and take advantage of mathematical methods. These methods/models merit a predominant position in current air pollution assessment.

Nevertheless, place-based assessment methods cannot address individual air pollution exposure dose accurately. In order to solve this problem, individual-based air pollution exposure assessment studies have begun to emerge; these studies take individuals as research objects. Individual-based methods can portray air pollution exposure conditions at the individual level and are especially useful for individual air pollutant health effect evaluation. Along with the rapid developments of information technologies (e.g., location acquisition technology (Lu and Liu 2012) and mobile wireless communication technology) and biotechnology, direct individual-based air pollution measures (i.e., real-time individual air pollutant monitoring) and indirect individual-based air pollution measures (such as air pollutant biomarker methods) show their advantages for data acquisition and high data accuracy (Kwan 2009).

To date, along with the shift of academic focus from place-based to individual-based air pollution exposure measures, several prototypes and pilot studies of individual-based air pollution exposure measures have been conducted (AbuJayyab et al. 2006, AIR 2010, Chiang et al. 2008, Raftery 2009). Few of them investigate individual air pollution exposure context from a geographical space-time point of view. This dissertation research investigates individual space-time activities as well as air pollution exposure scenarios to portray individual near real-time air pollutant exposure, intake accumulation, and

potential adverse health risk. The results of this dissertation research shed light on people-based geography and air pollution exposure assessment studies.

Research Questions and Working Hypotheses

This dissertation research will develop a pseudo individual near real-time measurement for assessing air pollution (i.e., O_3) exposure in selected Texas cities (i.e., Houston, Austin, and San Antonio) and evaluate the effectiveness of it. This dissertation research addresses the following research questions:

Question 1: Does the pseudo individual near real-time air pollution monitoring model effectively assess individuals' personal exposure to air pollution?

Question 2: Is the pseudo individual near real-time air pollution monitoring model equally effective in different cities and regions?

To investigate the research questions, two corresponding working hypotheses will be tested:

Hypothesis 1: The pseudo individual near real-time air pollution monitoring model can accurately assess individuals' actual exposure to air pollution. The monitoring model is not a pure individual-based near real-time air pollution monitoring model because it has both an individual-based component and a place-based component. The monitoring model will integrate the near real-time space-time air pollution scenarios with the global positioning system (GPS) recorded individual travel trajectories to estimate individuals' personal exposure to O_3. The ground truth data for individual air pollution exposure corresponding to the selected space-time trajectories will be obtained by using portable air pollution monitor/sampler to evaluate the hypothesis.

Hypothesis 2: The pseudo individual near real-time air pollution monitoring model is equally effective in different cities and regions. Because the pseudo individual near real-time air pollution monitoring model is developed by integrating near real-time space-time air pollution scenario cubes and individual space-time trajectories, the model's accuracy is related to space-time air pollution scenario cubes. The accuracy and effectiveness of space-time air pollution scenario cubes across different cities and regions will directly impact the effectiveness of the proposed model.

Significance

In recent years, major air pollution studies have changed from episode forms to place-based time-series forms. Typical place-based time-series air pollution researches (such as hospital admission studies) may simplify research processes, but they cannot portray individuals' air pollution exposure scenarios (Brunekreef and Holgate 2002). Integrating individuals into a time-series air pollution research frame is the best solution for investigating individuals' air pollution exposure (Kwan 2009). For this purpose, individual-based air pollution exposure measures have developed rapidly in recent years.

Recent individual-based air pollution exposure assessment studies investigate individual real-time air pollution exposure, life course air pollution exposure, air pollutant biomarkers, and air pollutant inhalation dose. Few of them integrate individual spatiotemporal air pollution exposure context with individual space-time trajectory. Individual travel behaviors, especially travel patterns and daily activities, are significantly related to both air pollution exposure and pollutant intake. Fail to consider individual

travel behaviors can lead to errors in air pollution exposure assessment and adverse health effect analysis.

Instead of considering air pollution generation theories and air pollution dispersion theories, this dissertation research takes advantage of **time geography**, **geographic information science**, and **health geography**. Generally speaking, this dissertation research is a geography-oriented and individual-centered air pollution exposure study. Consequently, this dissertation research will have four contributions. First, it can help in understanding air pollution and individual exposure from a people-based geography perspective. Second, this dissertation research will enrich the individual-based air pollution exposure measure theory by emphasizing individual travel behaviors in the individual air pollution exposure context. Third, this dissertation research's results can reveal the characteristics of the individual real-time air pollution exposure, which will contribute to local air pollution policy making. Fourth, the pseudo individual real-time air pollution monitoring platform only needs one handheld device terminal (HHDT), such as a GPS smartphone, which ensure a good end user experience and the commercial value.

CHAPTER II

LITERATURE REVIEW

Geography: Place-Based or People-Based?

Human-Environment Identity of Geography

Contests of the identities of geography are never stopped (Turner 2002). Widely accepted dualism – spatial-chorological identity and human-environment identity – gives current geography research different emphases: 1) physical space and place versus 2) human-environmental interaction. Along with the flourishing and waning of environmental determinism, the emerging of Berkeley and Chicago schools, and the outbreak of the quantitative revolution in 1950s, human-environment identity of geography seems to be more and more valued in the last hundred years (Butzer 2002). Turner (2002) noted several highlights in recent human-environment geography development: the relationship between physical world and human beings is still the subject for human-environment geography; both empirical and quantitative approaches (such as GIS) are important human-environment research methods; a compromise between two views of research – agent-based and structure-based – is increasingly accepted; the boundaries between theoretical and applied human-environment geography research is vanishing, but new boundaries (such as descriptive and quantitative research

8

barrier) are being generated; human-environment studies are still highly influenced by spatial-chorological geography.

In Pattison's (1990) four traditions of geography, i.e., spatial tradition, regional tradition, human-environment tradition, and earth science tradition, he points out that human-environment tradition includes not only the impact of environment on human beings but also the impact of human beings on the environment. Based on Pattison and Turner's statements, it is clear that human-environment study needs to involve a people-place process interaction. Furthermore, common human-environment geography study topics, such as disease and the environment, environmental justice and risk, and political ecologies, without exception, refer to people-place interaction. Facing the problem of which one (i.e., environment or human beings) should be the research priority of geography discipline, two branches of geography study – place-based geography and people-based geography – arise in recent years.

Environmental dynamic processes are commonly represented following two frameworks – place-based representation and individual-based representation. Eulerian reference framework is place-based representation; an object's movement is observed through a fixed observation framework or reference system. Differently, individual-based representation shows individual object's motions in a dynamic reference framework – Lagrangian framework, in which the object being observed is followed by the observer (Doyle and Ensign 2009, Setton et al. 2011). When these two frameworks are applied to human-environment geography, two different groups of geography research methods exist – place-based geography and people-based (or individual-based) geography (Kwan 2009, Miller 2007). Place-based geography reflects human-environment interaction at

certain locations without considering human beings' activities thoroughly. By contrast, focusing on human beings' activities at a given time and place, people-based geography consider individual's daily activities and their interaction with environment in detail (Kwan 2009). People-based geography approaches connect human beings and environment through individual space-time investigation and are people-centered dynamic analyzing methods.

Place-Based Geography

When investigating human-environment activities, spatial-chorological approaches are commonly used. This preference leads the place-based research perspective to be dominated in human-environment geography study. Based on the straightforward mathematical representation of Eulerian reference framework, place-based geography is a natural choice for investigating simple objects or homogeneous objects (Benenson and Torrens 2004), such as urban land-use change. Within the place-based geography framework, all components – environmental objects and human beings – are related to geographic places. For example, a traditional place-based geography may use such a process to study human air pollution exposure: one or more hypothetical homogeneous region(s) (such as census block) are defined by place-based geographers; one observed value is used to represent the air pollution concentration for each region; people who live in one region are believed to have same air pollution exposure level (Matthews 2008).

However, disadvantages of place-based geography should not be ignored. The modifiable areal unit problem (MAUP) is a major additional challenge for place-based

geography. Due to MAUP, the observation outcomes for a specified study area may vary if different scales or zoning methods are applied (Haynes et al. 2007). Despite the development of new approaches to handle MAUP (such as scale-space clustering method (Mu and Wang 2008) and creating homogeneous zones approach (Riva et al. 2009)), MAUP cannot be eliminated because theoretically a region can always be subdivided into sub-regions. The second challenge is an ecological fallacy (NationalResearchCouncil 2002). Because human beings are not objects for place-based geography, researchers tend to use the average characteristic of a group to represent individual's characteristic, which is not true. For example, the neighborhood residential exposure or ambient outdoor air pollution exposure may not be the only exposure source for all individuals who live in a residential block.

People-Based Geography

Traditional place-based geography takes macrocosmic geographic entities, phenomena, processes, and spatial environments as objects; it is short of robust analytical approaches for investigating individual behaviors and activities in the human-environment interaction. Generally speaking, people-based geography is a microcosmic approach. Instead of focusing on place or environmental process itself, people-based geography places emphasis on individual behavior, aims at the subtle and complex relationship among human beings, physical places, and regional geographic environment, and investigates the human-society interaction and the human-environment interaction.

The development of people-based geography is closely related to modern technologies, which make significant impact on human being's perspective of the world.

Transportation development is the first influence factor. Along with the quick development of transportation technologies, the space-time distance seems to be shortened, which is called time-space convergence (Janelle 1969). For example, it takes Columbus more than two months to sail across the Atlantic Ocean in the fifteenth century; a transatlantic flight only costs several hours at present. People's increasing mobility and accessibility weaken constrains of traditional "places" and make place-based geography unsuitable for investigating the rapidly changing human-environment interaction. Information and communications technologies (ICTs) aid the evolution of people-based geography too (Kwan and Weber 2003). ICTs, especially the Internet, shorten the physical distance between individuals, simplify the human-environment interaction, and help to construct the "global village" (Massey 1997). For example, by the aid of virtual reality (VR) technology, people can easily experience a sky dive without leaving their physical locations. The neo-human-environment interaction raises a claim for people-based geography.

One outstanding advantage of people-based geography is that it can apply object-oriented representation to study environmental phenomena. Among the eight common environment phenomena, mobile individuals, sedentary individuals, regions of individuals, sedentary regions in mass, and mobile regions in mass are spatial objects; while masses of individuals, continuous solid mass, and continuous fluid mass are spatial fields (Bian 2007). Usually, people-based geography investigates mobile individuals (e.g., people in movement); place-based geography investigates continuous solid mass or continuous fluid mass (e.g., air pollution dispersion). Object-oriented representation gives people-based geography several merits. First, objects (i.e., individuals) in people-based

geography are independent. Because individuals are independent from any environmental processes, individual observer's travel behavior will not impact observation accuracy. So the outcomes of people-based geography studies have higher accuracy than those of place-based geography studies. Second, object-oriented representation increases people-based geography's universality. Based on speculative or abstract reasoning, the outcomes of people-based geography studies can be easily applied to related areas. For example, a people-to-store accessibility study may shed light on emergency evacuation routing selection, and vice versa. Last, object-oriented representation gives people-based geography a high flexibility. The human-environment interaction is very complex because both human and environmental phenomena are constantly changing. In a people-based representation, individual objects can be replaced without harming the integrity of the human-environment interaction. For example, a people-based air pollution exposure assessment model may investigate air pollution exposure conditions for different individuals. Given these merits, although place-based geography is still dominated currently, people-based geography is attracting more and more attention.

People-based geography involves many theories and questions, such as acquisition methods for people-based information, people-based space-time modeling, and social network modeling. Along the developments of information technology, time geography, which focuses on individual space-time moving behavior observation and analysis, becomes an important branch of people-based geography (Kwan 2002).

Time Geography

Time geography is not a new discipline. In late 1960s, Swedish geographer Torsten Hägerstrand brought up time geography to facilitate the human migration behavior study. The well-known paper "*What about People in Regional Science?* (Hägerstrand 1970)" was published in 1970 and believed to be an early classical time geography work. In his paper, Hägerstrand put forward several critical viewpoints. First, he indicated that individuals, instead of human groups, should be objects of the human moving pattern study. Second, he thought highly of time factors in interpreting human activities and used space-time path to analyze human spatial travel behaviors. Last, he applied three constraints to confine individual spatial patterns and recommended investigating the disaggregated moving behaviors (Hägerstrand 1970). Hägerstrand's space-time theory not only leads to the birth of time geography, but also introduces geography a humanistic thought (GranÖ 2008).

According to Hägerstrand, time geography study is full of constrains of space and time, i.e., individual moving behavior is always limited by a series of constrains. The first group of constrains is *authority constrains*, which are limits that do not allow the individual to enter forbidden territories. For example, travelers can drive their own cars, but they are not allowed to take the bus if they do not have tickets. *Capability constrains*, the second group of constrains, indicate that human physical nature affects individual's moving pattern. For example, people cannot fly without necessary equipment. *Coupling constrains* belong to the last group; they indicate all individuals need to be in the same place before they can have interaction. For example, students attend class in a fixed classroom (Weber and Kwan 2003).

Space-time path and space-time prism are core models of time geography. The space-time path model is a three dimensional model, which uses a two dimensional plane to record individual fixed locations and a perpendicular dimension to represent time. Space-time path is generated by connecting individual fixed activity locations. The slope of space-time path segment is related to average travel speed between locations; the steeper the slope is, the lower the travel speed will be; when the slope is 90 degrees, the individual stays (Miller 2007). So space-time path can visually show individual's moving patterns: fixed activity locations, length of stay in fixed locations, travel velocity, travel time, and travel distance. Space-time path can also portray the interaction between individuals. The interaction is expressed by the space-time path segment overlapping, which is limited by coupling constrains. For example, two individuals leave each home, meet in a café for an hour, and then go to work respectively (see Figure 2.1).

As an extension of space-time path, space-time prism concerns individual's spatial accessibility within a time range. Space-time prism investigates individual's travel possibility instead of fixed-location connection, which is an emphasis of space-time path. Consequently, outcomes of space-time prism are closer to reality than those of space-time path. The projections of fixed locations are called as anchors; the projection of a space-time prism is called as potential path area, which limits the movement range between two fixed locations (anchors) (see Figure 2.2).
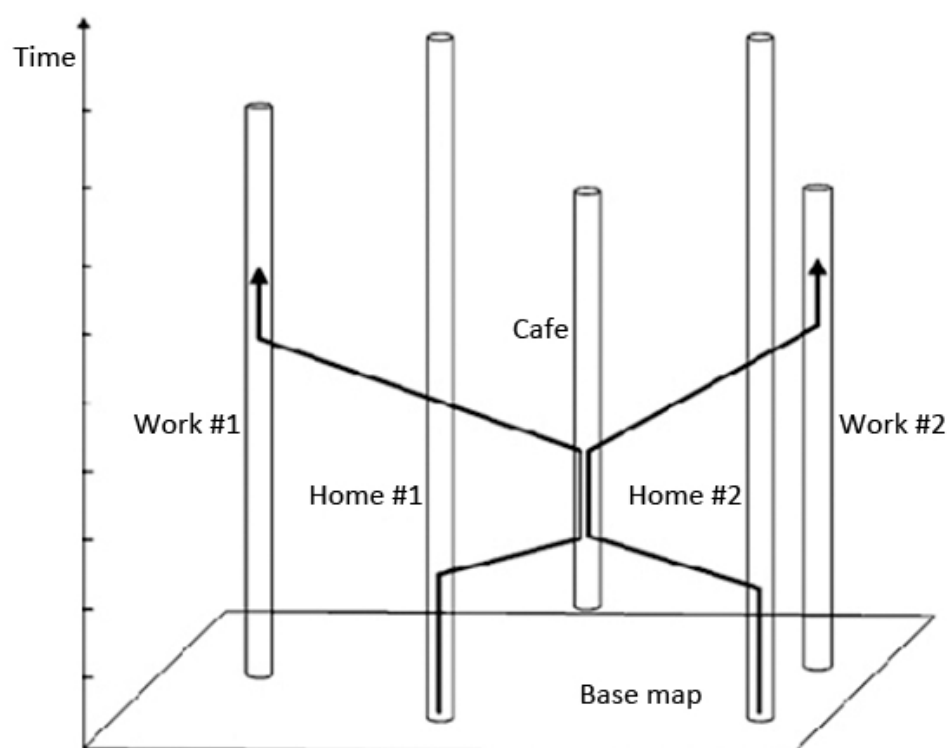
Figure 2.1. The Space-Time Path.

Note: Adapted from Miller 2007.
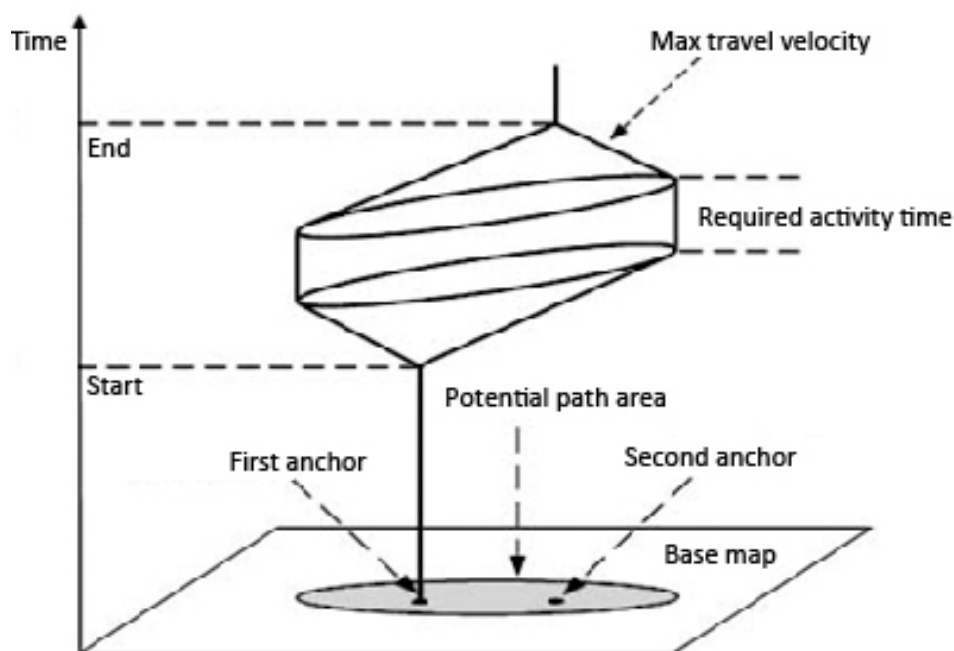
Figure 2.2. The Space-Time Prism.

Note: Adapted from Miller 2007.

Classical time geography suffers from three disadvantages. The first disadvantage is that classical time geography assumes that individual has a constant travel speed. The constant speed assumption can simplify the time geography theory, but it omits the reality of travel speed variations. The second disadvantage is that classical time geography applies descriptive method instead of analytical method to explain human moving patterns. The last disadvantage is that classical time geography concentrates on traditional physical interaction (e.g., face to face communication) and seldom considers virtual interaction (Miller 1991).

Time geographers take the lead in seeking solutions for these disadvantages in recent years. In 1996, Okabe and Kitamura applied a network transformation approach to

investigate the association between consumers and stores (Okabe and Kitamura 1996). In 1999, Miller used potential network area (PNA) to explain individual's travel coverage within a time range (Miller 1999). In 2001, Wu and Miller explored PNA's application in a dynamic transportation network (Wu and Miller 2001). In 2003, Kwan and Weber noted that recent developments in ICTs have significant influence on individual accessibility and must be taken into consideration (Kwan and Weber 2003). In the same year, Kwan et al. investigated established accessibility studies from three aspects – representation, methodology, and application (Kwan et al. 2003). In 2006, Yu extended the classical space-time path model by using both physical space-time path and virtual space-time path (Yu 2006). In 2009, Miller and Bridwell put forward a field-based theory to facilitate the analytical function for time geography (Miller and Bridwell 2009).

Air Pollution Exposure Assessment

Air Pollution

Air pollution generally refers to the contamination of the atmosphere that may lead to adverse health effects to human beings, animals, plants, and environments (EPA 2009a). Air pollution has complex components, which can be chemical gas, suspended liquid, or suspended solid. Generally speaking, emission source and generation mechanism are two major criteria for air pollution classification. According to the source of emission, air pollutants are divided as natural pollutants and man-made pollutants. Common natural air pollutants include sulfur dioxide (SO_2), nitrogen oxide (NO_x), O_3, PM, and volatile organic compounds (VOCs); they are mainly released from volcanic eruption, biological decay, ocean emission, and biological emission (ACE 2010).

Generally speaking, the proportion of natural air pollutants is higher than that of man-made air pollutants. Along with the rapid industrialization and urbanization worldwide (especially in developing countries such as China and India) in recent decades, man-made air pollutants become increasingly common and important. Most man-made air pollutants are released from stationary sources (such as power plants) and mobile sources (such as diesel engine automobiles) (EPA 2010c). According to the generation mechanism, air pollutants are divided as primary and secondary. Primary air pollutants are released directly through emission process. For example, SO_2 is a common air pollutant that is emitted from coal combustion. Secondary air pollutants are formed through primary air pollutant reaction. Ground-level O_3 is a typical secondary air pollutant that is formed by NO_x-catalyzed VOCs and carbon monoxide (CO) oxidation (Cape 2008).

Air pollution concentration is different for the indoor / outdoor environment. In smoker's homes, tobacco smoke is the primary source for indoor PM (Wallace 1996). In non-smoking homes, air pollutant types and air pollution concentrations may vary. To investigate indoor air pollution conditions, Wallace (2006) investigated suburban indoor-air-pollution-related activities such as gas stove cooking and candles burning through a thirty-seven months sample collection. Wallace found that 1) the complex gas stove cooking is the primary ultrafine particulate matter (UFP) emission source and gas powered dryer is the secondary source, and 2) the UFP concentration varies with environment, i.e., indoor level with emission source (i.e. gas cooking) greater than outdoor level greater than indoor level without emission source. Biomass fuels, such as wood, straw, charcoal, and animal dry dung are common rural household energy sources for some places, while coal and charcoal are main energy sources for urban residents in

developing counties. The total population who uses (e.g., cooks or heats) biomass fuels and coal is about 3 billion (Ezzati 2005), so the indoor air pollution from biomass fuel combustion has generated widespread concern in recent years. Gimbutaite and Venckus (2008) investigated indoor air pollutants for different kinds of wood structures. They found that firewood combusting generates most CO and sawdust firewood combusting generates most NO_x. Besides, Kang et al. (2009) reported the high in-tent total suspended particulate matter (TSP) level due to burning yak dung for the purpose of cooking and heating in the Tibetan Plateau. They also found high in-tent concentration of cadmium (Cd), arsenic (As) and lead (Pb), which are well known toxic elements.

Household products and materials are the main sources for indoor VOCs, which include "alkylbenzenes, alkanes, terpenes, aliphatic aldehydes, and some chlorinated aliphatic hydrocarbons" (Kostiainen 1995). Massolo et al. (2010) applied a three-year noncontiguous VOCs monitoring study for investigating indoor and outdoor winter air quality in La Plata, Argentine. They found that the VOCs concentration is relevant to both outdoor emission sources and human activities, e.g., indoor daily activities are the primary source for "*C9–C11 alkanes, toluene and xylenes*", vehicle emission for benzene, and industrial factories for "*hexane, heptane and benzene*".

Traffic emissions and industrial emissions are major sources for outdoor air pollution (Zou et al. 2009b). Topographic factors and meteorological changes, such as elevation, terrain, wind speed, wind direction, pressure, relative humidity, sunshine duration, cloud cover rate, and temperature, may affect the generation and concentration of these air pollutants (Arain et al. 2009, Li et al. 2010, Mikhailuta et al. 2009).

To regulate air pollution emission, numerous air pollutant emission standards and clean air acts have been developed worldwide since 1950s (Kramer, Cullen and Faustman 2006). The U.S. Clean Air Act is enacted in 1963; the current amendments are the Clean Air Act Amendments of 1990 (1990 CAAA), which designate 188 air pollutants (EPA 2008b). Based on 1990 CAAA, the EPA formulates the National Ambient Air Quality Standards (NAAQS) to guide air pollution hazards (EPA 2010b). NAAQS is finalized in 2010 and contains primary standards and secondary standards for six major air pollutions: CO, Pb, nitrogen dioxide (NO_2), particulate matter (PM_{10} – airborne particulate matter smaller than 10 micrometers, and $PM_{2.5}$ – airborne particulate matter smaller than 2.5 micrometers), O_3, and SO_2 (as reported in Table 1). Primary standards are applicable to guiding adverse health effects of human beings; secondary standards are applicable to non-health-effects issues.

Table 2.1. The U.S. National Ambient Air Quality Standards (NAAQS) by the EPA.

Pollutant	Primary standards		Secondary standards	
	Level	Averaging time	Level	Averaging time
CO	9 ppm (10 mg/m^3)	8-hour	None	
	35 ppm (40 mg/m^3)	1-hour		
Pb	0.15 μ g/m^3	Rolling 3-Month Average	Same as Primary	
	1.5 μ g/m^3	Quarterly Average	Same as Primary	
NO$_2$	53 ppb	Annual (Arithmetic Average)	Same as Primary	
	100 ppb	1-hour	None	
PM$_{10}$	150 μ g/m^3	24-hour	Same as Primary	
PM$_{2.5}$	15.0 μ g/m^3	Annual (Arithmetic Average)	Same as Primary	
	35 μ g/m^3	24-hour	Same as Primary	
O$_3$	0.075 ppm (2008 std)	8-hour	Same as Primary	
	0.08 ppm (1997 std)	8-hour	Same as Primary	
	0.12 ppm	1-hour	Same as Primary	
SO$_2$	0.03 ppm	Annual (Arithmetic Average)	0.5 ppm	3-hour
	0.14 ppm	24-hour		
	75 ppb	1-hour	None	

Source: EPA, 2010b.

Individual Air Pollution Exposure and Intake

Duan (1982) and Lioy (1990) introduced the model of human exposure to air

pollution that human exposure occurs when a person contacts with air contaminants in a

place and at a time. So personal exposure to air pollution is an accumulated process that is related to not only air pollutant concentrations but also the periods of exposure time (Lioy 1990):

$$E = \int_{t_1}^{t_2} C(t)dt$$ Equation 2.1.

where E is the personal exposure, $C(t)$ is the real-time pollutant concentration, and dt is the time span (t_1 to t_2) of exposure.

Air pollution exposure is related to a series of environment-human interaction processes, including human contacting with the air pollutants, air pollutants intake, and the accumulation of air pollutants over time (Monn 2001) (see Figure 2.3).

exposure (contact, in ambient media)
-integrated exposure:
integral (t=0..t$_a$) c$_i$ (t) dt [e.g. ppbhr]
-average exposure:
integr. exposure/time [e.g. ppb]

dose (in the body)
-intake:
integrated exposure x ventilation rate [e.g ng]
-average intake:
integrated uptake/time [e.g. ng day^{-1}]

or: direct dose measurement of a biomarker [ng, or ng ml^{-1} body fluid]
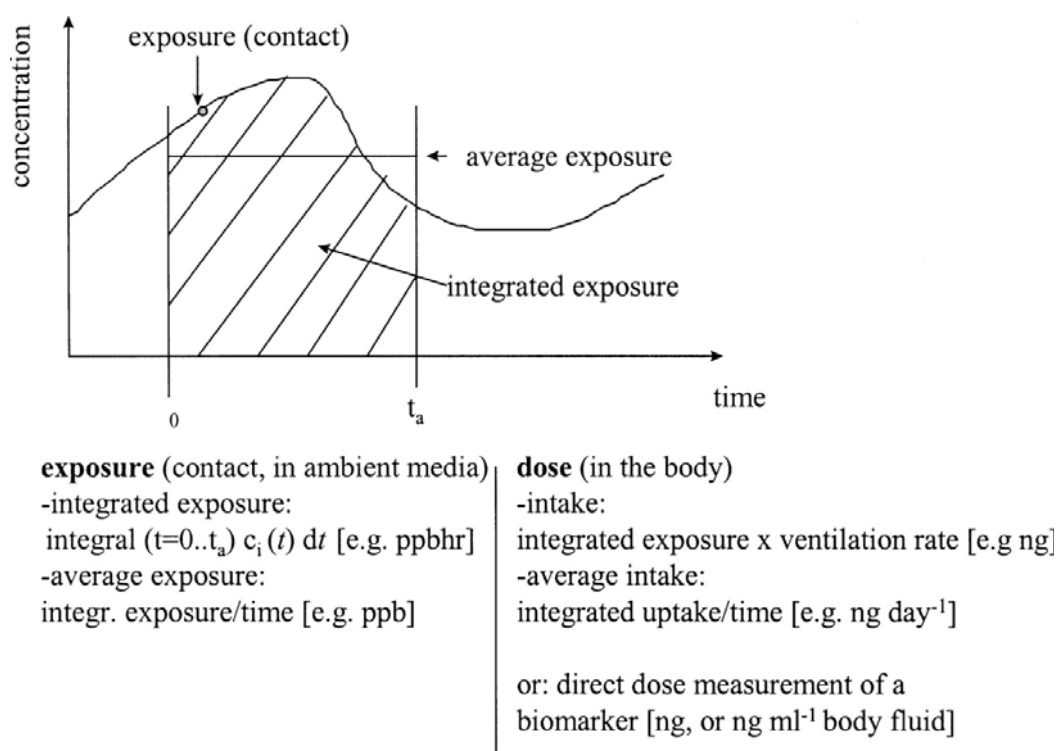
Figure 2.3. Air Pollution Exposure: Concentration and Exposure Duration.

Source: Monn, 2001.

Individual air pollution intake is related to a series of environment-human interaction processes, including human contacting with the air pollutants, intaking of the air pollutants, and the concentration of the air pollutants over time. Among different intaking ways of the air pollutants, inhalation is the major way for air pollutants to enter human body (Weisel 2002). Because of the influences of many human factors, e.g., respiratory frequency, air pollution intake can be different for individuals exposed to the same level of air pollution. Besides, health effects of air pollution are related to both air pollutant exposure and individual sensitivity toward air pollutants (Silverman and Ito 2010). Consequently, the individual is one key factor for air pollution exposure assessment in epidemiological studies.

$$I = \int_{t_1}^{t_2} C(t)Rdt$$ Equation 2.2.

where I is the individual air pollutant intake (inhalation dose), and R is the real-time inhalation rate (Lioy 1990).

Individual physical condition is a critical factor for deciding air pollutants intake. For example, children and adult can have different air pollution intake when the air pollution exposure level is same. Based on age, height, gender, and physical activities, it is possible to decide rough breathing capacity and average respiratory rate. In Holmes's (1994) report, several air intake groups were categorized. Based on Holmes's data, a simplified air intake categories are built (see Table 2.2).

Table 2.2. Individual Average Air Intake Volume per Minute.

Group	Staying/Sleeping/In car		Walking		Running/Cycling		Playing/Light physical labor	
	Speed	Air volume	Speed	Air volume	Speed	Air volume	Speed	Air volume
Children	< 1 or >24	5-10	1-5	12.5-17.5	5-24	30-35	< 2	15-20
Adult females	< 1 or >24	5-10	1-5	17.5-22.5	5-24	45-50	< 2	15-20
Adult males	< 1 or >24	7.5-12.5	1-7	25-35	7-24	55-60	< 2	20-30

Note: Unit: Speed (km/h), Air volume (liter). Adapted from Holmes 1994.

The Spatial Heterogeneity of Air Pollution and Exposure

The spatial heterogeneity of air pollution is a major issue for air pollution exposure study because different spatial locations may have different air pollution concentrations (Riva et al. 2009). This becomes a major challenge for place-based exposure measures. As a compromise, the conventional placed-based exposure studies commonly rely on air pollution monitoring site based spatial interpolation approaches and other regional spatial statistical modeling methods instead of precise and detailed local measure (Abrahamowicz et al. 2003) (see Figure 2.4).
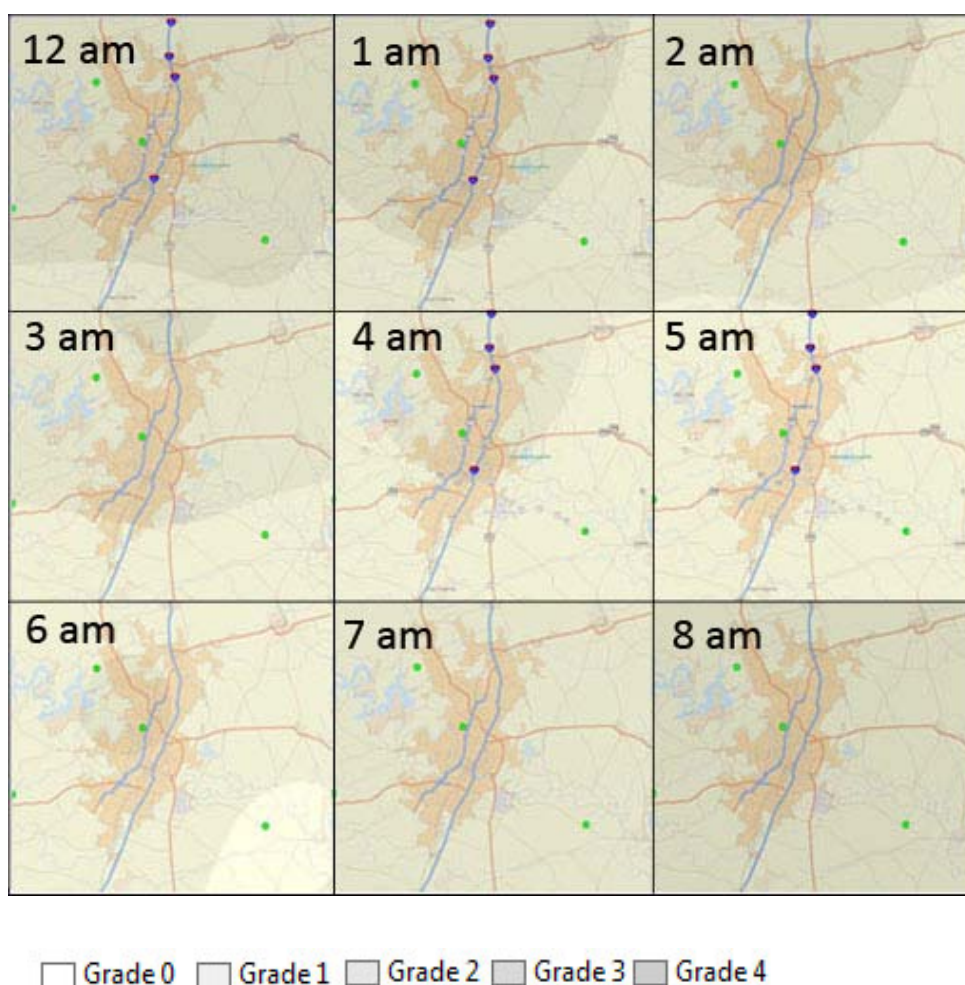
Figure 2.4. Hourly Average O₃ Concentrations in the Austin Area, Texas on August 1ˢᵗ, 2010.

Data source: TCEQ, 2010.

Note: The levels of concentration are: (Grade 0: 0-5ppb, Grade 1: 5-10ppb, Grade 2: 10-15 ppb, Grade 3: 15-20 ppb, and Grade 4: 20-25 ppb). Green points are the EPA air monitoring sites. The spatial interpolation method used is kriging (exponential model with five neighbors).

Air pollutants can have different originations and diffusion patterns; the spatial heterogeneity of air pollution is related to pollutant type (O'Neill et al. 2003). Recently, air pollutants were investigated separately in most studies. For example, Sahsuvaroglu and Jerrett (2007) used SO_2 to study local industrial pollution, NO_2 and CO to study traffic pollution, $PM_{2.5}$ to study long-distance transportation and power station generated secondary sulfates, and O_3 to study the secondary photochemical pollution mixture.

Among the major air pollutants, PM and its spatial heterogeneity were examined frequently. Recent studies found that fine particulate matter distribution is not as homogeneous as former studies indicated (Kim et al. 2005); sedimentation and coagulation activities made PM to distribute heterogeneously (Monn 2001). Vehicle emission is a main PM source; variation of traffic conditions on major roads impact the spatial dynamics of PM. A study in the three European countries found that the $PM_{2.5}$ densities at traffic areas are about 17% higher than those at other urban areas and the $PM_{2.5}$ absorption rates in traffic areas are 31% to 55% higher than those in other urban areas (Hoek et al. 2002).

Moore and colleagues (2009) examined the community-scale spatial and temporal heterogeneity of UFPs variation in two typical communities in Los Angeles, California. They concluded that 1) the spatial variation of UFP concentration is related to heavy-duty diesel vehicle densities; 2) the temporal change of UFP concentration during different times of the day and different seasons is related to vehicle volume changes; and 3) the spatial and temporal heterogeneity of UFP concentration may lead to inaccuracy in place-based UFP exposure measurements.

Besides PM and UFPs, spatial heterogeneities of other air pollutants have been investigated by recent studies.SO_2, CO, NO, NO_2, and O_3 were found to tend to concentrate in relatively small regions; their spatial distributions were related to local industries, major roads, and household fuel combustion (Bell et al. 2004b, Yang, Wang and Zhang 2008, Zhou et al. 2006). The spatial concentration of airborne metals, i.e. ferrum (Fe), zinc (Zn), cuprum (Cu), vanadium (V), and chromium (Cr) were found to be strongly related to the locations of industrial zones and traffic emission (Nerriere et al. 2007). The spatial heterogeneity of atmospheric PAH was influenced by biofuel combustion and traffic emissions (Tian et al. 2009).

To date, the major methods to investigate the spatial heterogeneity of air pollutants include proximity models, the land use regression (LUR) models, air dispersion models, hybrid models, questionnaires, and surveys (Barzyk et al. 2009, Ryan et al. 2007b, Wilhelm, Qian and Ritz 2009, Zou et al. 2009a). For example, Dockery et al. (1996) examined the average acidic air pollution exposure level for 24 communities in the US and Canada, and assumed that the community average exposure level as the personal exposure for children who lived in the community. To examine the effect of long-term traffic black smoke (BS) and NO_2 exposure toward mortality, Hoek et al. (2001) assumed that the residents in a small region had a homogenous PM exposure. However, few of these studies take individual's physical condition and spatiotemporal activity into consideration. Without considering individual factors, these studies fail to provide accurate individual-level air pollution exposure estimation and do not apply to individual air pollution exposure assessment for epidemiologic studies.

Air Pollution Exposure and Microenvironment

Pure place-based air pollution exposure measures fail to describe the accurate and real-time dose that a person is exposed to over a period. To mitigate this problem, the concept of microenvironment was developed (Georgopoulos and Lioy 1994). According to microenvironment and geographically spatial interaction, a person's daily activities are related to a series of microenvironments, such as home, workplace, traveling route, and recreation place. The air pollution level can be assumed to be homogeneous in each microenvironment. Despite the fact that human beings' spatiotemporal activities and the microenvironments where these activities occur are very complicated, microenvironment approach believes that daily activities follow certain routine that consists of a series of repeating routes and locations, such as commuting to work, staying at workplace, commuting back home, and staying home (Srivastava 2005). Weisel (2002) described an individual's total air pollution exposure at different microenvironments as:

$$E = \sum_{i=1}^{n} c_i \Delta t_i \qquad \text{Equation 2.3.}$$

where E is the individual air pollution exposure, i represent a certain microenvironment, c_i is the air pollution concentration in the ith microenvironment, and Δt_i is the time spent in the ith microenvironment.

The commonly studied microenvironments include indoor environment and outdoor environment. The modeling of air pollution at indoor microenvironments is important since most people spend a significant portion of their time indoor. The indoor air pollution environment is closely related to both indoor-generated air pollutants and outdoor-penetrated air pollutants (Massey et al. 2009, Spengler et al. 1981, Wallace

1996). Individuals' habits and customs may affect indoor-generated air pollution. For example, tobacco smoke (Wallace 1996), indoor wood burning and gas cooking (See and Balasubramanian 2006, Wallace 2006), biomass fuels, coal, and charcoal (Ezzati 2005, Gimbutaite and Venckus 2008, Kang et al. 2009) may increase indoor air pollution significantly. Household products and materials are the main source for indoor VOCs, which include alkylbenzenes, alkanes, terpenes, aliphatic aldehydes, and some chlorinated aliphatic hydrocarbons (Kostiainen 1995, Massolo et al. 2010). Besides, there are some indoor microorganisms and unexplained indoor air pollutants, such as house dust mite (HDM), pet, mold, cockroach, mouse, fungi, and bacteria, which may emit or generate microbial volatile organic compounds (MVOCs) (Gaffin and Phipatanakul 2009, Korpi, Jarnberg and Pasanen 2009).

Based on the indoor-outdoor air pollution exchange theory, indoor air pollution can be modeled. The indoor PM$_{2.5}$ concentration is related to the outdoor-penetrated air pollution, cigarette smoking, cooking, and other unknown indoor source emissions (Wallace 1996).

$$C_{PM\_in} = \frac{\lambda}{\lambda+0.4} \cdot C_{PM\_out} + 14 \cdot \frac{Sm}{V} + 4 \cdot \frac{Co}{V} + c \qquad \text{Equation 2.4.}$$

where C_{PM_in} is the indoor PM$_{2.5}$ concentration (mg/m^3), C_{PM_out} is the outdoor PM$_{2.5}$ concentration (mg/m^3), λ is the air change per hour (ACH) (hr^{-1}), Sm is the number of cigarettes smoked indoors, V is the volume of the indoor space (such as home and office) (m^3), Co is the cooking time in minutes, c is the constant, which represents other indoor emissions, such as the unknown source air pollution (mg/m^3).

Formula 3 can be simplified through following steps. First, according to

Yamamoto et al.'s (2010) ACH study in three US cities, the medians of the ACHs in

Texas cities are $0.38hr^{-1}$, $0.37hr^{-1}$, $0.48hr^{-1}$, and $0.63hr^{-1}$ in the spring season

(March through May), the summer season (June through August), the fall season

(September through November), and the winter season (December through February),

respectively. Second, the standard floor-to-ceiling height is assumed to be 8.5ft (Thatcher

et al. 2001). Last, because other indoor sources emit a small proportion of indoor air

pollution, and their emissions are hard to be quantified, the indoor emissions from the

unknown sources will be omitted in this dissertation research.

In Texas:

$$C_{PM\_in\_sp} = 0.49 \cdot C_{PM_{out}} + 58.17 \cdot \frac{Sm}{Ar} + 16.62 \cdot \frac{Co}{Ar} \qquad \text{Equation 2.5.}$$

$$C_{PM\_in\_su} = 0.48 \cdot C_{PM_{out}} + 58.17 \cdot \frac{Sm}{Ar} + 16.62 \cdot \frac{Co}{Ar} \qquad \text{Equation 2.6.}$$

$$C_{PM\_in\_fa} = 0.55 \cdot C_{PM_{out}} + 58.17 \cdot \frac{Sm}{Ar} + 16.62 \cdot \frac{Co}{Ar} \qquad \text{Equation 2.7.}$$

$$C_{PM\_in\_wi} = 0.61 \cdot C_{PM_{out}} + 58.17 \cdot \frac{Sm}{Ar} + 16.62 \cdot \frac{Co}{Ar} \qquad \text{Equation 2.8.}$$

where $C_{PM\_in\_sp}$, $C_{PM\_in\_su}$, $C_{PM\_in\_fa}$, and $C_{PM\_in\_wi}$ are the indoor PM$_{2.5}$ concentrations

in spring, summer, fall, and winter in Texas cities (mg/m^3), Ar is the area of the indoor

space (ft^2).

The accumulation process of indoor O$_3$ is similar to that of indoor PM$_{2.5}$. But the

proportion of the indoor-generated O$_3$ is very low. If the indoor-generated O$_3$ and the

ventilation-filter-removed O$_3$ are not considered, the indoor O$_3$ concentrations are related

to outdoor O$_3$ concentrations and the ACH (Du and Liu 2009). For example, the mean

indoor/outdoor ratio of O_3 concentrations is roughly around 0.2 in 145 Mexican homes (Romieu et al. 1998).

$$C_{O3\_in} = \frac{\lambda}{\lambda+1} \cdot C_{O3\_out}$$ Equation 2.9.

In Texas:

$$C_{O3\_in\_sp} = 0.28 \cdot C_{O3\_out}$$ Equation 2.10.

$$C_{O3\_in\_su} = 0.27 \cdot C_{O3\_out}$$ Equation 2.11.

$$C_{O3\_in\_fa} = 0.32 \cdot C_{O3\_out}$$ Equation 2.12.

$$C_{O3\_in\_wi} = 0.39 \cdot C_{O3\_out}$$ Equation 2.13.

where C_{O3_in} is the indoor O_3 concentration (ppm), $C_{O3\_in\_sp}$, $C_{O3\_in\_su}$, $C_{O3\_in\_fa}$, and $C_{O3\_in\_wi}$ are the indoor O_3 concentrations in spring, summer, fall, and winter in Texas cities (ppm).

Outdoor microenvironment air pollution is believed to be associated with traffic emissions and industrial emissions (Zou et al. 2009b). Roadway air pollutants mainly include PM, black carbon (BC), CO, NO_x, benzene, and polycyclic aromatic hydrocarbons (PAHs), while industrial emitted air pollutants may vary according to different industrial activities (Cook et al. 2008). A number of recent place-based studies have been carried out to investigate air pollution in these outdoor microenvironments (Cook et al. 2008, Liu et al. 2007). Traveling microenvironment is a special outdoor microenvironment. Vehicle's inside and outside air exchange makes drivers and passengers to be exposed to the same level of pollution as roadway ambient (Fruin et al. 2008).

Through examining and connecting multiple microenvironments, researchers attempted to assess individual's exposure to air pollutants. Liu and colleagues conducted a pilot study in the early 1990s to measure children's O_3 exposure by examining both indoor and outdoor data (Liu et al. 1993). In the last twenty years, a number of studies were conducted to investigate air pollution exposure based on microenvironment, which include rural versus urban environments, indoor versus outdoor residential environments, and indoor versus outdoor workplace environments (Edwards and Jantunen 2009, Edwards et al. 2001, Edwards et al. 2005, Ilgen et al. 2001).

Microenvironment has an application potential in individual air pollution exposure assessment if it is integrated with time geography. By investigating individual time-microenvironment-activity (TMA), individual air pollution exposure context can be assumed as a series of independent microenvironment exposures (Ballesta et al. 2008). For example, in Delgado-Saborit et al.'s (2009) individual VOC exposure study, different microenvironment pollutant concentrations were measured separately; individuals' spatial locations over time were collected through individual activity diaries.

Air pollution exposure measures based on microenvironment method cannot substitute for individual-based measures. Individual's daily activities are different, so is individual's air pollution exposure. Individuals who live in the same residential community may have different air pollution exposure levels. It is very hard to delineate people's exposure levels by just using air pollution concentrations in several fixed microenvironments such as residential community, workplace, and outdoor (Kwan 2009). Integrating microenvironment and individual-based measures is a good solution for accurate individual exposure assessment.

Air Pollution Exposure Assessment Methods: Place-Based vs. Individual-Based

When investigating air pollution exposure, two groups of methods (i.e., place-based measures and individual-based measures) are applied (Fang and Lu 2012). Place-based measures take places as objects, while individual-based measures take people as objects. Place-based measures are based on Eulerian reference framework and are applicable to areal air pollution exposure studies. Individual-based measures are based on Lagrangian reference framework and are superior to place-based measures in conducting individual level air pollution exposure (Doyle and Ensign 2009).

Place-Based Air Pollution Exposure Measures

Using the straightforward mathematical representation of Eulerian reference framework, place-based method is a natural choice for investigating simple objects or homogeneous objects, such as urban land-use change (Benenson and Torrens 2004, Juda-Rezler 2010). Following the place-based approach, the conventional air pollution exposure measures commonly define one or more hypothetical homogeneous region(s), and use one fixed value to represent the air pollution concentration for each region. A number of place-based exposure assessment methods have been developed, including proximity modeling, air dispersion modeling, etc. (Zou et al. 2009a). Census units ranging from census block to city level or other predefined boundaries are commonly used as homogeneous regions (Matthews 2008) for better data access and easier integration. The summary of the major characteristics of place-based methods as well as the related major literature are reported in the end of next section (Individual-Based Air Pollution Exposure Measures) (see Table 2.3).

However, disadvantages of place-based measures should not be ignored. First, the hypothesis on homogeneous air pollution concentration region is problematic. Due to the spatial heterogeneity of air pollutant concentration, it is risky to assume homogeneous air pollutant levels across a region. Second, the spatial and temporal resolutions for place-based measures are coarse. Place-based measures usually utilize neighborhoods, census blocks, or census tracks as measuring units, and utilize daily, monthly, and even quarterly intervals as time spans (Samet et al. 2000). Third, due to MAUP, the air pollution exposure measuring for a specified place may vary when different scales or zoning methods are applied (Haynes et al. 2007). Last, it can be very inaccurate to assume that different individuals in a hypothetical homogeneous region have the same air pollution exposure level. This may cause the ecological fallacy. For example, the neighborhood residential exposure or ambient outdoor air pollution exposure may not be the only exposure source for all individuals in an identical block.

Place-based air pollution measurement methods involved in this dissertation research include the LUR modeling and the spatial interpolation methods.

LUR Modeling

The land use regression (LUR in short) modeling is a discrete environmental exposure simulation approach (Ryan and LeMasters 2007). It combines air pollution monitoring data and land use data with geographic information system (GIS) techniques (Hoek et al. 2008). According to the LUR model, there is a linear relationship between the dependent variable, air pollution level, and the independent variables, such as land use, traffic, meteorological factors, demographic factors, and geographic factors (Ryan et

al. 2007b). Through a multiple linear regression, the parameters can be calibrated. The model, after validation, can then be used to predict the air pollution.

$$y = \beta_1 \cdot x_1 + \beta_2 \cdot x_2 + \cdots + \beta_n \cdot x_n + \beta_{n+1}$$
<div style="text-align: right">Equation 2.14.</div>

where y is the outdoor air pollution concentration, $\beta_1 \cdots \beta_{n+1}$ are the parameters, $x_1 \cdots x_n$ are the variables.

Since 1990s, researchers have developed a number of LUR models to simulate air pollution in intra-urban environment (Briggs et al. 1997). Ryan et al. (2007b) applied a multiple linear LUR traffic exposure model to assess the relationship between air pollution along the road and wheezing in infants in Cincinnati. Arain et al. (2007) added the impact of wind flow to the LUR model to predict the concentration of nitrogen dioxide (NO_2) in a heavily polluted region in Canada. Clougherty et al. (2008) simulated the comprehensive effects of fine articulate matter ($PM_{2.5}$), NO_2, and elemental carbon (EC) in urban neighborhoods of Boston using a multi-variable LUR model. Rosenlund et al. (2007) noted that the LUR model may successfully simulate the traffic-air pollution (NO_2) without air pollution emission data. However, as Hoek et al. (2008) pointed out after reviewing 25 recent LUR modeling studies, that the great challenge for LUR modeling is its transferability – most studies developed / tested for area-specific LUR models.

The LUR model used in this study shows two unique aspects. First, it models ground-level O_3. Most recent LUR studies examined other air pollutants such as articulate matter (PM) and NO_2 (Hoek et al. 2008). Because ground-level O_3 is known to be related to NO_2, sunshine length and intensity, temperature, and air humidity (Pudasainee et al. 2006), it is possible to use the LUR model to simulate urban O_3 level.

Second, this study used near real-time (with a three-hour lag) hourly data to build a series of hourly LUR models. Traditional LUR studies usually utilize the average air pollution concentration over a period of time for the LUR model (Ross et al. 2007). These studies neglected to the variation of air pollution over their study time. Recently researchers have noticed this shortcoming and begun to use the LUR modeling to simulate the temporal change of air pollution. For example, in Mölter et al.'s (2010) LUR modeling study, the annual mean air pollutants (PM_{10} and NO_2) concentration was simulated for the 13 consecutive years. However, finer time scales (e.g. weekly, daily, or hourly) modeling is still missing, which is important for understanding the short-term health effect of air pollution.

Spatial Interpolation

Spatial interpolation is a group of methods for predicting values of un-sampled locations from scattered set of observations (Lam 1983). There are many spatial interpolation methods including the local neighborhood approaches (e.g., inverse distance weighting (IDW)), the geostatistical approaches (e.g., kriging), and the variational approaches (e.g., thin plate spline (TPS)) (Coulibaly and Becker 2007). Considering away any possible causal relationship or spatial association between the measured attribute and other characteristics of a location and / or its surroundings, spatial interpolation methods have been widely used in air pollution simulation. Fuentes (2002) utilized spatial interpolation based on spatial spectra to predict the nonstationary O_3 concentrations. Wong et al. (2004) compared four spatial interpolation methods (i.e., spatial averaging, nearest neighbor, IDW, and kriging) to predict PM_{10} and O_3 concentrations in the U.S. using the EPA sites data. They found that the densities of EPA

sites were related the performance of these spatial interpolation methods. Janssen et al. (2008) applied a detrended kriging model, named RIO, to assess air pollution conditions. In their study, land use data was integrated with spatial interpolation to model the concentrations of O_3, NO_2, and PM_{10} in Belgium.

Individual-Based Air Pollution Exposure Measures

Individual-based air pollution exposure methods measure air pollution exposure at individual level (Fang and Lu 2012). The advantages are in several aspects. First, individual-based measures involve both air pollution exposure and individual factor and facilitate the study of individual air pollution health effects. Individual-based measures are more robust in individual air pollution exposure assessment for epidemiologic studies than place-based measures. Second, individual-based measures acquire accurate and continuous spatiotemporal data for individuals. The spatial resolution can be accurate to sub-meter and temporal resolution to second (Nethery et al. 2008). To measure a person's everyday air pollution exposure, locations and time spent in each location are two critical factors (Kwan and Weber 2008). Third, individual-based measures can mitigate MAUP (Kwan 2009). Tobler's theory of frame independent spatial analysis (Tobler 1989) states that 1) geographical data may be independent to any spatial scales and zoning methods, and 2) appropriate spatial analysis approaches can eliminate the MAUP. Under the frame of individual-based exposure study, measurement objects are individuals, and the conventional areal measurement objects – neighborhoods, communities, census blocks, and even cities lose their area characteristics. Last, recent development in communication and information technology lends strong support to individual-based measures. While place-based measures suffer from limited data sources (such as air pollution monitoring

sites and field recording) (Tomlin et al. 2009), individual-based measures take advantage of such technologies as global positioning system (GPS) and biological indicators, which make real-time monitoring and recording practical (Nieuwenhuijsen, Paustenbach and Duarte-Davidson 2006).

Nevertheless, individual-based measures have several limitations. The first challenge comes from individual's representativeness. Lagrangian reference framework suffers from a shortcoming that the representativeness of the selected individual objects is questionable. The individual-based measures inherit this adverse characteristic. It is a major issue for individual-based air pollution exposure measures to ensure that the selected individuals are representative regarding their air pollution exposure. For this purpose, a large population sample is often required for individual-based measures. But this may cause other problems. A large sample tends to result in excessively complicated computational processes. Moreover, statistical analysis results for large population are not always reliable (Doyle and Ensign 2009). The second challenge to individual-based methods is to acquire large data set delineating population's exposure to air pollution. The cost for such monitoring units is high; so is that for recruiting large samples. The problem of sample size may restrict the application of individual-based air pollution exposure measures (Honicky et al. 2008). The last challenge is related to the current technologies for location and air quality measuring and recording. Ideal individual-based measuring equipment needs to be small enough for long-term carry-on use, to have long battery life for continuous recording, and to provide steady performance under bad environmental conditions. Unfortunately, to date neither real-time location acquisition

tools (i.e., GPS) nor real-time environmental monitoring tools (i.e., portable air quality

meter), can fully meet these conditions.

Table 2.3. Characteristics of Place-Based vs. Individual-Based Air Pollution

Exposure Measures.

	Place-based measures		Individual-based measures	
	Characteristics	**Related literature**	**Characteristics**	**Related literature**
Reference framework utilized	• Eulerian reference framework • Simple mathematical structure	(Juda-Rezler 2010)	• Lagrangian reference framework • Complex mathematical structure	(Doyle and Ensign 2009)
Observation and recording method	• Observe and record movements of an object through fixed observation points	(Greaves, Issarayangyun and Liu 2008)	• Observer follows an object to observe and record	(Chiang et al. 2008)
When measuring many objects	• Lose detailed characteristics for individuals • Take all objects as a group and measure the group's attributes • No demographic heterogeneity or air pollution concentration heterogeneity in the group	(Hoek et al. 2008)	• Reserve all individuals' distinctive characteristics • Individual behaviors may not be representative to others • Use statistical approaches to simulate the group's attributes	(Gerharz, Kruger and Klemm 2009)

Table 2.3-Continued

	Place-based measures		Individual-based measures	
	Characteristics	**Related literature**	**Characteristics**	**Related literature**
Measuring unit	• Predefined census units, which usually ranged from census block to city level • Hypothetical homogeneous exposure regions	(Matthews 2008)	• Individuals • People related moving objects, such as cars	(Raftery 2009)
The amount of measuring object	• Usually limited number	(Benenson and Torrens 2004)	• Sample size needs to be very large to facilitate regional air pollution mapping • One object is enough for individual level measuring	(Honicky et al. 2008) (Kim, Paulos and Gross 2010)
Scale	• Aggregate level • Fine spatial and temporal resolution for a point, but limited for a region	(Samet et al. 2000)	• Individual level • Fine spatial and temporal resolution	(Jensen 2006)
MAUP	• MAUP exists • May be mitigated through new approaches such as scale-space clustering method and creating homogeneous zones	(Mu and Wang 2008) (Riva et al. 2009)	• Can mitigate MAUP	(Kwan 2009)

Table 2.3-Continued

	Place-based measures		Individual-based measures	
	Characteristics	**Related literature**	**Characteristics**	**Related literature**
Measuring accuracy	• High accuracy for a limited number of sample sites • Low accuracy for individuals	(Hoek et al. 2002)	• Usually high spatiotemporal accuracy for individuals • Low accuracy for place	(Dutta et al. 2009)
Measuring methods	• Monitoring data from governmental and private air pollution monitoring sites • On site air pollution measuring • Air pollution exposure modeling • Historical air pollution libraries and data warehouses • Questionnaires and surveys	(Zou et al. 2009a)	• Carry-on real-time monitor • Life course measures • Longitudinal studies • Agent-based modeling • Biological monitoring methods • Inhalation exposure modeling • Survey and diaries	(Adams, Riggs and Volckens 2009) (Clougherty et al. 2007) (Naess et al. 2007) (Kalapanidas and Avouris 2002) (Delfino et al. 2008) (EPA 2008c)
Current developing status	• Conventional • Many new air pollution exposure assessment methods and data sources	(Barzyk et al. 2009)	• Exploratory • Rapid development with great potential	(Dutta et al. 2009)

Current Progresses in Individual-Based Air Pollution Exposure Measures

Individual-based air pollution exposure can be measured directly or indirectly. Two groups of methods are normally used for direct measure: individual real-time monitoring method and space-time activity measuring method (such as life course measures and longitudinal studies) (Miller 1999). Indirect measure methods, which include biomarker, inhalation exposure modeling, and agent-based modeling, are important surrogates for direct individual-based air pollution exposure measures. This section discusses each of these methods in details; see Table 2.4 at the end of this section.

Individual Real-Time Air Pollution Exposure Monitoring

Individual real-time air pollution exposure monitoring continuously collects in situ air pollution exposure data for individuals across space and through time (Morabia et al. 2009). In early 1980s, Wallace and Ott pointed out that with high portability and all day recording capability, individual air pollution exposure monitors "*could transform the way in which human exposure to air pollution*" be measured (Wallace and Ott 1982, p.601). Individual real-time monitoring, supported by location acquisition technology and portable air pollution sampler, enables continuous reporting of the dynamics of personal space-time tracks and air pollution exposure levels (Croner, Sperling and Broome 1996).

Real-time location acquisition instruments emerged along with the development of information and communication technologies (Warren 2006). Common real-time location acquisition instruments (location-aware systems) such as civilian handheld GPS and global system for mobile communications (GSM) have great potential for spatiotemporal data collection (Bell et al. 2004b, Lu and Liu 2012, Xin, Li and Di 2005).

Many researchers have applied GPS or GSM to collect location data for their epidemic studies (Bell et al. 2004b, Duncan, Badland and Mummery 2009, Greaves et al. 2008, Matejicek, Engst and Janour 2006, Trandabat et al. 2007, Trandabat et al. 2005, Xin et al. 2005, Zhan et al. 2006).

Individual real-time environmental monitoring instruments, such as portable air pollution sampler, are being developed. For example, a team in Carnegie Mellon University has developed a prototype of low-cost VOCs sensor embedded T-shirt named WearAir; it can indicate VOCs levels with light-emitting diodes (LEDs) (Kim et al. 2010). However, because WearAir does not have real-time locations recording module, the exposure measures cannot be connected to spatiotemporal context directly.

A true individual-based real-time air pollution exposure monitor needs to be able to sense and record both spatiotemporal information as well as air pollution exposure at individual level simultaneously and continuously. For example, Adams and colleagues (2009) developed a PM exposure monitoring package. The package includes a portable GPS receiver to track individual time and location tracking, a miniature aerosol nephelometer to monitor PM exposure level, and a thermocouple sensor to record temperature. Depending on how tightly coupled the measurement of location is with that of air pollution exposure, a real-time air pollution exposure monitoring tool can be a "genuine" system or a "pseudo" one (see Table 2.4).

Integrated Genuine Individual Real-Time Air Pollution Monitoring   A basic integrated genuine individual real-time monitoring tool has two components, i.e., an individual real-time location acquisition unit and an individual real-time environmental monitoring unit (Sensaris 2010). Because all components of it are individual-based, an

integrated genuine individual real-time monitoring tool has a very high measuring accuracy.

Recent projects such as Area's Immediate Reading (AIR) and the Common Sense project are examples of genuine real-time exposure monitoring studies (Dutta et al. 2009). Launched in 2006, AIR project uses real-time portable GPS-air monitoring devices to delineate individual air pollution exposure. Individual air pollutants, such as NO_x, CO, and O_3, are measured and transmitted to the network database center. AIR device can display real-time ambient air pollution information as well as regional air pollution concentration (AIR 2010). The Common Sense project, co-developed by Intel Research and the University of California, Berkeley, is an ongoing people-base exposure study that aims at measuring personal on site air pollution exposure through mobile network (Raftery 2009). The integrated CO, NO, O_3, and other air pollutants sensors are built in the handheld device; the mobile phone chip can record individual spatial location; the mobile phone network functions as a user-based air pollution information sharing and mapping service network (Honicky et al. 2008). In addition to the Common Sense project, N-SMARTS is another ongoing project at the University of California, Berkeley that provides a real-time individual moving exposure measuring platform for CO, NO_2, and SO_2 (Chiang et al. 2008).

To date, complete genuine individual real-time monitoring studies are few. Two major challenges hinder the application of the integrated genuine individual real-time monitoring tool. The technological challenges for developing such an integrated genuine individual real-time monitoring tool are how to keep its size small for ease of carry by an individual without significantly impact his/her daily function, battery life long to support

continuous recording, and cost low to ensure affordability for various users. The smallest integrated real-time monitoring tool has the size of handheld portable PDA (Raftery 2009). Besides technological challenges, the bad end-user experience is a key adverse factor. Although Public are aware of air pollution health effects, few of them will like to carry air quality meters in everyday life.

Integrated Pseudo Individual Real-Time Air Pollution Monitoring   An integrated pseudo individual real-time air pollution monitoring tool has one or more non-individual-based components; the two functional aspects, monitoring of location and that of air pollution, are loosely coupled in the system. Most pseudo individual real-time air pollution monitoring studies use GPS or GSM to collect real-time individual spatial trajectory information and use separately derived air pollution measurements to delineate individual air pollution exposure levels (Jensen 2006).

The measuring accuracy of integrated pseudo individual real-time air pollution monitoring tools is not as good as that of integrated genuine individual real-time air pollution monitoring tools. Nevertheless, integrated pseudo individual real-time air pollution monitoring tools are more suitable for individual air pollution exposure assessment. Integrated pseudo individual real-time air pollution monitoring tools have very flexible structures; location acquisition and air pollution monitoring are operated separately; numerous mobile phone users make location acquisition through GPS or GSM easy; thousands public air monitoring sites in the U.S. make on site air pollution measurement very convenient. Even more important, integrated pseudo individual real-time air pollution monitoring tools can provide great end-user experience. Individuals do not need to carry portable air quality meters; a daily-used smartphone is the only personal

equipment needed. The whole monitoring process is automatic; individual daily activities are not affected.

An early pseudo system was proposed ten years ago using atmospheric and meteorological sensors as air quality monitor and GSM-based message passing protocol as the communication component (Garcia-Alegre et al. 2001). Initiated in early 2000s, National Environmental Research Institute in Denmark developed a traffic air pollution exposure modeling system named AirGIS (Hertel et al. 2006, Jensen 2006). AirGIS system included two levels. The first level was to simulate urban air pollution environment using Danish Operational Street Pollution Model (OSPM), road network, and traffic information. The second level was personal location module – individual-carried cell phones with built-in GPS receivers, which send location information to AirGIS tracking center at twenty seconds intervals. The third example is PolluMap, a GSM supported automatic urban air pollution surveillance system launched in Dubai, United Arab Emirates (AbuJayyab et al. 2006). In this system, multiple location and air pollution concentration data were collected by moving or fixed monitors; the data were sent through wireless communication to a web server to delineate a citywide air pollution map. Projects such as AirGIS and PolluMap integrate convenient non-individual-based air pollution surveillance and real-time individual location acquisition monitoring. There is a rapid increase of studies on similar integrated pseudo individual real-time monitoring in the recent years (Gerharz et al. 2009).

A few pseudo real-time monitoring studies used real-time monitoring units as place-based survey tools instead of individual-based spatiotemporal data collectors. The location acquisition units were used to collect location information for certain fixed

locations or locations on a route, rather than for individual's moving trajectory. In a study that investigated PM, UFP, and noise exposure of car drivers and bike riders in the twelve selected short routes in the Netherlands, GPS was used to collect a series of coordinate data along routes (Boogaard et al. 2009). Similarly, $PM_{2.5}$ meter and GPS units were used in another study (Morabia et al. 2009) to assess the air pollution exposure level for the drivers, subway riders, and pedestrians on selected routes in New York City.

Table 2.4. Individual Real-Time Monitoring Studies.

Groups		Advantages	Drawbacks	Related literature
Location monitoring	GPS	• Collect site or route coordinates • Rapid • Low cost	• Every sensor collects only limited data	(Zhan et al. 2006) (Duncan et al. 2009)
	GSM SMS and GSM GPRS	• Acquire real-time location data • Quick response, low cost, and large coverage network	• Data delay • Low temporal resolution • Low spatial resolution	(Bell et al. 2004b) (Xin et al. 2005)
Environmental monitoring	Stand-alone environmental monitoring	• High air pollution concentration measurement accuracy • Good for individual use	• Hard to delineate regional air pollution condition	(Kim et al. 2010)

Table 2.4-Continued

Groups		Advantages	Drawbacks	Related literature
Integrated real-time monitoring	Integrated pseudo real-time monitoring	• Use both individual-based measures and place-based measures • Low cost • Save time	• All components are not individual-based • Individual exposure is based on simulation instead of real-time monitoring • Limited temporal resolution • Limited spatial resolution	(Garcia-Alegre et al. 2001) (AbuJayyab et al. 2006) (Hertel et al. 2006) (Boogaard et al. 2009) (Morabia et al. 2009)
	Integrated genuine real-time monitoring	• All components are individual-based • High spatial resolution • High temporal resolution	• Expensive instrument • Need large sample size for delineating regional air pollution • Handheld equipment needed • Immature technology	(Chiang et al. 2008) (Honicky et al. 2008) (Adams et al. 2009) (Dutta et al. 2009) (Raftery 2009) (AIR 2010)

Other Individual-Based Air Pollution Exposure Measures

Besides individual real time monitoring, there are several common individual-based air pollution exposure measures such as life course measure and longitudinal studies, biomarkers technology, inhalation exposure modeling, and agent-based modeling (Avruskin et al. 2004, Butz and Torrey 2006, Martin et al. 2008, Ryan et al. 2007a, Sokolova and Fernandez-Caballero 2009).

Pope and Dockery (2006) indicated that effective dose depends on not only exposure concentration but also exposure length. In other words, the adverse effect from extended long-term air pollution exposure is more serious than that from accumulated short-term air pollution exposure. To address the comprehensive effect from long-term air pollution exposure, the space-time activity measuring methods such as life course measures and longitudinal studies are frequently used. Life course measures and longitudinal studies commonly collect long-term individual air pollution exposure data through questionnaires, diaries, surveys, and neighborhood observation (Gerharz et al. 2009, Miller 1999, Schaefer-McDaniel et al. 2009).

Biomarkers measure is a typical indirect individual-based air pollution exposure measure. Individual air pollution exposure is not measured by air pollution monitoring instrument but estimated through biomarkers. Generally speaking, biomarkers are a series of markers relevant to host's intake of air pollutants. They help understanding the relationship between air pollution exposure and its potential impact on the host person as they reveal the dose of air pollutants that entered human body (Delfino et al. 2009, Lewtas 2007, Swenberg et al. 2008). The widely accepted trichotomy for biomarkers are

biomarkers of exposure, susceptibility, and effect; these three types of biomarkers are not mutually independent (Metcalf and Orloff 2004, WHO 1993).

A critical objective for individual-based air pollution exposure measures is to decide the total air pollution intake. If ambient air pollution concentration and inhalation rate are decided, individual air pollution exposure dosage can be quantified. Inhalation exposure modeling is an effective way to model individual air pollution inhalation in different scenarios. In other words, measuring individual inhalation dosage and seeking the relationship between inhalation dose and adverse health effects are primary research tasks for inhalation exposure modeling (Ott 1982). Early in the 1980s, inhalation exposure modeling was developed to simulate individual air pollutant inhalation rate. To examine the air pollution exposure-inhalation relationship, individuals were exposed to 2-butoxyethanol (20 ppm) for two hours (Johanson et al. 1986). Similar studies were carried out to analyze individual inhalation of UFP and SO_2 (Shah et al. 2008, Sheppard et al. 1981). In these studies, personal biophysical parameters are pre-measured; biomarkers for air pollutants, such as air pollutants amount of residue and metabolites in blood or urine, disease attack, and blood pressure change, were measured to examine the exposure-inhalation mechanism.

In early 1970s, based on *"interactive dynamics of discriminatory individual choices"*, Schelling (1971, p.143) introduced agent-based modeling (ABM). With the three advantages – emergency decision, automatic operation, and high felxibility, ABM has been widely applied in simulating social behavior of individual or groups under certain rules (Bonabeau 2002). When a direct exposure measure is not available, ABM can be used to estimate individual-based air pollution exposure. ABM is suitable for

individual-based air pollution exposure for two reasons. First, taking individuals as agents, ABM has a great potential to simulate individual spatiotemporal travelling patterns and individual air pollution exposure scenario (Sun 2007). Second, ABM has very powerful flow simulation function, which enables air pollution diffusion analysis (Bonabeau 2002).

Recent Information Technological Advances to Promote Individual-Based Air Pollution Exposure Measures Studies

Mobile Positioning Technology

Mobile positioning technology emerges along with the development of information and communication technologies in recent years (Warren 2006). Mobile positioning technology does not collect air pollution information by itself. But it can be used to quickly collect a person's location information through a time period, which is the component of many personal exposure assessment methods.

Common mobile positioning technologies include Global Satellite Navigation System (GNSS), radio frequency identification (RFID), cellular network positioning, and other networks (such as Wireless Fidelity (Wi-Fi) network and Internet Protocol (IP) address) positioning technologies. To date, the most successful GNSS is GPS, which is fully operated and has a full global coverage. Other GNSSs in preparation include the Russian GLONASS, the Chinese Beidou (also called as Compass) navigation system, and the European Union's Galileo positioning system (IGS 2009). As technology progresses, the horizontal error of a GPS receiver/data-logger is reduced to less than 5 meters under cloudless condition (Keita, Carfagna and Mu'Ammar 2010); the size of a GPS

receiver/data-logger is small enough to be integrated into a watch or a mobile phone. The accuracy of cellular network positioning is decided by the location of near base station and therefore is not high. Assisted GPS (A-GPS) positioning is a hybrid approach that combines standalone GPS positioning and cellular network positioning (LaMance, DeSalas and Jarvinen 2002). Recently, many researchers applied mobile positioning technologies to collect persons' location data for their environmental assessment studies (Duncan et al. 2009, Greaves et al. 2008, Maisonneuve et al. 2009, Zhan et al. 2006).

Mobile Wireless Communication Technology

Mobile wireless communication technology (or called as cellular network technology) has evolved four generations. The first generation (1G) only provides mobile voice communication service. The second generation (2G) begins to support data communication with a low speed of 10KBps. The third generation (3G) is currently the most widely used high speed mobile wireless data communication technology. With 3G network, mobile cellular subscribers can easily access to internet. The fourth generation (4G) is a new technology that provides a higher data communication speed than 3G. Although 4G is better, there's still a long way to go before 4G replaces 3G because of issues such as network upgrading (Arshad, Farooq and Shah 2010).

Mobile wireless communication technology, especially 3G and 4G technology, allows mobile cellular subscribers to acquire and disseminate information at all times and places. Air pollution exposure assessment can take advantage of this feature. For example, a smart mobile phone becomes a mobile air pollution monitoring platform when it is integrated with a portable air pollution sampler (Raftery 2009). According to the

International Telecommunication Union (ITU), the mobile cellular subscribers worldwide reached 5.3 billion in 2010. Among these subscribers, about 940 million had 3G service (ITU 2010). The huge amount of mobile cellular subscribers set me thinking on what the future of personal exposure assessment studies will be since there are so many potential participants/contributors.

Web 2.0 and VGI

First introduced by Darcy DiNucci (1999) and clearly defined by Tim O'Reilly (2005), the term "Web 2.0" indicates the new World Wide Web that is featured as read-write function and bottom-up structure. Web 2.0 has the advantage of user-generated content (UGC). Any individual or group can publish information to the internet conveniently. In other words, there are "six billion sensors" on the earth (Goodchild 2007b).

The spatial information (including air pollution exposure data) created by the untrained voluntary persons (e.g., common net users) is called volunteered geographic information (VGI) (Goodchild 2007a). VGI has the virtue of fast reponse, low cost, and large volume. So the VGI system is applicable to collect a person's environmental exposure. For example, CoCoRaHS (the Community Collaborative Rain, Hail and Snow Network) relies on about twenty thousand volunteers nationwide with different social backgrounds to measure and report the precipitation amount in their backyards. Using these data, CoCoRaHS publishes U.S./state/county daily precipitation maps (CoCoRaHS 2010).

The mobile VGI system – a mobile wireless communication technology supported VGI system – can achieve real-time data collection and publishing through smart mobile phones (Song and Sun 2010). For example, when a person finds poor air quality near a street block, he can use his iPhone to report the information onto Twitter using the Schmaps & Schnaps app. Then those who follow him receive a map that shows the event location and other information. If the reporter carries a portable air pollution sampler, his personal real-time exposure to air pollution can be measured and published synchronously.

Health Effects of Air Pollution Exposure

Air pollutants have many effects on human health (Curtis et al. 2006, Mauderly and Samet 2009). These health effects can be either long-term or short-term. Major long-term health effects include diseases of the respiratory system (e.g., chronic asthma and lung cancer), other internal diseases (e.g., cardiovascular and cerebrovascular diseases), and shortened life expectancy (Neupane et al. 2010, Puett et al. 2009). Major short-term health effects include allergy, upper respiratory infections, acute asthma, and even death (Belleudi et al. 2010, Kan et al. 2010). Individual sensitivity toward air pollutants is different. Generally speaking, children and older persons are more sensitive to air pfollutants (He et al. 2010, Silverman and Ito 2010). Air pollutants can have different human health effects (Kampa and Castanas 2008, Pope, Ezzati and Dockery 2009). It is necessary to investigate different air pollutants separately.

Health Effects of Ground-Level O_3 Exposure

Ground-level O_3 may cause airway inflammation, airway hyperresponsiveness (AH), respiratory infection, pulmonary injury, and heart disease (Weinhold 2010). A Thailand study found that short term ground-level O_3 exposure is associated with cardiovascular diseases (RR=1.239, 95% CI=0.901, 1.705) and respiratory diseases (RR=1.157, 95% CI=0.791, 1.692) (Ruangdej and Chaosuansreecharoen 2008). A recent study reported that of climate change induced O_3 increase may cause daily mortality increases in 50 U.S. cities (Bell et al. 2007). In their study, sixty years climate change (1990 through 2050) was simulated; the estimated summertime O_3 concentrations increased significantly (high O_3 summer days increased 68%); O_3-related mortality would increase 0.11% to 0.27% daily. Lin et al. (2008) applied a birth cohort study to assess the association between chronic O_3 exposure and the risk of asthma among children in New York and reported a positive correlation (OR: 1.16-1.68). Moore et al. (2008) investigated the asthma hospital discharge during high O_3 seasons in southern California. They found that O_3 level is associated with children asthma hospital admission. Rage et al. (2009) examined the asthma severity among 328 samples from the French Epidemiological study on the Genetics and Environment of Asthma (EGEA). They reported that summertime O_3 (over 110mg/m^3) is positively associated with the severity of adult asthma (OR=2.22, 95% CI=1.61, 3.07). Lin and Lu (2009) reported that the global association between O_3 exposure and children respiratory diseases is not significant in Houston, Texas in 2001 summer, but they noted that there is a significant association in three sub-areas.

Because the generation of ground-level O_3 is related to temperature, humidity, and solar radiation, O_3 concentrations vary with time and season. Generally speaking, O_3 concentrations are higher in urban area during summer daytime (Khoder 2009). In the APHEA-2 (Air Pollution and Health: a European Approach) project, Samoli et al. (2009) reported the positive relationship between ground-level O_3 and respiratory mortality and cardiovascular mortality in summer. They found that for every 10 mg/m^3 O_3 increase, the lag 0 respiratory mortality and the lag 0-20 respiratory mortality increase 0.36% (95%CI=0.002–0.009) and 3.35% (95%CI=0.002–0.048) respectively. But they failed to build the O_3 health effect relationship for other seasons. Another French study investigated summer O_3 concentrations in nine cities and found a significant association between O_3 and mortality (Filleul et al. 2006). For every 10 mg/m^3 O_3 increase, the mortality increased 1.01% (95%CI=0.006, 0.014).

Health Effects of PM Exposure

PM is a common name of a series of air pollutants in air; it includes BS, haze, TSP, PM_{10}, $PM_{2.5}$, and UFP (Bell, Samet and Dominici 2004c). Recent epidemiologic studies have supported that PM is associated with increases in acute and chronic respiratory illness, cardiovascular illness, and death. Early studies such as the Harvard Six-City study found that the indoor air particulate levels in is associated with pulmonary function decrease (Spengler et al. 1981). In the U.S., Dominici et al. (2006) investigated the national hospital admission data for 1999 through 2002 and found that the short-term $PM_{2.5}$ exposure is significantly related to cardiovascular and respiratory diseases hospital admission. de Bilderling et al. (2005) investigated a 2289 cases United Kingdom questionnaire survey cohort study and indicated that maternal smoking is positively

associated with children (7-8 years old) wheezing (OR=1.90, 95% CI: 1.06, 3.39) and children-adolescent (7-8 years old and 15-18 years old) wheezing (OR= 2.18, 95% CI: 1.15, 4.14). Furthermore, they found that exposures to gas heating and gas cooking may increase the risk of children and adolescent wheezing, although the adverse effect of gas burning is inferior to that of smoking. Lin and colleagues reviewed 43 tobacco smoke-tuberculosis (TB) or indoor air pollution-TB papers and found that indoor tobacco smoking may increase the risk of TB infection (Lin, Ezzati and Murray 2007). In 1970s and 1980s, researchers reported the association between indoor burning-related air pollution and the prevalence of children respiratory disease (Honicky, Akpom and Osborne 1983, Melia et al. 1977). See and Balasubramanian (2006) explored the relationship between Chinese cooking style (gas stove coking with stir-frying method in a wok) and suspending concentrations of $PM_{2.5}$ and metals. They found the average $PM_{2.5}$ and metals concentrations during cooking hours increase significantly, which are 11.7 and 10.4 times higher than those during non-cooking hours, respectively. Their findings support that the long-term cooking exposure may increase health risk.

Health effects of roadway/traffic PM exposure attract extensive research interests. An 8-year cohort study found that children who live near to major roads have an inferior lung development than those who live away from major roads (Gauderman et al. 2007). The California Teachers Study investigated the monthly PM exposure for about 45000 females between 2002 and 2007. The $PM_{2.5}$ exposure was found to be associated with increased cardiopulmonary, pulmonary, ischemic heart disease, and all non-traumatic causes mortality (Ostro et al. 2010). Edwards et al. (2006) initiated a lung cancer case-control study and measured the life course exposure for heavy industry ambient air

pollution in Teesside, England. They took residents who lived within a range of 5km of

heavy industry for more than twenty five years as life course exposure objects. They

found that the association between industrial air pollution and women lung cancer is

significant (age and confounding factors adjusted OR= 1.83, 95% CI: 0.82, 4.08).

Health Effects of Other Air Pollutants

NO_2 is found to be associated with lower respiratory tract infections and lung

damage. A recent indoor NO_2 exposure health effect study for non-atopic children

reported high indoor NO_2 concentration (29.8 ppb on average) is associated with children

asthma attack (RR=1.75, 95%CI=1.10-2.78) and peak flows rate (RR=1.46,

95%CI=1.07-1.97) (Kattan et al. 2007).

Health effects of NO_2 are related to both exposure concentration and exposure

duration. Latza, Gerdes and Baur (2009) reviewed 214 NO_2 health effects studies that are

published during 2002-2006. They found that 1) very-short-term high NO_2 exposure (1

hour mean<$200\mu g/m^3$) may not have adverse health effects, 2) short-term low NO_2

exposure (24 hour mean<$50\mu g/m^3$) may increase respiratory morbidity and mortality, and

3) long-term low NO_2 exposure (annual mean<$40\mu g/m^3$) may also increase respiratory

diseases and mortality.

Samoli et al. (2007) investigated CO mortality in 19 European cities. They found

that for every $1mg/m^3$ (two day mean value) CO increase, the cardiovascular mortality

and the total mortality increase 1.25% (95%CI=0.003–0.022) and 1.2% (95%CI=0.006–

0.018) respectively. An Italy study reported that CO can impair the function of lung of

adults who have asthma history (Canova et al. 2010). They found that for every $1mg/m^3$ CO increase, peak expiratory flow (PEF) of samples decreases 2.6% to 2.8%.

There are several studies relevant to other and unexplained indoor source air pollution. Gaffin and Phipatanakul (2009) indicated that HDM, pet, mold, cockroach, and mouse may cause asthma attack. Indoor microorganisms such as fungi and bacteria emit microbial VOCs, which can irritate eye and upper respiratory tract (Korpi et al. 2009).

Multiple air pollutants may have comprehensive health effects. For example, Andersen et al. (2008) found that the multiple ambient air pollutants such as PM_{10}, NO_2, NO_x, and CO can simultaneously trigger to infants' wheezing symptoms.

<center>Air Quality Index</center>

Air quality index (AQI) or called as Air pollution index (API) is a positive number that is used to indicate the degree of air pollution and potential air pollution health effects. AQI standard varies by nation. In the U.S., based on five major air pollutants, i.e., ground-level O_3, $PM_{2.5}$, PM_{10}, CO, NO_2, and NO_x, the EPA calculates AQI to report to public air quality (EPA 2010c). EPA classified AQI into six color-coded levels, as reported in Table 2.3 (EPA 2009b). Local and national AQI (such as $PM_{2.5}$, O_3, and $PM_{2.5}$-O_3 combined) reports and forecasts are updated hourly (AIRNow 2010b, EPA 2010a) (see Equation 2.15).

$$I = \frac{I_h - I_l}{B_h - B_l}(C - B_l) + I_l \qquad \text{Equation 2.15.}$$

where I is the AQI value, C is the air pollutant concentration, B_h is the high breakpoint ($\geq C$), B_l is the low breakpoint ($\leq C$), I_h is the high AQI limit corresponding to B_h, I_l is the

low AQI limit corresponding to B_l. Breakpoints for the AQI (B_h and B_l) are available in the breakpoint table (EPA 2009b).

Table 2.5. The U.S. AQI Standard.

AQI	Health concern	Color	Explanation
0-50	Good	Green	Clean air, no health risk
51-100	Moderate	Yellow	Light air pollution, little health risk
101-150	Unhealthy for sensitive groups	Orange	Only sensitive groups are affected
151-200	Unhealthy	Red	Unhealthy air for everyone
201-300	Very Unhealthy	Purple	Serious health effects for everyone
301-500	Hazardous	Maroon	Severe adverse health effects, even death

Source: EPA, 2009.

AQI maps, i.e., maps covered with AQI color information layers, are usually used for AQI reporting and forecasting. For example, a public web site – WWW.AIRNOW.GOV provides near real-time hourly AQI maps for the U.S. and AQI readings for major U.S. cities (see Figure 2.5).
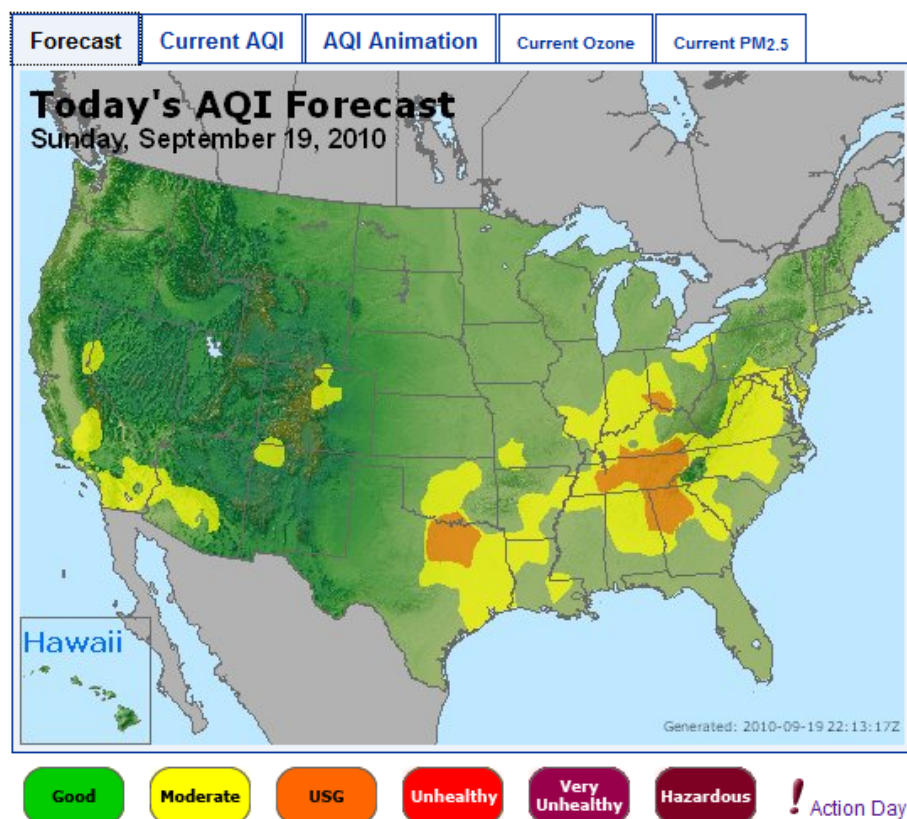
Figure 2.5. National PM$_{2.5}$-O$_3$ Combined AQI Forecast on September 19th, 2010.

Source: AIRNow, 2010.

AQI maps provide a good visualization of national / state air quality. However, when they are applied to personal exposure visualization, they have two drawbacks. First, public AQI maps only show AQIs on city level. Their low spatial resolutions are not suitable for visualizing personal exposure to air pollution. Second, AQI maps are 2D maps, which mean that only AQIs at one specific time point or average AQIs over a period of time are shown in one map. Temporal information is missing.

CHAPTER III

STUDY AREA

Houston, Austin, and San Antonio are the three selected Texas cities for this dissertation research (see Figure 3.1). Houston is situated in the southeast Texas; Austin and San Antonio are situated in the central/south-central Texas. According to the U.S. census (2010), Houston, Austin, and San Antonio are among largest cities in the U.S. in 2009 as reported in Table 3.1.

The air pollution conditions in these three cities are different (see Figures 3.2, 3.3, and 3.4) (EPA 2010a). Houston is a notorious heavily polluted city because of its numerous oil and petrochemical industries and large population. According to the ALA (2010), Houston ranks the seventh among the most O_3-polluted U.S. cities, and the sixteenth among the most $PM_{2.5}$-polluted U.S. cities. Austin is the capital of the state of Texas; it has a lightly polluted air quality because of its limited traditional industry. San Antonio does not have serious air quality problem, but the daily average AQI in San Antonio is higher than that in Austin. Consequently, Austin, San Antonio, and Houston can represent the large subtropical cities with different air pollution levels – the lightly polluted, the moderately polluted, and the heavily polluted (EPA 2010a).
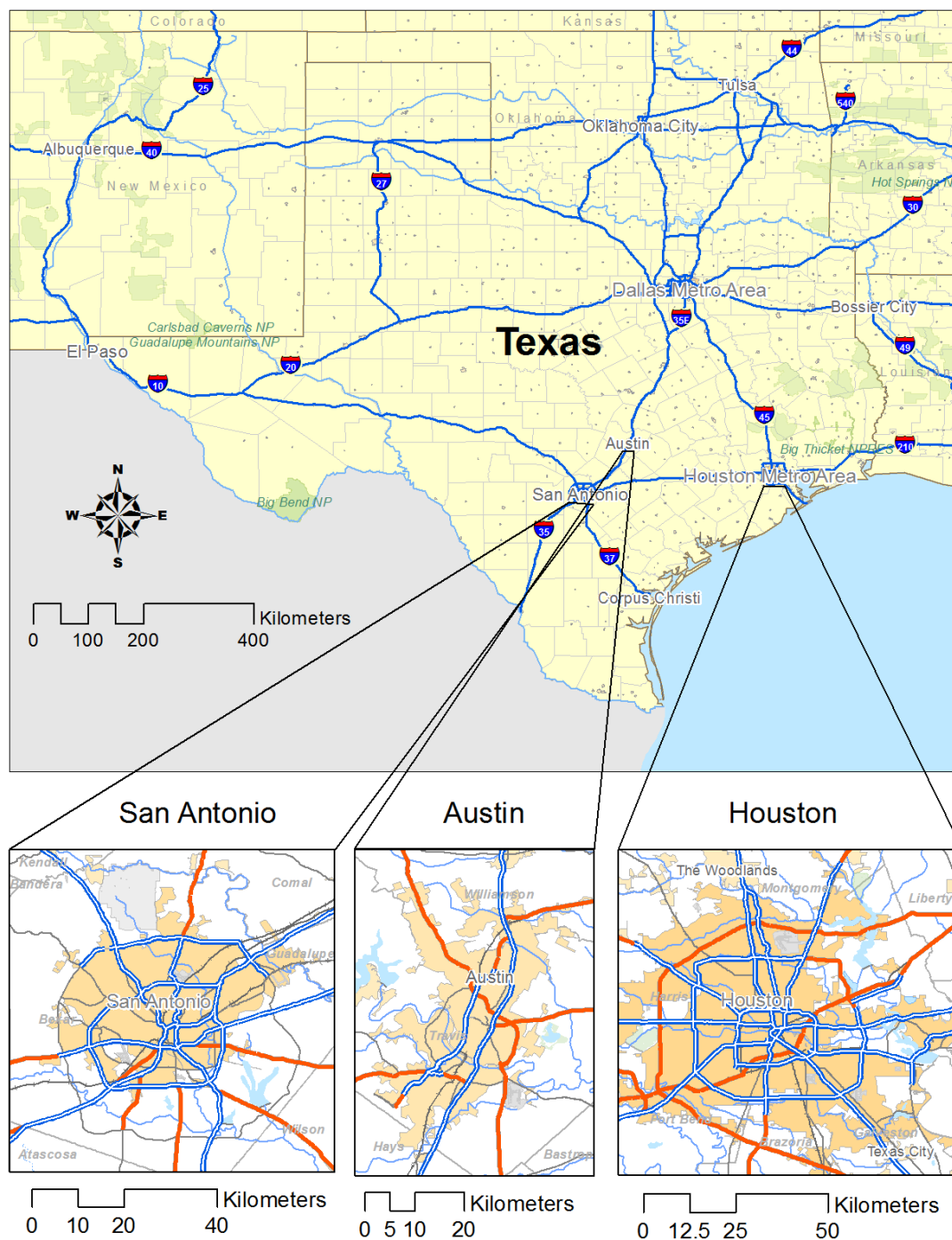
Figure 3.1. The Geographic Locations of Houston, Austin, and San Antonio in

Texas.

Source: U.S. Census, 2010

Table 3.1. Basic Area, Population, and Air Pollution Conditions of Houston, Austin, and San Antonio.

	Houston	Austin	San Antonio
Area (mi^2)	656.3	296.2	412.1
Population (million)	2.26	0.79	1.37
State rank by population	1	4	2
National rank by population	4	15	7
County	Harris	Travis	Bexar
Air pollution condition	Heavily polluted	Lightly polluted	Moderately polluted
Outstanding air pollutants	$PM_{2.5}/O_3$	$PM_{2.5}$	$PM_{2.5}$
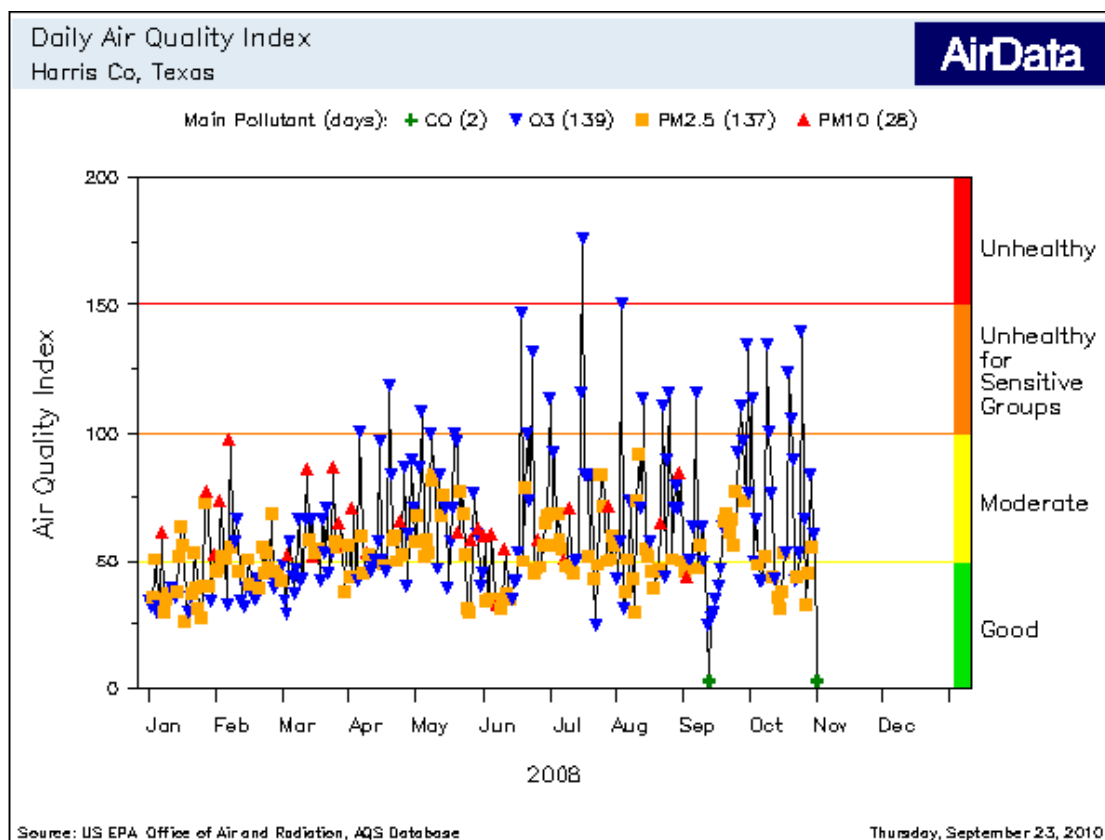
Figure 3.2. Daily AQI of Harris County (Houston), Texas in 2008.

Source: EPA, 2010a.
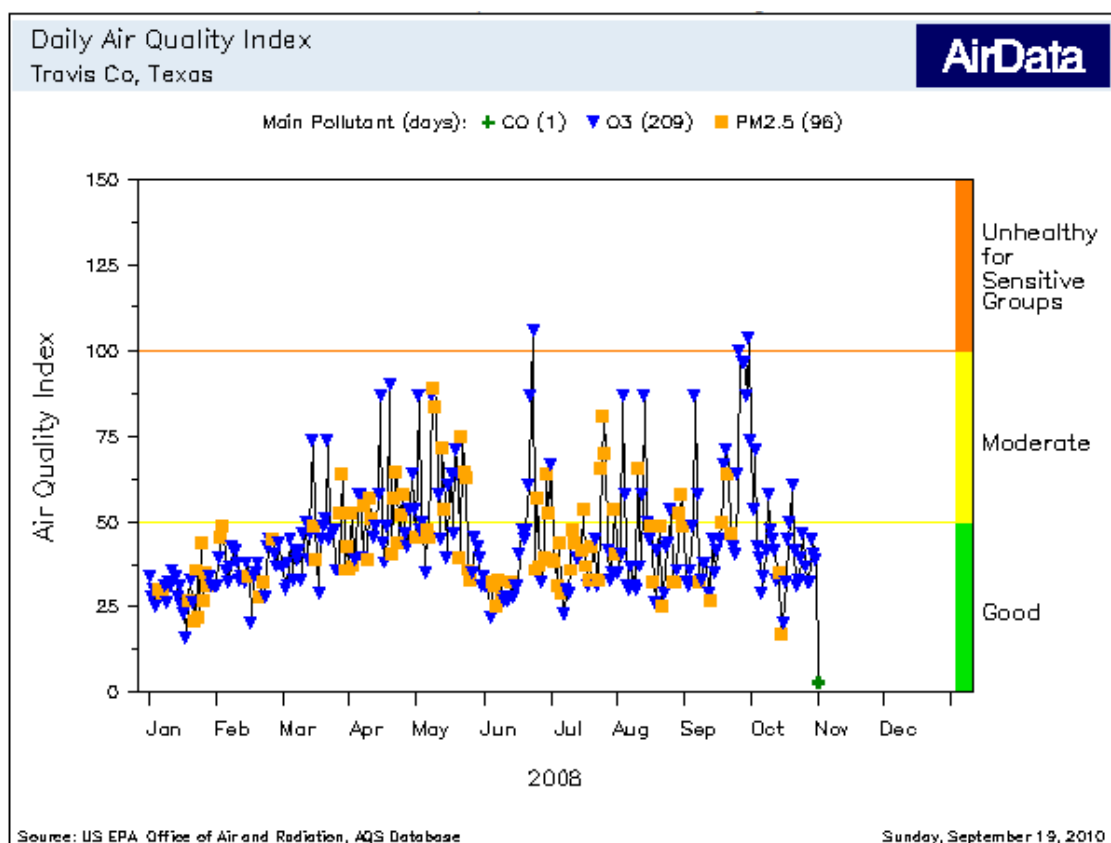
Figure 3.3. Daily AQI of Travis County (Austin), Texas in 2008.

Source: EPA, 2010a.
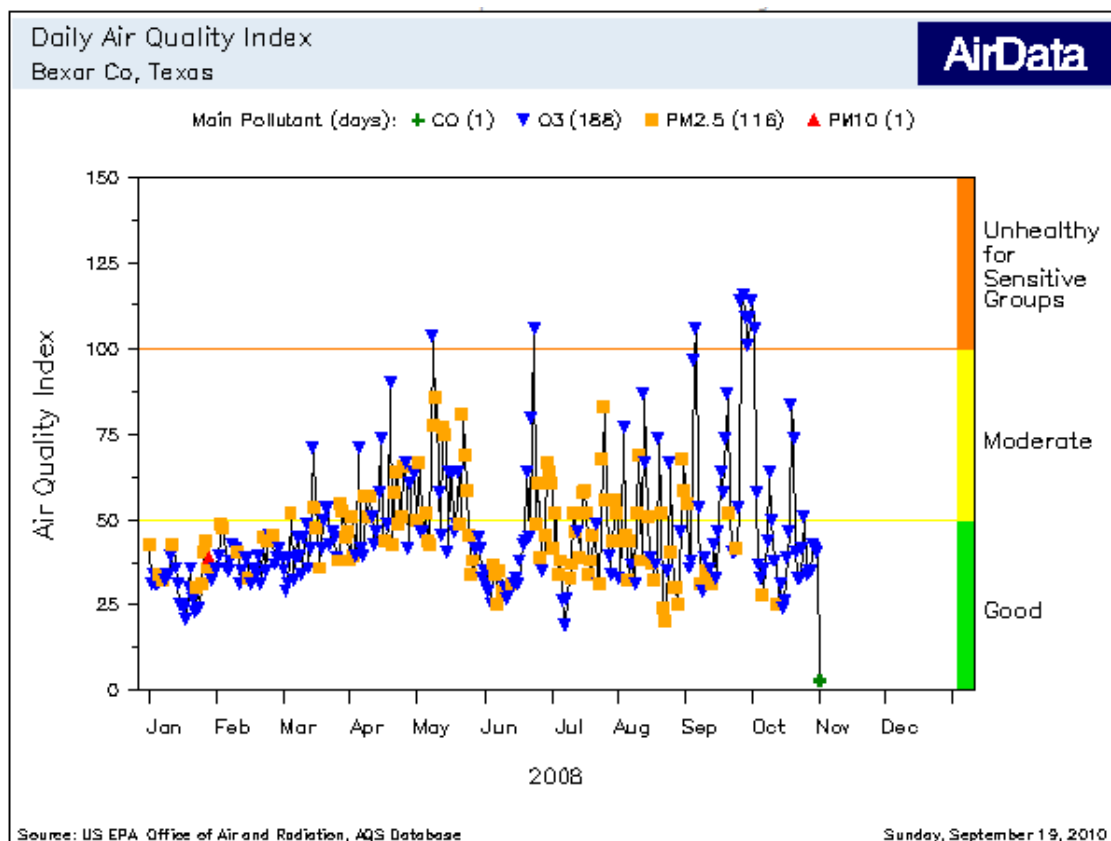
Figure 3.4. Daily AQI of Bexar County (San Antonio), Texas in 2008.

Source: EPA, 2010a.

CHAPTER IV

RESEARCH FRAMEWORK AND RESEARCH DESIGN

Research Framework

This dissertation research focuses on investigating the individual air pollutant (i.e., O_3) exposure by considering the individual travel behavior. So the research framework has three concerns – the space-time air pollution scenarios, the individual travel behavior, the individual-based air pollution exposure and intake (see Figure 4.1).

```
┌─────────────────┐
│ Individual daily│
│   activities    │
└─────────────────┘

┌─────────────────┐        ┌─────────────────┐        ┌─────────────────┐
│ Space-time air  │        │ Individual-based│        │ Individual-based│
│   pollution     │   →    │  air pollution  │   →    │  air pollution  │
│   scenarios     │        │ exposure models │        │  intake models  │
└─────────────────┘        └─────────────────┘        └─────────────────┘

┌─────────────────┐
│Individual travel│
│  trajectories   │
└─────────────────┘

┌─────────────────┐
│   Individual    │
│    physical     │
│   conditions    │
└─────────────────┘
```
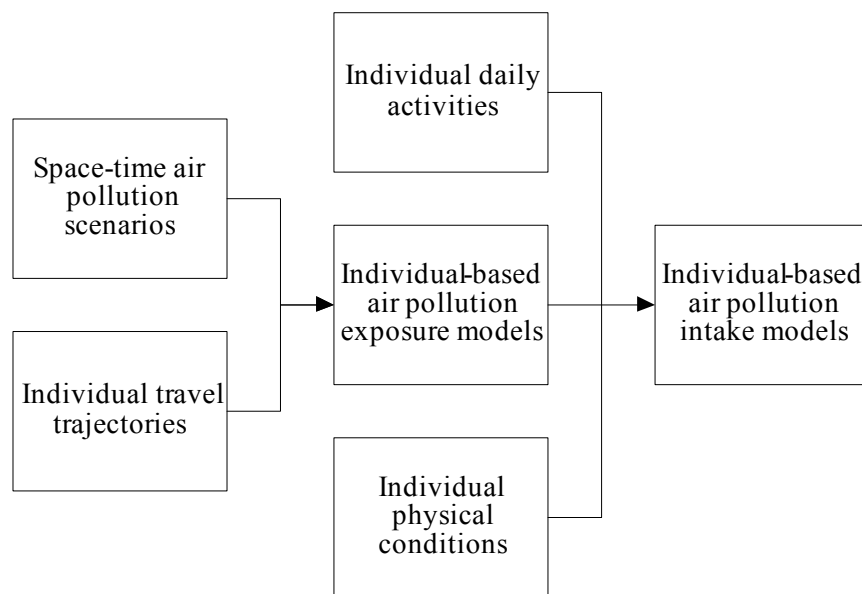
Figure 4.1. The Research Framework of the Dissertation.

Research Design

Based on the research framework, the research design includes three major blocks: development of near real-time space-time air pollution scenario cubes, individual real-time space-time behavior 3D mapping, and integrating space-time cubes and space-time behaviors to develop the pseudo individual near real-time air pollution monitoring model, see Figure 4.2 for the detailed process of developing the pseudo individual near real-time air pollution monitoring and dose simulation model.

The content and process of the research design are:

1) Data involving human participant's individual physical condition and main indoor environment air conditions will be collected from volunteer interview and travel diary.

2) Hourly outdoor air pollution raw data will be downloaded from the EPA air pollution monitoring web site.

3) Regional indoor-outdoor microenvironment map will be generated from land use / land cover data.

4) Regional near real-time space-time air pollution scenario cubes will be constructed based on main indoor environment air conditions, hourly outdoor air pollution raw data, and indoor-outdoor microenvironment map.

5) Individual real-time space-time behavior data, including travel trajectories, stops, speeds, and accelerations, will be obtained by a handheld GPS navigator.

6) The Pseudo Individual near Real-time Air pollution Monitoring (**PIRAM** in short) model will be developed by integrating space-time air pollution cubes and individual travel trajectories.

7) The ground truth data for individual air pollution exposure corresponding to the selected space-time trajectories will be obtained by using portable air pollution monitor/sampler to validate the PIRAM model.

8) The integrated Pseudo Individual near Real-time Air Quality Index (**PIRAQI** in short) model is generated from the PIRAM model by converting estimated individual air pollution exposure levels to the AQI values using the AQI calculator.

9) Participant's real-time air intake volume per minute is decided by individual physical condition and daily physical activities, which will be estimated by analyzing travel diary and GPS collected data (i.e., stops, speeds, and accelerations).

10) The integrated Pseudo Individual near Real-time Air pollution Dose Simulation (**PIRADS** in short) model is generated by integrating the PIRAM model and participant's real-time air intake volume per minute.
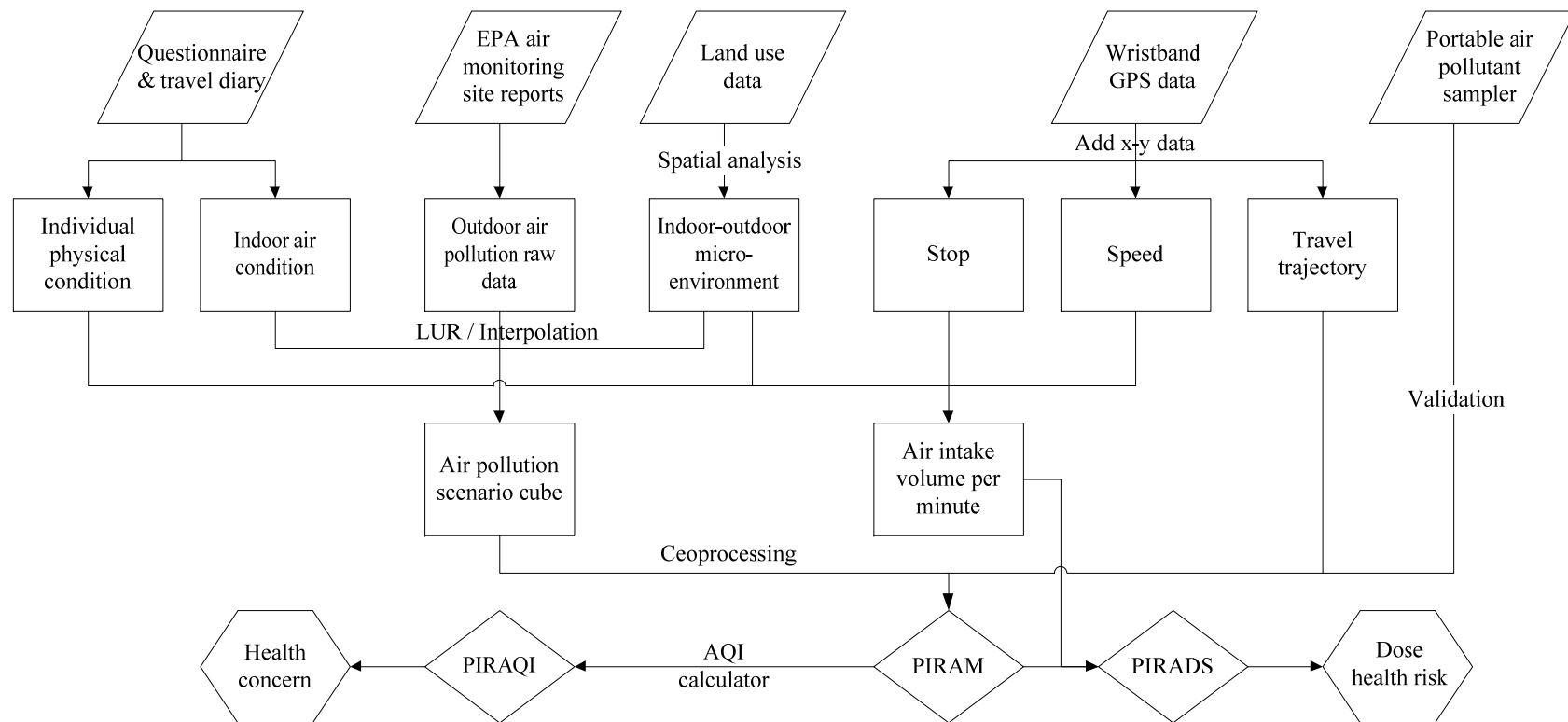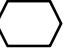
Figure 4.2. The Process Flowchart of the Pseudo Individual Near Real-Time Air Pollution Modeling.

Graphic symbols: initial data - ⬰ ; intermediate data - ▢ ; result models - ◇ ; health effect profile - ⬡ .

Near Real-Time Space-Time Air Pollution Scenario Cube Design

In the early 1970s, Hägerstrand proposed a space-time cube to integrate space and time together for the purpose of analyzing life histories of people and how they interact (Hägerstrand 1970). In his space-time cube, the base is the traditional 2D geographical space, while the height is used to represent time. This way, people's life trajectory can be visualized across space and through time in this space-time cube. However, due to computational limitation, Hägerstrand's space-time cube was restricted to conceptual level until the recent years start seeing its adoption by GIS researchers for visualization (Kraak 2003) as well as analysis purposes (Demšar and Virrantaus 2010, Gatalsky, Andrienko and Andrienko 2004).

I propose to extend Hägerstrand's space-time cube from the traditional geospace-time cube to a specific air pollution cube in space-time dimensions. A space-time air pollution scenario cube integrates the air pollution scenarios into a three-dimensional space-time cube. The base of this cube describes the spatial variation of air pollution across a traditional 2D space; the height dimension represents time so that, as time progresses, the change of air pollution for each location within the base 2D space is continuously represented in the cube at the corresponding time. On the operational level, depending on the time resolution of air pollution scenarios, an air pollution cube consists of a series of component time layers and reveals the dynamic change of air pollution concentration (see Figure 4.3).
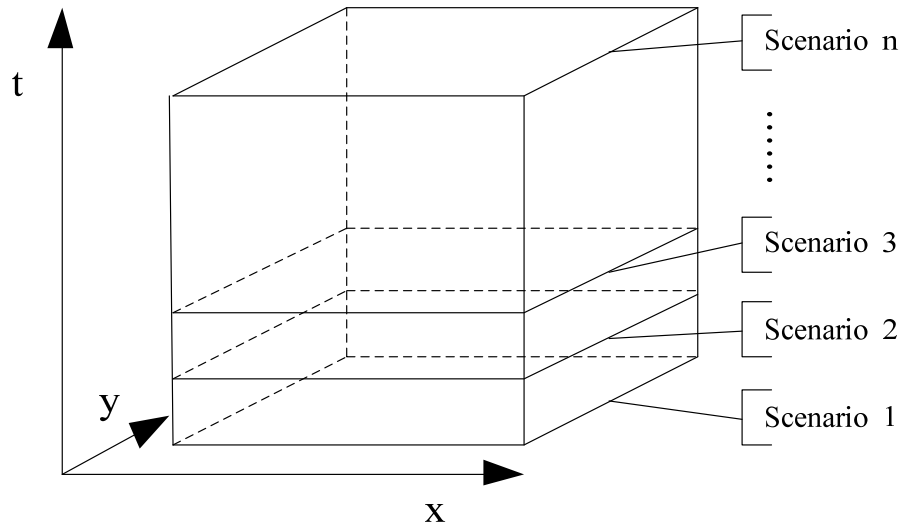
Figure 4.3. Space-Time Air Pollution Scenario Cube.

Note: In the three-dimensional graph, the x-axis and the y-axis represent the air pollution

scenario (spatial dimension) at a certain time stamp; the t-axis represents temporal

dimension. The air pollution scenarios change over time and collectively form the

cube. A series of stacked layers of air pollution scenarios through time constitute a

space-time air pollution scenario cube. For example, if the air pollution scenarios

are recorded every one hour, there are twenty four scenarios (air pollution

component layers) during a day.

A near real-time space-time urban ambient air pollution scenario cube is

constructed when continuous real-time air pollution data are not practically available. It is

made up of a series of component layers (i.e., air pollution scenarios) with equal intervals

of time (Fang and Lu 2011). Each component layer is a near real-time air pollution map,

which is generated using indoor-outdoor microenvironment and field air pollution data, normally subjecting to a certain time delay.

After identifying the preferred methods for air pollution prediction for a time point, the appropriate methods can be used to generate the air pollution component layers for a set of discrete time points throughout the study period. However, the space-time air pollution cube is not finished until the air pollution concentration at any time points can be predicted. This can be achieved using the air pollution concentrations of the two adjacent component layers and the time lag in-between. A comprehensive model to estimate pollution level for this in-between time point should consider not only the air pollution level at the same location from the two adjacent component layers, but also the air pollution level at the surrounding locations from the early time component layer. Furthermore, any known event that happened between that early component layer and the current time point should be considered. Equation 4.1 represents a general model of such (Fang and Lu 2011).

$$C^t = \sum c^t_{i,j} = f\left(c^{t-1}_{i,j}, c^{t+1}_{i,j}\right) + \sum g\left(c^{t-1}_{k,l}\right) + \sum h\left(e^{(t-1,t)}\right) \qquad \text{Equation 4.1.}$$

where C^t is a component layer at time t; $c^t_{i,j}$ is air pollution level at location (i, j) at time t; $c^{t-1}_{k,l}$ is air pollution level at location (k, l), which is within the neighborhood of location (i, j); $e^{(t-1,t)}$ is an event e that occurred between time $t - 1$ and t.

As a starting point for future more advanced exploration, this study takes a simple linear interpolation approach along time line to estimate the O_3 level for a location at a certain time. Equation 4.2 illustrates a linear interpolation for this step. The inter-layer pollution for any location can easily be calculated using raster calculation functions.

Other temporal interpolation functions, when proved sound, can be implemented
following same procedure.

$$
\begin{cases}
C_{n\sim m} = \overline{C}_n + \frac{m-30}{60}\left(\overline{C}_{n+1} - \overline{C}_n\right) & 30 \leq m < 60 \\
C_{n\sim m} = \overline{C}_{n-1} + \frac{m+30}{60}\left(\overline{C}_n - \overline{C}_{n-1}\right) & 0 \leq m < 30
\end{cases}
\qquad \text{Equation 4.2.}
$$

where $C_{n\sim m}$ is the air pollution concentration at hour n minute m, $\overline{C}_n$ is the average air
pollution concentration between hour n and $n + 1$.

Compared to the traditional space-time cube, an air pollution cube is distinctive in
three-folds. First of all, the cube describes the patterns of air pollution across space and
through time compared to the traditional space-time cube where the cube itself is an
empty container to simply provide reference for space and time. Put another way, the air
pollution cube itself provides attribute information (air pollution level) for any reference
point in the space-time cube. Secondly, for the air pollution cube to caring attribute
information, as described above, the cube needs to be "constructed" technically using
spatial and mathematical methods rather than just being conceptualized as the traditional
space-time cube. Thirdly, the air pollution cube has the potential to support individual-
based exposure studies. Connecting to Peuquet's conceptual work on time geography
(Peuquet 1994), the traditional space-time cube describes *where* (space) and *when* (time)
only and leave the description of *what* (object) to the actors that move around in the
container. The air pollution cube, on the other hand, describes *where*, *when*, and *what* (air
pollution level) simultaneously. This allows for the power of an individual-based
description of *what* (in this case, individual level air pollution exposure) when actors are
introduced into the cube. More specifically, the air pollution cube can serve as a
background container where, when discrete locations or continuously trajectories be

"planted" inside, predictions of air pollution exposure can be derived and actions be recommended to control for pollution exposure.

Individual Real-Time Space-Time Behavior Monitoring Design

The individual real-time monitoring provides two groups of data: the individual real-time space-time behavior data and the genuine individual real-time air pollution exposure data. The individual real-time space-time behavior data are indispensable components of the individual near real-time air pollution exposure models. The individual real-time space-time behavior data include the travel trajectories, the moving speeds, and the frequent stops. The individual travel trajectories are used to decide individual's space-time path in the near real-time space-time air pollution scenario cube (see Figure 4.4); the individual moving speeds and the individual frequent stops are integrated with the individual physical conditions and the indoor-outdoor microenvironments to calculate individual real-time air intake volume per minute (see Table 2.2, Equations 2.9 through 2.13).
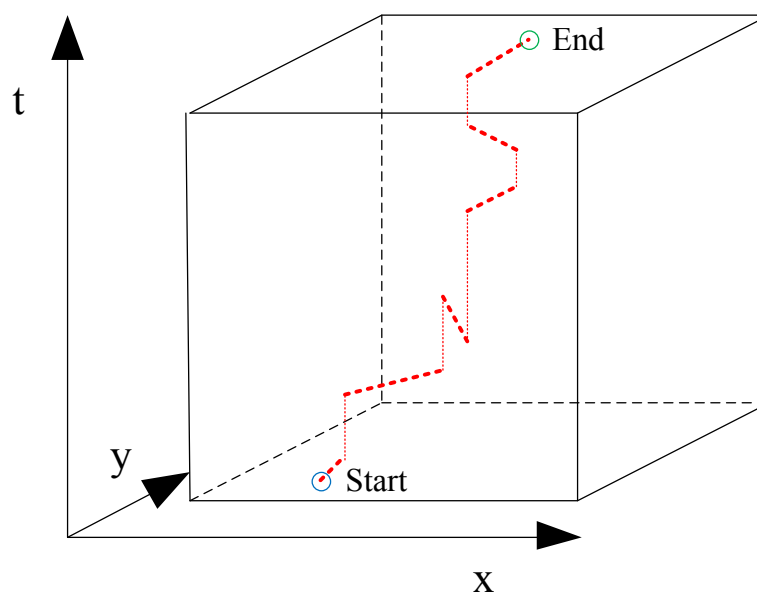
Figure 4.4. An Individual Travels through A 3D Space.

Note: The dashed curve is the virtual space-time travel path of the individual.

A few volunteers in the three selected cities were asked to carry handheld GPS units and portable air pollution samplers (see next section) for a few of days. The Garmin eTrex Vista H handheld GPS navigator was used to record the individual real-time space-time behavior data. It collected data at 10 second intervals (see Figure 4.5). The volunteers were asked to write a travel diary to validate GPS recorded travel information.

Figure 4.5. Garmin eTrex Vista H Handheld GPS Navigator.

Indoor-Outdoor Microenvironment

Indoor-outdoor microenvironment was used in this dissertation for two specific purposes. First, indoor-outdoor microenvironment was integrated with main indoor environment air conditions and hourly outdoor air pollution raw data to construct regional near real-time space-time air pollution scenario cubes. Second, indoor-outdoor microenvironment was integrated with the individual moving speeds, the individual frequent stops, and the individual physical conditions to calculate individual real-time air intake volume per minute.

Individual Real-Time Air Pollution Exposure Monitoring Design

The genuine individual real-time air pollution exposure data is the true real-time ambient air pollution concentration (i.e., the ground truth data). The BW GasAlert Extreme single gas detector (O_3) with 10 ppb increments was used as the air pollution sampler (see Figure 4.6). It collected data at 10 second intervals.

Figure 4.6. BW GasAlert Extreme Single Gas Detector (O_3).

PIRAM, PIRAQI, and PIRADS

Based on the near real-time space-time air pollution scenario cube (see the details in Chapter 5) and the individual real-time space-time behavior monitoring data (see the

details in Chapter 6), the integrated Pseudo Individual near Real-time Air pollution

Monitoring (**PIRAM** in short) model will be generated (see Figure 4.7). An individual's

air pollution exposure at any time point within the cube can be estimated by intersecting

the individual's space-time path with the horizontal component layers (i.e., scenarios) and

of the cube and applying Equation 5.2.
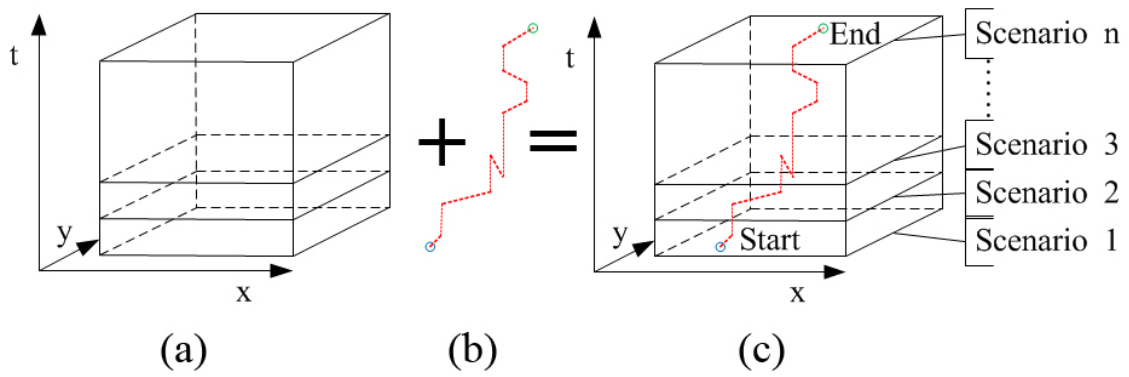
Figure 4.7. Integrating (a) the Near Real-Time Space-Time Air Pollution Scenario

Cube and (b) the Individual Real-Time Space-Time Behavior to Construct (c) the

Pseudo Individual Near Real-Time Air Pollution Monitoring Model.

When the individual air pollution exposures by the PIRAM model are converted

to the AQI values using the AQI calculator (AIRNow 2010a), the integrated Pseudo

Individual near Real-time Air Quality Index (**PIRAQI** in short) model is generated from

the PIRAM model. The PIRAQI model applies AQI values instead of air pollution

concentrations to depict the individual air pollution exposure. So it has good visual

effects and can effectively profile individual air pollution health concerns.

When the PIRAM model is integrated with the individual real-time air intake volume per minute, the integrated Pseudo Individual near Real-time Air pollution Dose Simulation (**PIRADS** in short) model is generated. The PIRADS model can portray individual real-time air pollution exposure doses such as daily exposure dose, hourly exposure dose, on-site exposure dose, and peak concentration exposure dose. Recent studies have reported that the intake of O_3 is associated with the health risks (Marshall et al. 2006). Because the PIRADS model can provide the detailed inhaled air pollutant dose, it is suitable to profile individual real-time air pollution health risk.

Principles

Several important principles are relevant to this dissertation research.

Individual-based near real-time air pollution measure is the first emphasis of this dissertation research. Different from the conventional place-based air pollution measures, this research takes individuals as measuring objects. At the same time some data are obtained through place-based methods, but are coupled with individual components. For example, the air pollution scenarios are acquired through place-based approaches.

Human travel behavior is the second emphasis. This dissertation research does not take all human travel behaviors into consideration. Two criteria for human travel behavior selection are 1) these travel behaviors need to be relevant to air pollution exposure and 2) only representative behaviors that are closely related to air intaking are selected. Individual travel-related physical activities, travel trajectories, stops, moving speed, and accelerations are selected human travel behaviors.

In this research, it is critical to **quantify** the individual near real-time air pollution exposure. All data (such as individual locations and air pollution concentrations) need to be quantified to support the monitoring models.

Repeatability is a criterion for testing effectiveness of the monitoring models. No interventions are applied in this research. The individuals and the air pollutant components are analyzed independently. Portable air pollution sampler recorded data, i.e., the ground truth data, are used to test the repeatability of the monitoring models.

CHAPTER V

DEVELOPMENT OF SPACE-TIME AIR POLLUTION SCENARIO CUBES

Data Source

EPA Air Monitoring Site Reports

EPA provides thousands of air monitoring sites nationwide for the purpose of outdoor air pollution conditions on site measuring. In Texas, there are about 237 EPA air monitoring sites managed by the Texas Commission on Environmental Quality (TCEQ) that provide hourly air and weather parameters such as O_3, CO, $PM_{2.5}$, PM_{10}, NO_2, SO_2, wind speed, wind direction, and outdoor temperature (TCEQ 2010). Although there is a three-hour lag for data transmission and display, the TCEQ web site can provide the approximately real-time ambient air pollutant concentration data. The information of the dissertation-research-involved EPA air monitoring sites is reported as Table 5.1 and Figure 5.1.

Table 5.1. The EPA Air Monitoring Sites Managed by the TCEQ in the Houston Region, the Austin Region, the San Antonio Region in 2010.

Region	Total	CO	NO_2	O_3	$PM_{2.5}$	PM_{10}	SO_2	TSP
Houston	47	8	21	46	11	0	8	0
Austin	9	1	4	8	4	0	2	0
San Antonio	18	3	5	11	7	1	1	5

Data source: TCEQ, 2010.
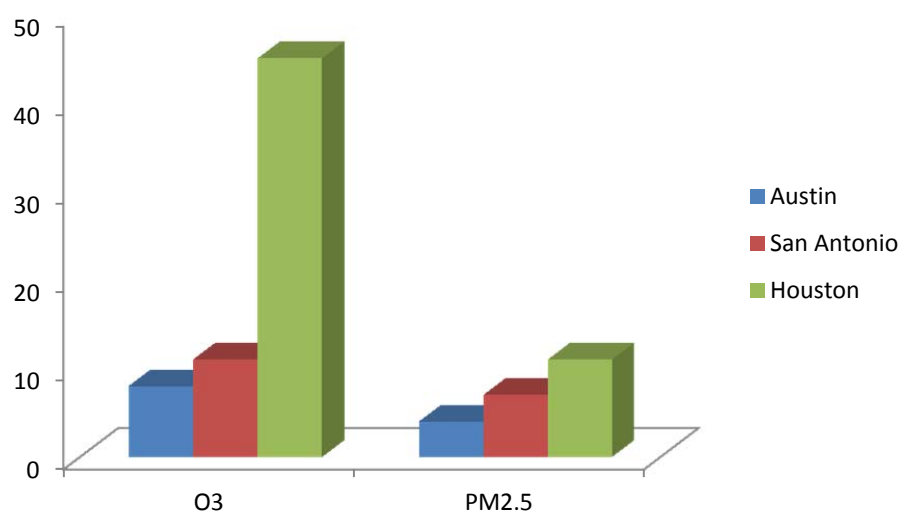
Figure 5.1. The O_3 and the $PM_{2.5}$ Air Monitoring Sites in the Houston Region, the Austin Region, the San Antonio Region in 2010.

Data source: TCEQ, 2010.

In this dissertation research, the initial outdoor air pollution concentration data were collected through place-based measures from the EPA air monitoring sites online reports for several reasons. First, although the portable air pollution sampler can collect fine individual real-time ambient air pollution concentration, its high cost, low reliability, and the poor end-user experience make it a challenge for the research. Second, the EPA air pollution monitoring sites reports are the only public source that can provide appropriate near real-time air pollution data. Other data sources have longer delay and cannot be used in the near real-time on-site research. For example, National Emission Inventory (NEI) Database air pollution data has a three-year lag (EPA 2008a). Last, data collected by the EPA air pollution monitoring sites are in standard format and can be easily processed.

Land Use / Land Cover Data

Through processing EPA air monitoring site data, the hourly outdoor air pollution conditions are generated. The next step is to build the indoor-outdoor microenvironment. Based on the land use / land cover data, the indoor-outdoor microenvironment maps for each city are created. The land use / land cover data are available on web sites such as the Capital Area Council of Governments' Information Clearinghouse (CAPCOG 2010), the City of San Antonio – Geographic Information Systems (COSA 2010), the City of Houston GIS Release (COHGIS 2010), and the Houston-Galveston Area Council (H-GAC) (2010).

According to the indoor-outdoor air pollution exchange theory, indoor air pollution includes indoor-generated and outdoor-penetrated air pollution. Data from the

individual questionnaires, such as the household smoking habits, the household cooking habits, and the areas of major indoor microenvironments, are used to decide indoor-generated air pollution. For example, the household smoking habit is related to the indoor-generated $PM_{2.5}$; the smoking-generated $PM_{2.5}$ concentration can be quantified by the number of cigarettes that are smoked indoors and the volume of the building. Other indoor air pollution (such as cooking smoke) will be also considered. Outdoor-penetrated air pollution is related to the ACH, which are reported in the literature (Yamamoto et al. 2010).

Based on this information, hourly outdoor air pollution scenario layers and indoor-outdoor microenvironment maps, a series of hourly indoor-outdoor-integrated air pollution maps are generated. These maps are component layers for the near real-time space-time air pollution scenario cube. In the research, there will be three such cubes – one near real-time O_3 cube for each selected city.

Houston Air Pollution Cube

In the Houston region, there are 46 EPA O_3 monitoring sites (see Figure 5.3). In other words, the number of monitoring sites is enough for the LUR modeling. Consequently, two groups of methods were used to predict outdoor air pollution concentration at non-sampled locations in the Houston region – discrete modeling methods (e.g., the land use regression (LUR) modeling) and continuous modeling methods (e.g., the spatial interpolation approaches) (Ryan and LeMasters 2007). The air pollution concentration at a time between any two adjacent component layers can be estimated based on the temporal trends at a location and its surroundings.

Two days (December 27th & 28th, 2010) diurnal ambient ozone (O_3) scenarios of the Houston region were modeled to build the Houston air pollution cubes. Through an online reporting system, EPA air monitoring sites provide near real-time (i.e., a three-hour lag) hourly averaged air and weather data such as O_3 level, wind information, relative humidity, and outdoor temperature (see Figure 5.2). These data were used as the major air pollution data source. These EPA monitoring sites were randomly divided into two subsets – the training data sets (thirty six sites for model building) and the test data sets (ten sites for model validation). Other data used for this study included land use / land cover data, transportation data, meteorological data, demographic data, and other geographic data. They were obtained from the web sites of the U.S. Census Bureau, the United States Naval Observatory (USNO), the Texas Natural Resources Information System (TNRIS), the Texas Department of Transportation (TxDOT), the TCEQ, the WebGIS, the Environmental Systems Research Institute (ESRI), the H-GAC, and the COHGIS.

Figure 5.2. The EPA Air Monitoring Sites Managed by the TCEQ in the Houston

Region in 2010.

Data source: TCEQ, 2010.

LUR Modeling

Hourly outdoor near real-time air pollution scenarios in the Houston region were built through the LUR modeling. In the LUR model, air pollution is a dependent variable; road network, road type, traffic count, elevation, population density, solar irradiance, temperature, precipitation, wind direction, and wind speed are variables. There is a multiple linear relationship between dependent variable and independent variables (Ryan

et al. 2007b). Through a multiple linear regression with SPSS, the parameters will be decided. Based on the parameters and the variables, the hourly outdoor air pollution exposure maps will be calculated.

Considering the local conditions of Houston, this research selected 19 independent variables for the LUR model. These independent variables were categorized into 6 classes and reported in Table 5.2 – physical geography, road, traffic, population, land cover, and meteorology. The distance to ocean for each EPA site was computed because the large body of water may affect the dispersion of air pollutants (Moore et al. 2007). The distance to power plants and/or refineries is important as these facilities form the major pollution sources in Houston. Roads are considered as they serve as indications of traffic, which is a well-known source for O_3. Annual Average Daily Traffic (AADT) count data in 2009 were obtained from the TxDOT and used as a direct representation of traffic condition. The 2009 traffic data were used as the data since 2010 were not available for this study. Population density is related to human activities and thus anthropogenic air pollution. The population density on block level was calculated using Census 2000 data.

Table 5.2. All Independent Variables Used in the LUR Modeling for Outdoor O₃

Prediction in the Houston Region.

Variable	Variable definition	Unit	Class
x1	Elevation	m	Physical geography
x2	Distance to Ocean	m	
x3	Distance to the nearest power plants & refineries	km	
x4	Distance to nearest primary road*	km	Road
x5	Distance to nearest secondary and minor road **	km	
x6	Length of secondary and minor road within 600m	km	
x7	Traffic count in nearest major road	10^6/day	Traffic
x8	Block population density	per km^2	Population
x9	Area of urban and built-up land within 150m	km^2	Land cover
x10	Area of agricultural land and forest land within 150m	km^2	
x11	Area of urban and built-up land within 300m	km^2	
x12	Area of agricultural land and forest land within 300m	km^2	
x13	Area of urban and built-up land within 600m	km^2	
x14	Area of agricultural land and forest land within 600m	km^2	
x15	Wind index	----	Meteorology
x16	Resultant wind speed	m/s	
x17	Temperature	F	
x18	Relative humidity	%	
x19	Solar relative radiance	----	

Note: * Primary road: Census feature class code (CFCC) first level categories A1 & A2.

** Secondary and minor road: CFCC first level categories A3 – A7.

Land cover variables measure urban and built-up areas, agricultural land, and forest/woods. Other types of land cover were not considered as they are negligible in size in the study area. Based on the literature (Ryan and LeMasters 2007), we chose buffer sizes of 150m, 300m, and 600m. Meteorological variables included wind index, resultant wind speed, temperature, relative humidity, and solar relative radiance. Wind index indicates the difference between the resultant wind direction and the nearest air pollution emission source direction (McCune and Keon 2002) (Equation 5.1). Data on the hourly resultant wind speed, the temperature, and the relative humidity for each EPA sites were obtained from the EPA online reports. The solar relative radiance was derived from the site's elevation, the sun altitude, and the sun azimuth.

$$w = \frac{1-\cos(\theta-\alpha)}{2}$$

Equation 5.1.

where w is the wind index, θ is the direction from the nearest road or air pollution emission source to the EPA sites (e.g., north=0/360, east=90), α is the hourly resultant wind direction for each EPA sites.

A backward multi-linear regression was conducted for the training data sets to calibrate the parameters for each hourly LUR model and the adjusted coefficients of determination (R^2) reported (see Table 5.3). The significant threshold for the predicting variables was set as 0.05. To validate the LUR models, the root mean square errors (RMSEs) and R^2 between the measured and the predicted values at the test sites were examined. Furthermore, statistics tests were applied to compare the predictions of O_3 pollution level with the actual measurements obtained at the test sites. Depending on the normality of the samples (examined using the Kolmogorov–Smirnov test for normality),

either a paired-sample t-tests or a Wilcoxon signed-rank test was conducted to examine if

the predictions are significantly different from the corresponding observations (see

Tables 5.5 and 5.6).

Table 5.3. Included Predicting Variables for the Hourly LUR Component Layer

Models for Outdoor O_3 Prediction in the Houston Region by the Multiple Linear

Regression Analysis in SPSS.

Model #	Time (date, hr:min)	Predicting variables	Adjusted R^2
1	27, 1:30pm	x4, x6, x9, x10, x11, x12, x13, x17, x19	0.46
2	27, 2:30pm	x1, x2, x8, x9, x19	0.39
3	27, 3:30pm	x4, x6, x9, x10, x11, x12, x14, x17, x19	0.52
4	27, 4:30pm	x1, x4, x6, x9, x10, x17, x19	0.60
5	27, 5:30pm	x1, x2, x4, x5, x6, x9, x11, x16, x19	0.76
6	27, 6:30pm	x1, x2, x3, x5, x6, x11, x13, x17	0.67
7	28, 7:30am	x1, x2, x3, x4, x6, x9, x14	0.69
8	28, 8:30am	x4, x9, x10, x17	0.52
9	28, 9:30am	x1, x2, x9, x11, x17	0.58
10	28, 10:30am	x4, x7, x9, x10, x13, x14, x18	0.55
11	28, 11:30am	x4, x11, x12, x18	0.45
12	28, 12:30pm	x3, x4, x7, x9, x10, x11, x12, x17, x19	0.78
13	28, 1:30pm	x3, x9, x11, x12, x13, x14, x17	0.71
14	28, 2:30pm	x1, x2, x3, x5, x9, x13, x15, x17	0.59
15	28, 3:30pm	x1, x3, x4, x8, x11, x12, x13, x14	0.46
16	28, 4:30pm	x1, x3, x4, x11, x12, x13, x14	0.59

Note: Meanings of the predicting variables are listed in Table 5.2.

Spatial Interpolation

According to the literature, for outdoor air pollution assessment, the LUR

generated discrete maps may be better than the continuous spatial interpolation maps

(Ryan and LeMasters 2007). To test for this, this dissertation research compared the LUR

generated maps with the spatial interpolation maps.

Due to the lack of agreement regarding which spatial interpolation method is the

best for O_3 prediction, this study compares three commonly applied spatial interpolation

methods to predict the hourly outdoor O_3 pollution in the Houston region. These methods

are IDW (power: 2, neighbors: 15), radial basis functions (RBF) (neighbors: 15), and

ordinary kriging with spherical semivariogram. RBF is a spline interpolation method used

in ArcGIS.

These EPA monitoring sites were randomly divided into two subsets – the

training data sets (thirty six sites for geostatistical model building) and the test data sets

(ten sites for geostatistical model validation).

The performance of the three spatial interpolation methods – IDW, RBF, and

kriging was assessed by examining the RMSEs and MEs for the training data sets (see

Table 5.4). The lowest RMSEs for each component layer model were highlighted in bold.

Among the three interpolation methods, IDW generated only 1 prediction with the lowest

RMSE; RBF prediction generated 8 lowest RMSEs; kriging method generated 7 lowest

RMSEs. It should be noted that because of the unexplained errors such as measurement

error and microscale variation, the nugget effect exists in kriging. This echoes the finding

from the *p*-values reported in Table 5.5 – the prediction from IDW is generally not as

good as that from the other two interpolation methods.

Table 5.4. The RMSEs and MEs for the Training Data Sets for Outdoor O$_3$
Assessment Using the 3 Spatial Interpolation Methods – IDW, RBF, and Kriging in
the Houston Region on December 27th & 28th, 2010.

Model #	Time	IDW		RBF		Kriging	
		ME	RMSE	ME	RMSE	ME	RMSE
1	27, 1:30pm	-0.81	3.22	-0.21	3.03	-0.11	**2.88**
2	27, 2:30pm	-0.78	4.43	-0.30	**4.17**	-0.21	4.22
3	27, 3:30pm	-0.95	4.21	-0.52	4.00	-0.17	**3.95**
4	27, 4:30pm	-1.29	4.67	-0.52	**4.27**	-0.26	4.33
5	27, 5:30pm	-1.40	3.86	-0.54	**2.95**	-0.29	3.18
6	27, 6:30pm	-1.03	4.79	-0.60	4.60	-0.31	**4.38**
7	28, 7:30am	-2.01	5.85	-0.90	5.30	-0.33	**5.18**
8	28, 8:30am	-2.04	5.68	-0.36	4.64	-0.26	**4.60**
9	28, 9:30am	-1.01	5.18	-0.40	**5.12**	-0.21	5.46
10	28, 10:30am	-0.97	5.18	-0.39	**4.97**	-0.31	5.23
11	28, 11:30am	-0.98	4.51	-0.48	**4.43**	-0.22	4.62
12	28, 12:30pm	-0.87	3.75	-0.49	3.77	-0.14	**3.60**
13	28, 1:30pm	-0.89	**5.40**	-0.54	5.45	0.01	5.58
14	28, 2:30pm	-0.99	4.03	-0.55	4.08	-0.15	**3.93**
15	28, 3:30pm	-0.63	4.48	-0.19	**4.14**	-0.29	4.37
16	28, 4:30pm	-1.49	4.84	-0.74	**4.23**	-0.44	4.63

Note: The units of the RMSEs and MEs: ppb. For each model, the lowest RMSE across

the different predicting methods is highlighted as bold.

The RMSEs and R^2 between measured and predicted values at the ten randomly

selected test sites were calculated to evaluate the performance of the different

interpolation methods. Furthermore, the paired-samples t-tests and the Wilcoxon signed-

rank tests were applied to evaluate the accuracy of the different interpolation methods

(see Table 5.5s and 5.6).

The Comparison between the LUR Modeling and the Spatial Interpolation Methods

A total of sixteen LUR models were built to generate the hourly component layers

for the space-time air pollution cube. Table 5.3 summarizes the predicting variables and

the adjusted R^2 for each component layer model. The numbers of predicting variables for

these models vary: model #8 and model #11 each has 4 predicting variables, whereas

model #1, model #3, model #5, and model #12 each has 9 variables. The values of

adjusted R^2 ranged from 0.39 to 0.78. Overall, the fitting results of these sixteen hourly

LUR models were good. Table 5.5 reports the RMSEs and R^2 between the measured and

the predicted values at the test sites. The values of the RMSEs of the LUR models ranged

from 2.26 ppb to 5.25 ppb. The accuracy of O_3 predictions across the sixteen models

were assessed using both paired-sample t-tests and Wilcoxon singed-rank tests. The

results are reported in Table 5.6. The *p*-values for all the sixteen LUR models were

greater than 0.05, indicating that the LUR predications at the test sites are statistically

similar to the EPA measured pollution levels.

Table 5.5. The RMSEs and R^2 Between Measured and Predicted Values at the O$_3$

Test Sites in the Houston Region by the LUR Models and the Spatial Interpolation

Methods (unit: ppb).

Model #	Time (date, hr:min)	LUR		IDW		RBF		Kriging	
		RMSE	R^2	RMSE	R^2	RMSE	R^2	RMSE	R^2
1	27, 1:30pm	**3.56**	0.40	5.01	0.01	5.07	0.02	5.11	0.01
2	27, 2:30pm	**2.41**	0.50	3.15	0.19	2.88	0.19	3.15	0.18
3	27, 3:30pm	4.74	0.35	3.61	0.45	**3.23**	0.50	3.39	0.47
4	27, 4:30pm	4.27	0.32	**3.90**	0.27	3.97	0.30	3.99	0.27
5	27, 5:30pm	**2.64**	0.40	5.26	0.15	6.41	0.14	4.99	0.18
6	27, 6:30pm	**2.34**	0.67	3.54	0.55	3.18	0.59	3.20	0.52
7	28, 7:30am	**2.27**	0.69	4.66	0.81	4.07	0.79	4.33	0.71
8	28, 8:30am	5.25	0.66	6.67	0.34	**5.01**	0.47	6.08	0.06
9	28, 9:30am	**2.87**	0.25	5.98	0.71	5.67	0.76	8.65	0.03
10	28, 10:30am	5.05	0.65	3.97	0.78	**3.76**	0.74	4.72	0.37
11	28, 11:30am	3.86	0.47	3.94	0.01	**3.39**	0.16	3.78	0.30
12	28, 12:30pm	**3.25**	0.18	4.27	0.09	3.52	0.51	3.90	0.12
13	28, 1:30pm	**2.26**	0.33	4.16	0.16	4.03	0.16	5.68	0.00
14	28, 2:30pm	**2.81**	0.50	4.45	0.32	4.18	0.47	3.80	0.47
15	28, 3:30pm	**3.06**	0.40	5.16	0.18	6.02	0.07	6.21	0.02
16	28, 4:30pm	3.83	0.39	4.07	0.17	4.22	0.20	**3.63**	0.34

Note: The units of the RMSEs: ppb. For each model, the lowest RMSE across the

different predicting methods is highlighted as bold.

Table 5.6. The Paired-Samples T-Tests and the Wilcoxon Signed-Rank Tests for the Hourly Outdoor O$_3$ Pollution Component Layer Predictions at the Ten Randomly Selected Test Sites in the Houston Region.

Model #	Time (date, hr:min)	p-value			
		LUR	IDW	RBF	Kriging
1	27, 1:30pm	0.249*	0.956*	0.807*	0.755*
2	27, 2:30pm	0.764*	**0.043***	0.121*	**0.040***
3	27, 3:30pm	0.203**	0.096*	0.064*	0.209*
4	27, 4:30pm	0.059**	0.871*	0.426*	0.662*
5	27, 5:30pm	0.207*	0.507*	0.908*	0.973*
6	27, 6:30pm	0.137*	0.053*	0.108*	0.234*
7	28, 7:30am	0.116*	0.433*	0.862*	0.961*
8	28, 8:30am	0.114**	**0.013****	0.068*	**0.044***
9	28, 9:30am	0.713*	0.616*	0.460*	0.445**
10	28, 10:30am	0.478*	**0.021***	**0.031***	0.091*
11	28, 11:30am	0.646**	**0.009****	**0.013****	0.059**
12	28, 12:30pm	0.959**	**0.003***	**0.003***	**0.015***
13	28, 1:30pm	0.268*	**0.024***	**0.034***	**0.028***
14	28, 2:30pm	0.508**	0.158*	0.295*	0.399*
15	28, 3:30pm	0.508**	0.251*	0.386**	0.342*
16	28, 4:30pm	0.285**	0.831*	0.694*	0.417*

Note: The p-values less than 0.05 are highlighted as bold.

* The paired-samples t-test for normally distributed samples.

** The Wilcoxon signed-rank test for non-normally distributed samples.

The normality of the samples was examined using the Kolmogorov–Smirnov test for normality.

The performance of the three spatial interpolation methods – IDW, RBF, and kriging were assessed by examining the RMSEs for the test data sets. Among the three interpolation methods, IDW generated 1 prediction with the lowest RMSE; RBF generated 4 lowest RMSEs; kriging method generated 1 lowest RMSEs. Similar patterns are observed when paired-sample t-tests or Wilcoxon signed-rank tests were applied to compare the predicted values at the test sites with the corresponding observed values. As can be seen from the *p*-values reported in Table 5.6, IDW produced more predictions that are significantly different from the observed values than RBF did.

When comparing the air pollution prediction results from the LUR models and the spatial interpolation methods, both the RMSE values and the statistical tests reveal that LUR models generated better results. The predictions from the LUR models are overall closer to the observed values at the test sites than the predictions from the spatial interpolation methods. The statistical tests show that all the LUR predications are statistically similar to the observed. The RMSE values for the LUR models are generally smaller than those for the spatial interpolation methods. Among the lowest RMSEs (highlighted in bold), ten were from the LUR models, and six were from the spatial interpolation methods. Overall, the LUR models were more accurate than the spatial interpolation methods.

After model validation, the hourly outdoor O_3 pollution component layers for Houston were generated (see Figure 5.3). The ambient O_3 levels in the Houston region ranged from 0 to 65 ppb.

O3 level (ppb)
High : 65
Low : 0

Kilometers
0 10 20 40 60 80

N

Projection: NAD 1983 StatePlane Texas
South Central FIPS 4204
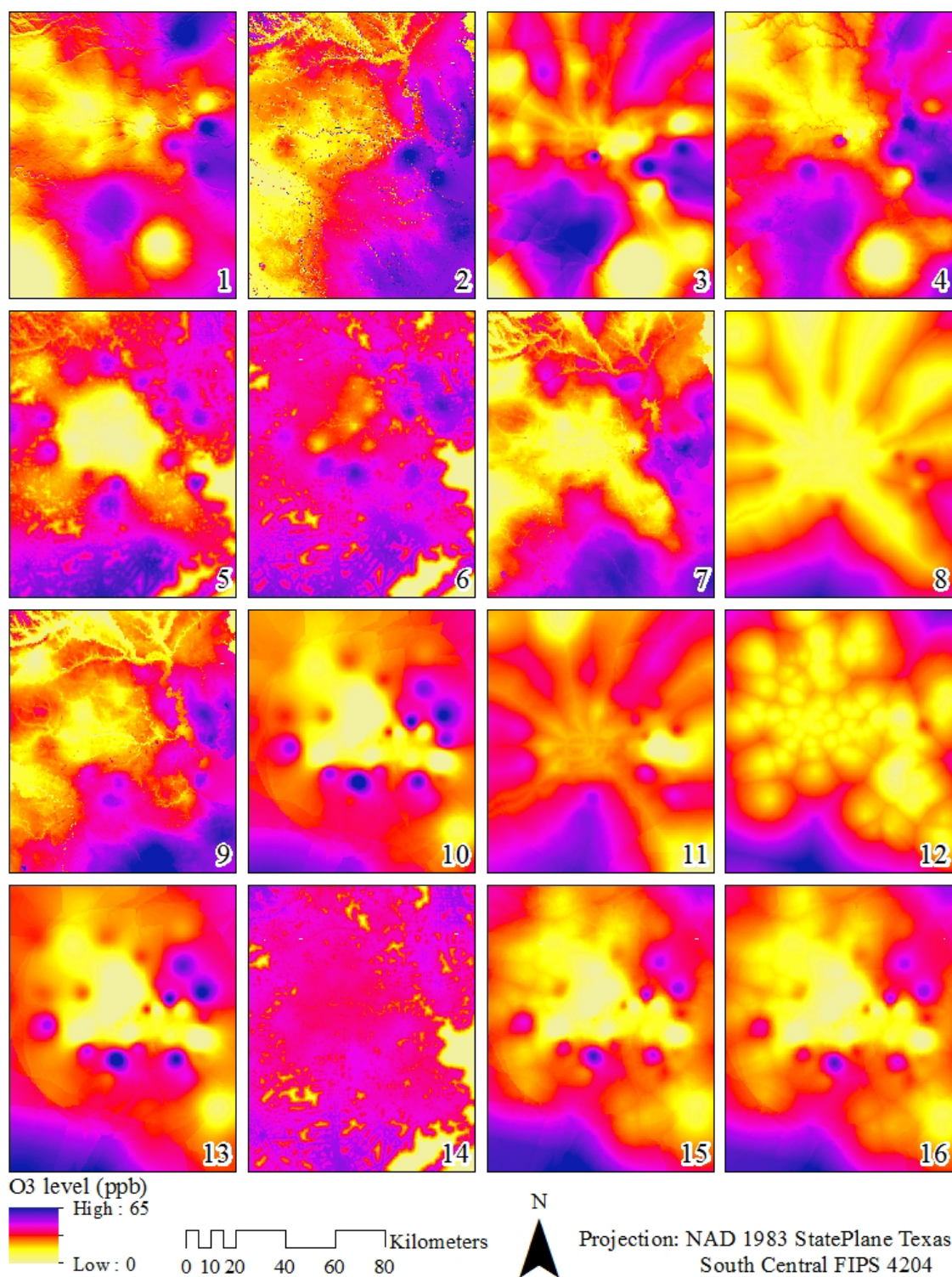
Figure 5.3. The Hourly LUR Component Layers (Model #1 - Model #16) for

Outdoor O₃ Prediction in the Houston Region on December 27th & 28th, 2010.

Indoor-Outdoor Microenvironment

The H-GAC 2008 land cover data set used a ten-category classification: Developed, Higher Intensity; Developed, Lower Intensity; Developed, Open Space; Cultivated; Grassland/Shrub; Forest; Woody Wetland; Herbaceous Wetland; Barren; and Water. In this dissertation, Developed, Higher Intensity land category was assumed to be indoor microenvironment; other nine land categories were assumed to be outdoor microenvironment.

The indoor-outdoor microenvironment was generated based on the H-GAC land cover data and was in raster format, which had a spatial resolution of 30m (see Figure 5.4).
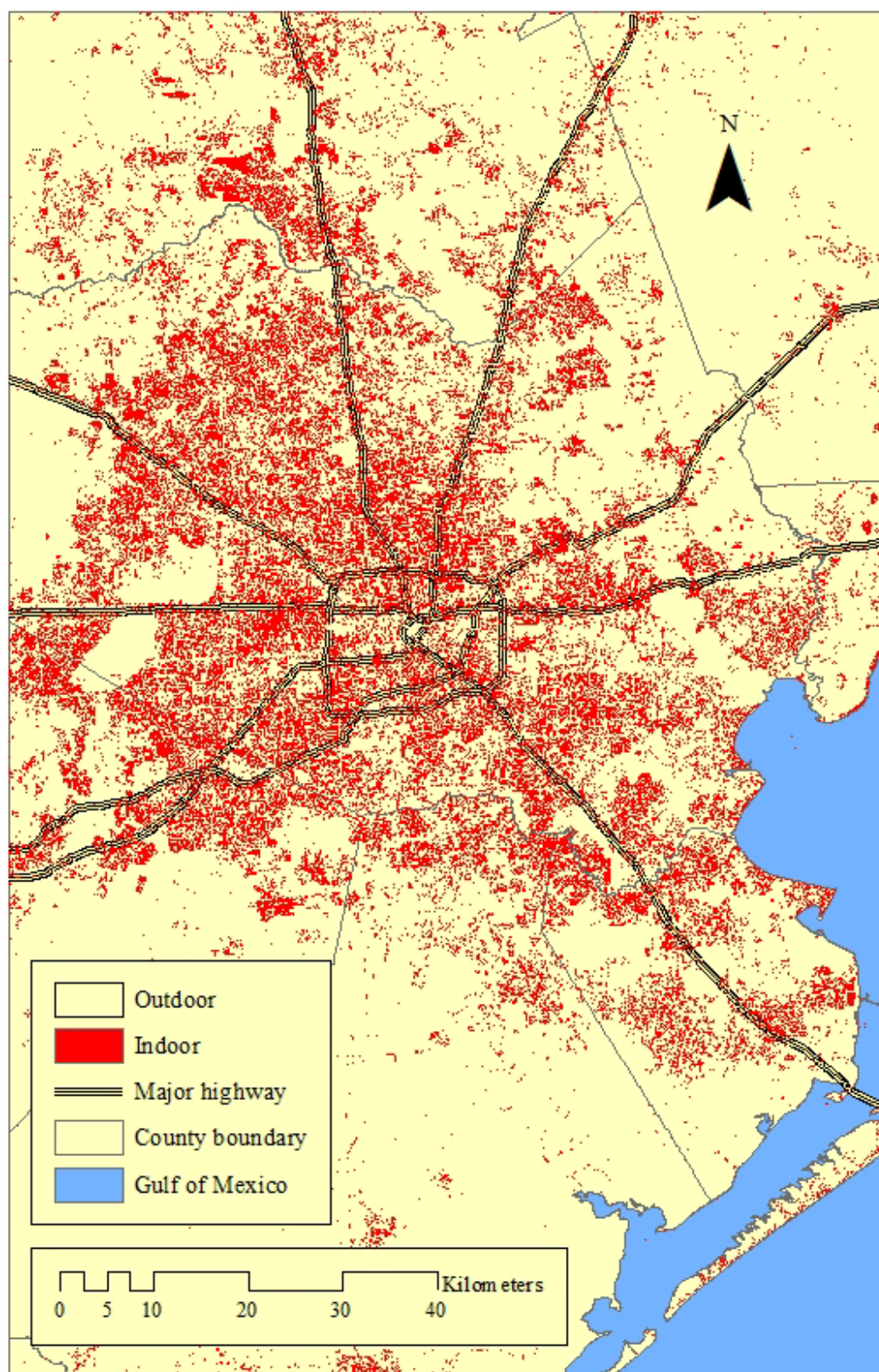
Figure 5.4. The Indoor-Outdoor Microenvironment in the Houston Region in 2010.

Constricting the Air Pollution Cube

Because the study period (i.e., December 27th & 28th, 2010) of constructing the Houston air pollution cube is in the winter season, Equation 2.13 was used to describe the indoor-outdoor O_3 relationship.

By integrating the hourly outdoor air pollution scenario layers and the indoor-outdoor microenvironment, the hourly near real-time space-time air pollution scenario layers were generated (see Figure 5.5).
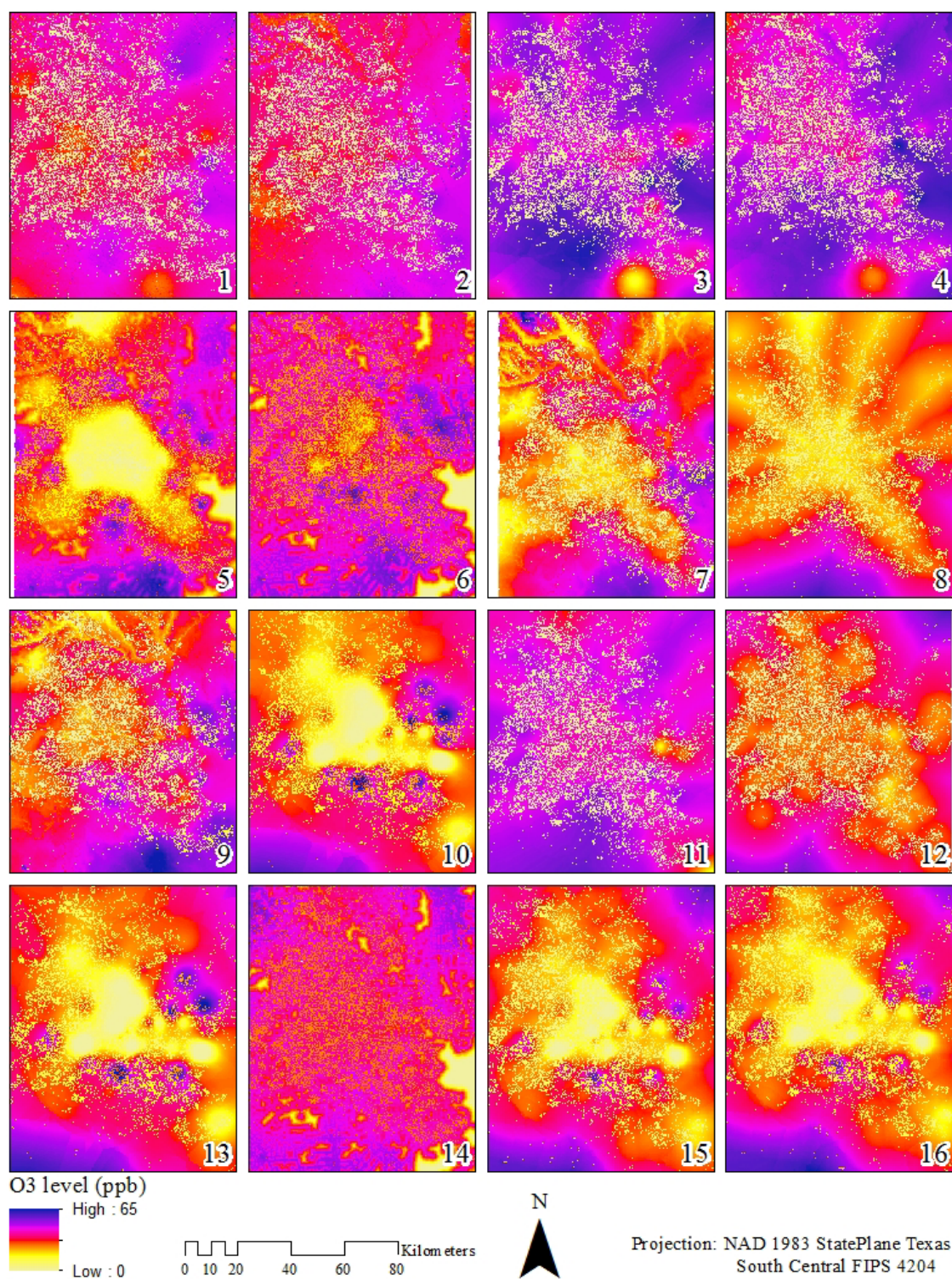
Figure 5.5. The Hourly LUR Component Layers (Model #1 - Model #16) for O₃ Prediction in the Houston Region on December 27ᵗʰ & 28ᵗʰ, 2010.

By registering and stacking the hourly O_3 pollution component layers, the backbones for the near real-time space-time O_3 pollution scenario cubes were built. Figure 5.6 illustrates the frame of the diurnal near real-time space-time O_3 pollution scenario cubes for the Houston region on December 27th & 28th, 2010. The between-layer pollution predictions were then generated using Equation 4.2.

(a)

4:30 pm

12:30 pm

7:30 am

O3 level (ppb)
High : 65

Low : 0
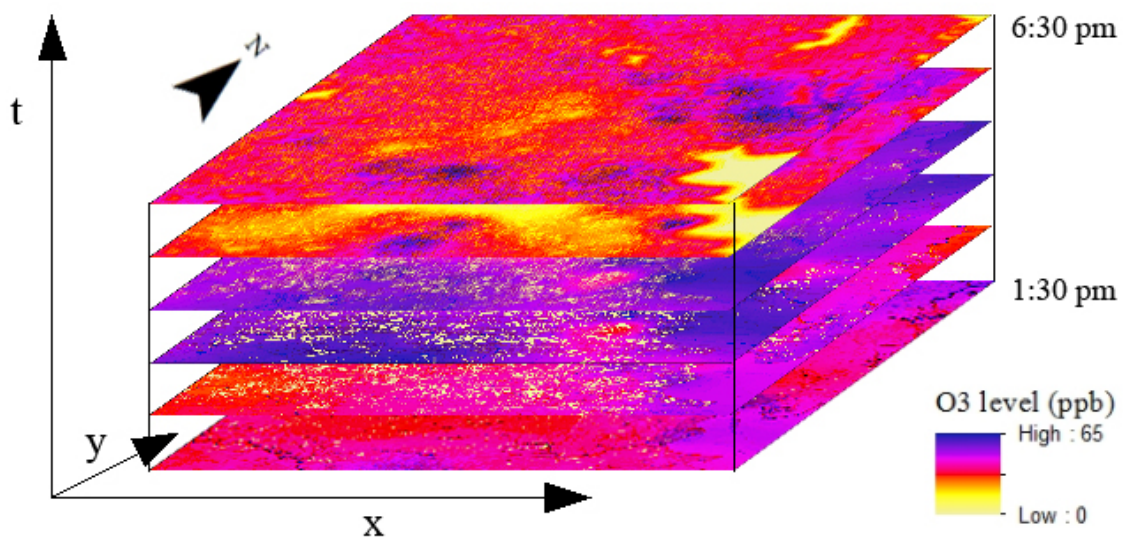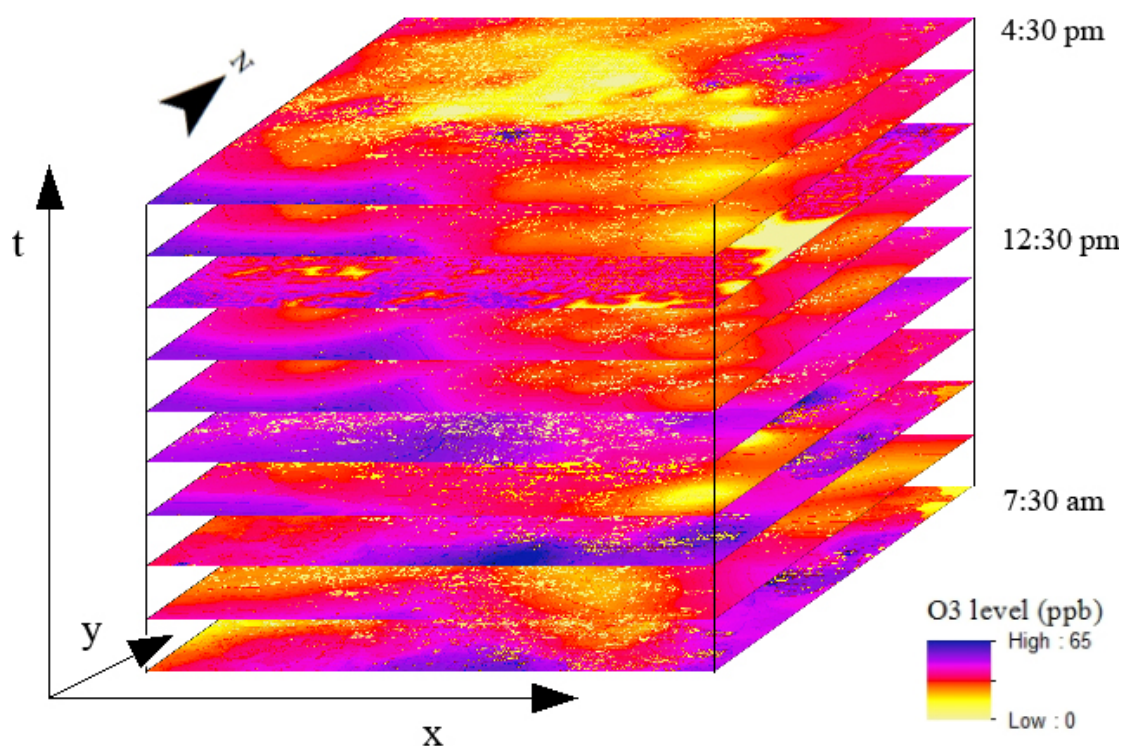
(b)

Figure 5.6. The Near Real-Time Space-Time O$_3$ Pollution Scenario Cube Constructed Using LUR Modeling Method in the Houston Region on December 27th & 28th, 2010.

Note: (a) December 27th, (b) December 28th.

Austin Air Pollution Cube

In the Austin region, there are only 8 EPA O$_3$ monitoring sites (see Figure 5.7). The number of monitoring sites is not enough for the LUR modeling. Only the spatial interpolation methods were used to predict the hourly outdoor O$_3$ pollution in the Austin region. EPA monitoring sites were not divided into the training subsets and the test data

sets because the number of involved EPA air monitoring sites was small in the Austin region.
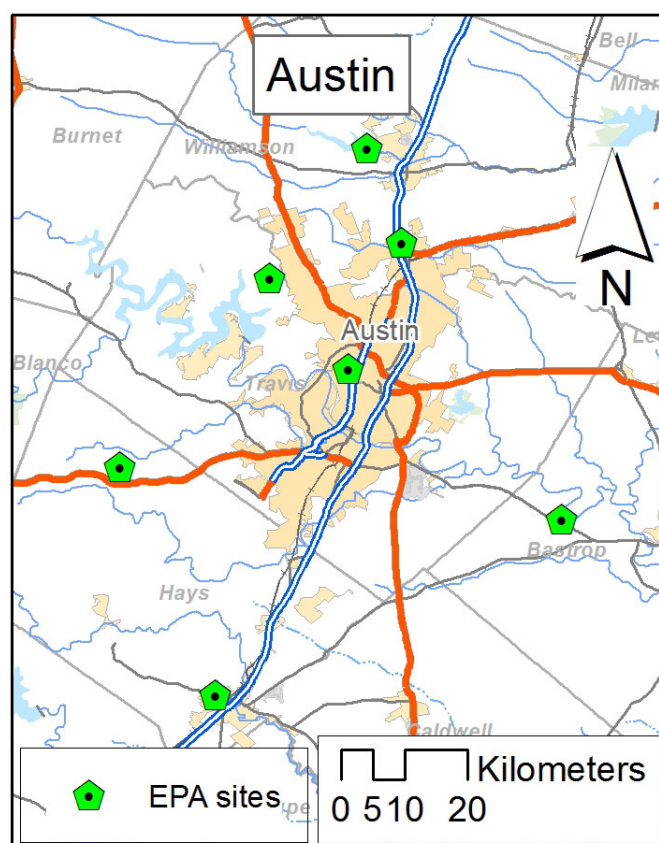
Figure 5.7. The EPA Air Monitoring Sites Managed by the TCEQ in the Austin Region in 2010.

Data source: TCEQ, 2010.

Spatial Interpolation

One day (November 2nd, 2010) diurnal ambient O_3 scenarios of the Austin region were modeled to build the Austin air pollution cubes. Three spatial interpolation methods – IDW (power: 2, neighbors: 5), RBF (neighbors: 5), and ordinary kriging with spherical semivariogram – were applied to create hourly outdoor near real-time air pollution scenarios in the Austin region.

The performance of the three spatial interpolation methods was assessed by examining the RMSEs and MEs of each model (see Table 5.7). The lowest RMSEs for each component layer model were highlighted in bold. Among the three interpolation methods, IDW and kriging method generated 3 predictions with the lowest RMSE, respectively; RBF prediction generated 6 lowest RMSEs. Consequently, results of RBF were best for the Austin region.

At each time point, maps with lowest RMSEs were selected as the hourly component layers for outdoor O_3 prediction in the Austin region on November 2nd, 2010 (see Figure 5.8). The ambient O_3 levels in the Austin region ranged from 0 to 48 ppb. In the noon time, O_3 concentrations were relative high.

Table 5.7. The RMSEs and MEs for Outdoor O$_3$ Assessment Using the 3 Spatial Interpolation Methods – IDW, RBF, and Kriging in the Austin Region on November 2nd, 2010.

Model #	Time (hr:min)	IDW		RBF		Kriging	
		ME	RMSE	ME	RMSE	ME	RMSE
1	8:30am	0.18	2.75	0.59	2.73	0.23	**2.32**
2	9:30am	0.27	3.03	0.78	3.18	0.40	**2.79**
3	10:30am	-0.41	2.66	0.22	**2.33**	0.04	2.58
4	11:30am	0.20	**3.34**	0.62	3.52	0.45	3.53
5	12:30pm	-0.07	3.14	0.46	3.05	0.14	**3.02**
6	13:30pm	-0.66	3.45	0.23	**1.64**	-0.29	2.04
7	14:30pm	-0.70	3.01	0.09	**2.13**	-0.36	2.16
8	15:30pm	-0.25	4.12	0.31	**2.45**	0.16	3.51
9	16:30pm	-0.48	4.64	0.70	**3.71**	0.21	3.89
10	17:30pm	0.62	4.27	0.76	**3.56**	0.41	3.82
11	18:30pm	1.09	**3.74**	0.67	3.96	0.83	3.95
12	19:30pm	1.51	**5.02**	1.46	5.05	1.09	6.00

Note: The units of the RMSEs and MEs: ppb.

For each model, the lowest RMSE across the different predicting methods is highlighted as bold.
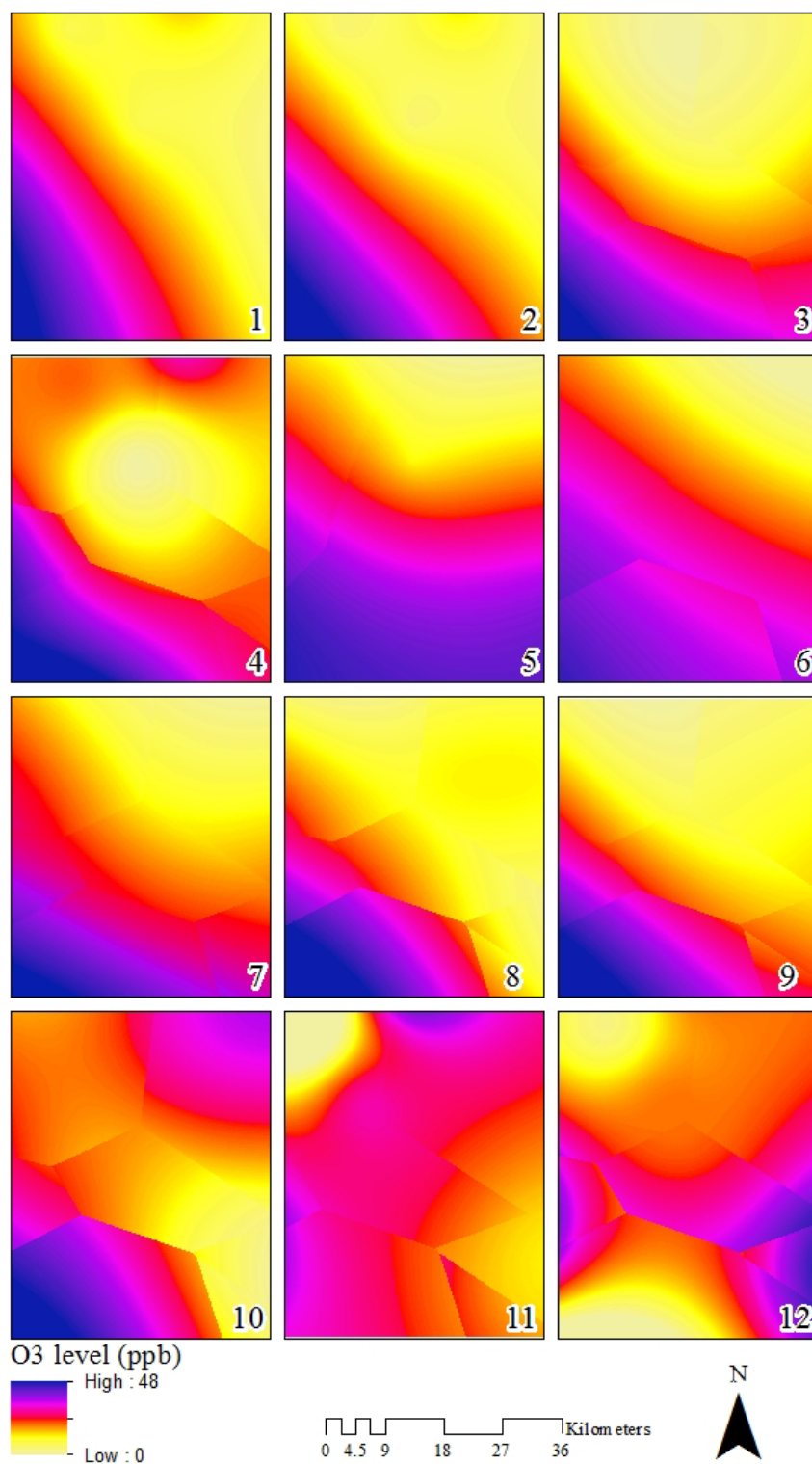
Figure 5.8. The Hourly Component Layers (Model #1 - Model #12) for Outdoor O₃ Prediction in the Austin Region on November 2nd, 2010.

Indoor-Outdoor Microenvironment

2008 land use parcel data of Bastrop, Caldwell, Hays, Travis and Williamson

Counties were obtained from the CAPCOG web site. Parcels with land use codes A (Real

Property: Single-Family Residential), B (Real Property: Multifamily Residential), C

(Real Property: Vacant Lots and Tracts), F1 (Real Property: Commercial), F2 (Real

Property: Industrial (Manufacturing)), L1 (Personal Property: Commercial), L2 (Personal

Property: Industrial (Manufacturing)), M1 (Mobile Homes (Owner different from

landowner)), and O (Real Property: Residential Inventory) were assumed to be indoor

microenvironment; other land was assumed to be outdoor microenvironment.

The indoor-outdoor microenvironment was generated based on the CAPCOG land

use data and was in raster format, which had a spatial resolution of 30m (see Figure 5.9).
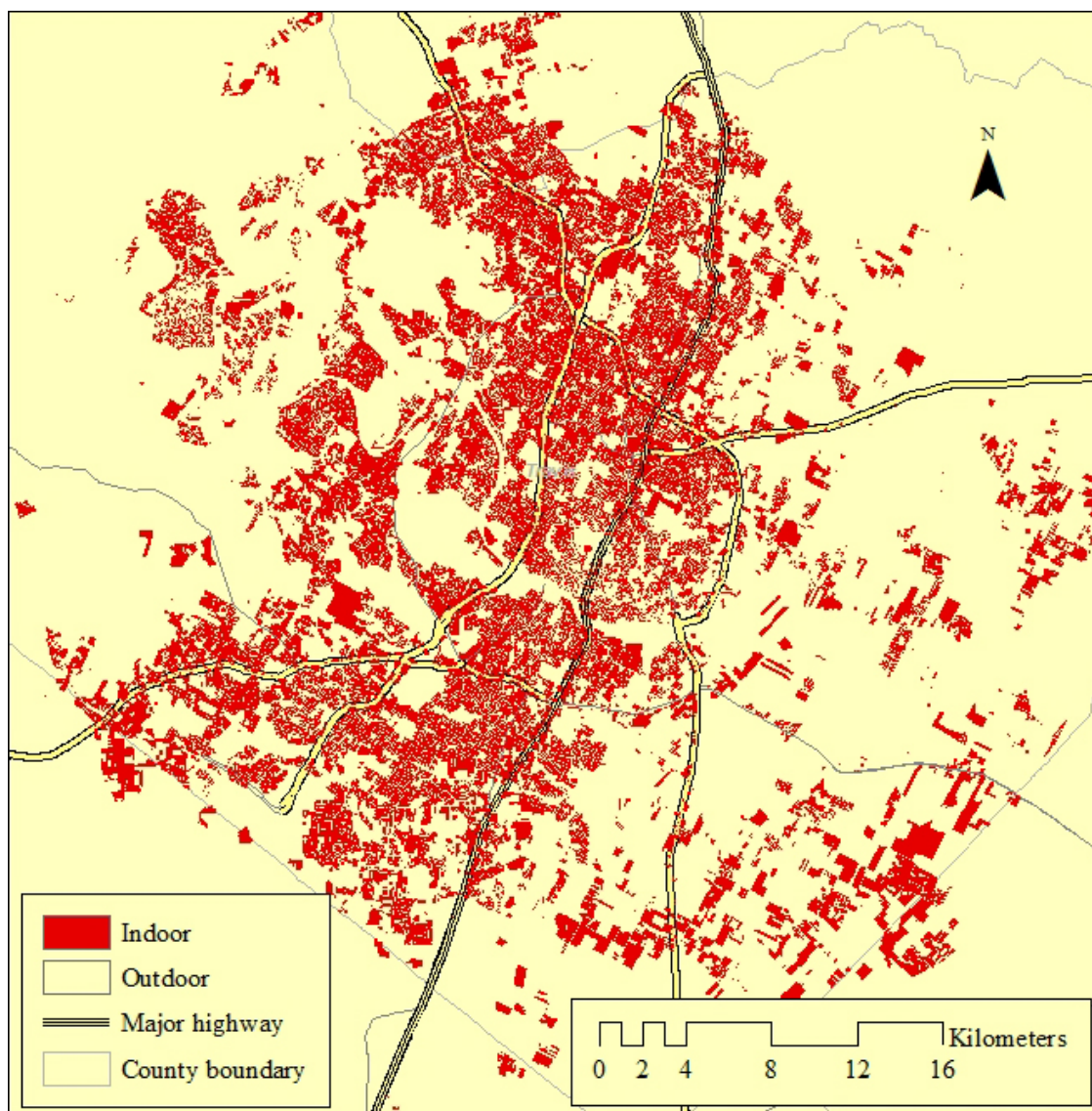
Figure 5.9. The Indoor-Outdoor Microenvironment in the Austin Region in 2010.

Constricting the Air Pollution Cube

Because the study period (i.e., November 2nd, 2010) of the Austin air pollution cube constructing is in the fall season, Equation 2.12 was used to describe the indoor-outdoor O_3 relationship.

By integrating the hourly outdoor air pollution scenario layers and the indoor-outdoor microenvironment, the hourly near real-time space-time air pollution scenario layers were generated (see Figure 5.10).
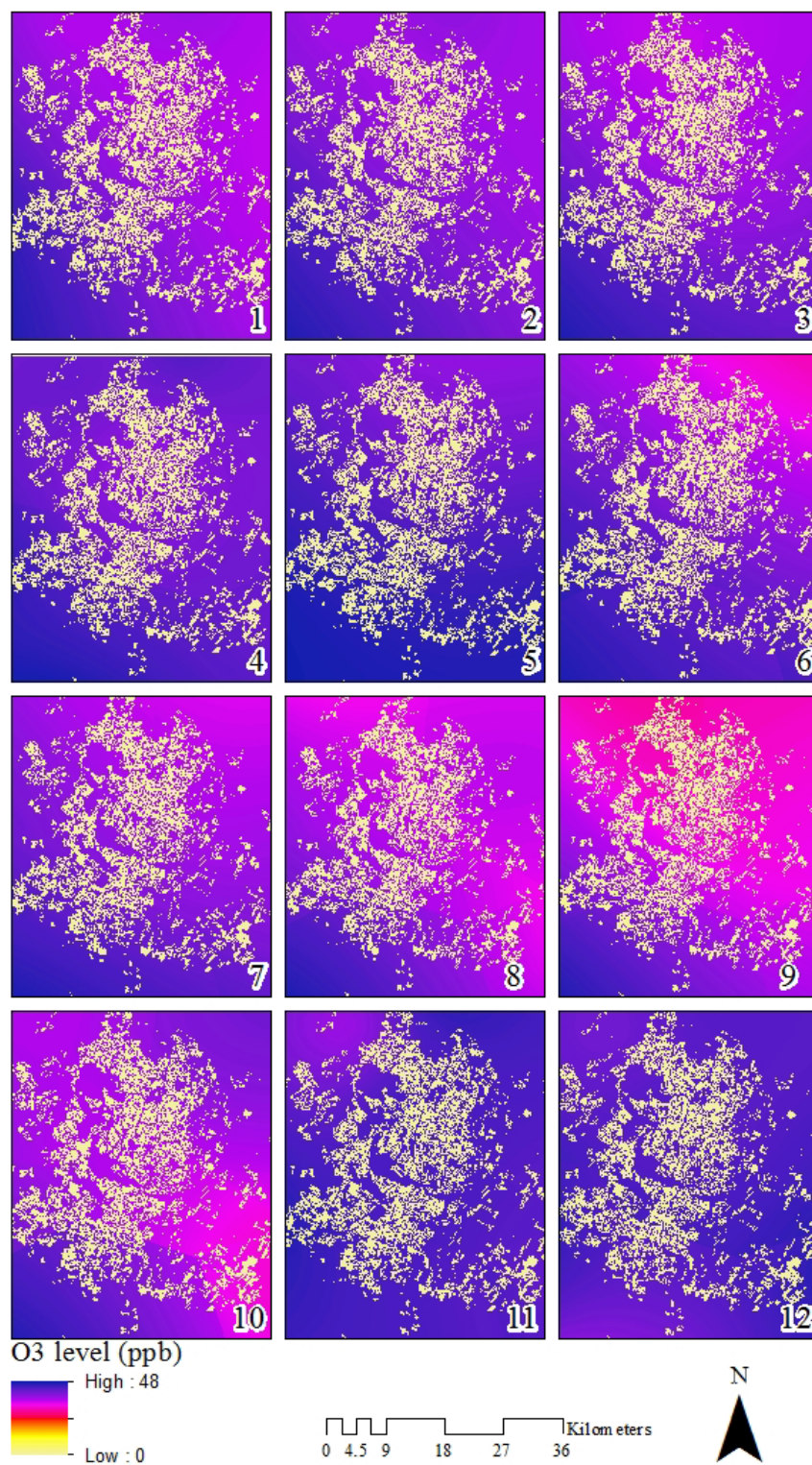
Figure 5.10. The Hourly Component Layers (Model #1 - Model #12) for O₃

Prediction in the Austin Region on November 2nd, 2010.

By registering and stacking the hourly O_3 pollution component layers, the
backbone for a near real-time space-time O_3 pollution scenario cube was built. Figure
5.11 illustrates the frame of the near real-time space-time O_3 pollution scenario cube for
the Austin region. The between-layer pollution predictions were then generated using
Equation 4.2.
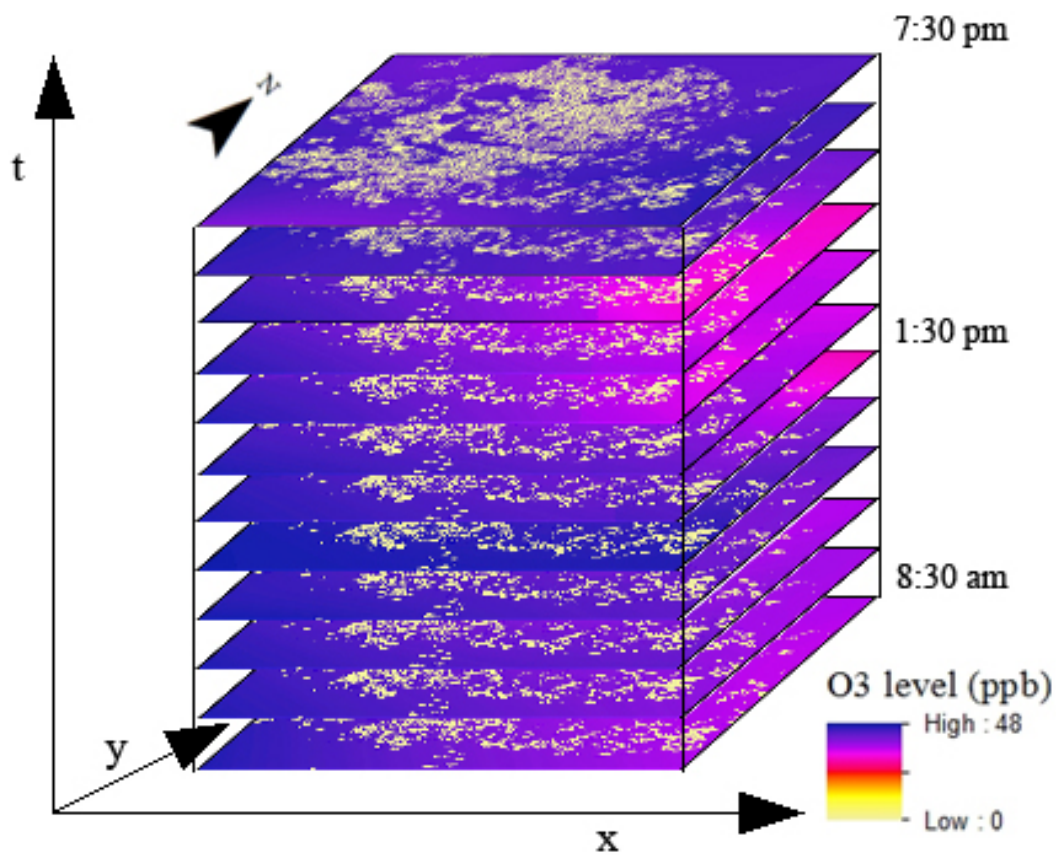
Figure 5.11. The Near Real-Time Space-Time O_3 Pollution Scenario Cube

Constructed Using the Spatial Interpolation Methods in the Austin Region on

November 2nd, 2010.

San Antonio Air Pollution Cube

Similar to the Austin region, there are 11 EPA O_3 monitoring sites in the San Antonio region (see Figure 5.12). The number of monitoring sites is not enough for the LUR modeling. Only the spatial interpolation methods were used to predict the hourly outdoor O_3 pollution in the San Antonio region. EPA monitoring sites were not divided into the training subsets and the test data sets because the number of involved EPA air monitoring sites was small in the San Antonio region.
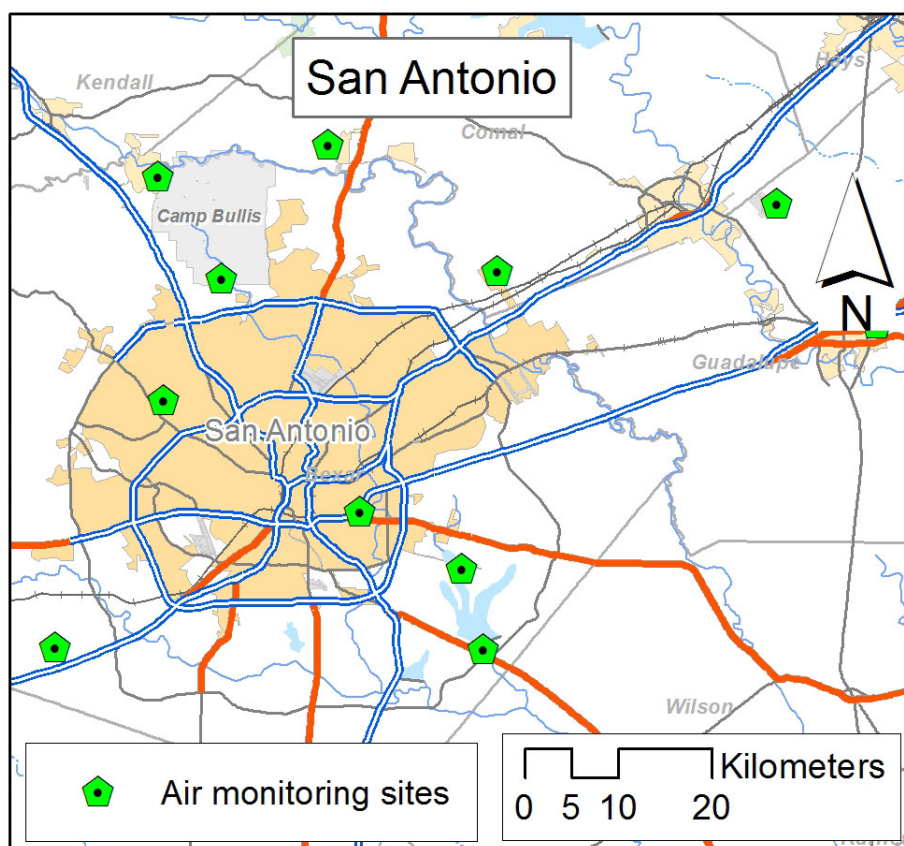
Figure 5.12. The EPA Air Monitoring Sites Managed by the TCEQ in the San Antonio Region in 2010.

Data source: TCEQ, 2010.

Spatial Interpolation

One day (October 26th, 2010) diurnal ambient O_3 scenarios of the San Antonio region were modeled to build the San Antonio air pollution cubes. Three spatial interpolation methods – IDW (power: 2, neighbors: 5), RBF (neighbors: 5), and ordinary kriging with spherical semivariogram – were applied to create hourly outdoor near real-time air pollution scenarios in the San Antonio region.

The performance of the three spatial interpolation methods was assessed by examining the RMSEs and MEs of each model (see Table 5.8). The lowest RMSEs for each component layer model were highlighted in bold. Among the three interpolation methods, IDW did not generate predictions with the lowest RMSE; kriging method generated 3 predictions with the lowest RMSE; RBF prediction generated 9 lowest RMSEs. Consequently, results of RBF were best for the San Antonio region.

At each time point, maps with lowest RMSEs were selected as the hourly component layers for outdoor O_3 prediction in the San Antonio region on October 26th, 2010 (see Figure 5.13). The ambient O_3 levels in the San Antonio region ranged from 0 to 53 ppb. In the noon time, O_3 concentrations were relative high.

Table 5.8. The RMSEs and MEs for Outdoor O$_3$ Assessment Using the 3 Spatial

Interpolation Methods – IDW, RBF, and Kriging in the San Antonio Region on

October 26th, 2010.

Model #	Time (hr:min)	IDW		RBF		Kriging	
		ME	RMSE	ME	RMSE	ME	RMSE
1	8:30am	0.56	3.86	0.81	**3.05**	0.26	3.91
2	9:30am	0.54	3.42	0.41	**3.41**	0.04	3.52
3	10:30am	0.40	3.20	0.25	3.16	0.05	**3.15**
4	11:30am	0.45	2.82	0.55	**2.62**	0.03	2.87
5	12:30pm	0.52	2.87	0.66	**2.62**	0.12	2.81
6	13:30pm	0.57	3.22	0.65	**2.95**	0.15	3.09
7	14:30pm	0.62	2.72	0.52	2.59	0.46	**2.58**
8	15:30pm	0.32	2.70	0.31	**2.65**	0.31	2.87
9	16:30pm	0.09	3.92	0.46	**3.36**	-0.07	3.99
10	17:30pm	0.61	6.19	1.01	**5.68**	0.23	6.13
11	18:30pm	0.61	10.77	0.28	9.88	0.67	**9.74**
12	19:30pm	0.56	14.75	0.12	**13.66**	0.83	14.34

Note: The units of the RMSEs and MEs: ppb.

For each model, the lowest RMSE across the different predicting methods is

highlighted as bold.
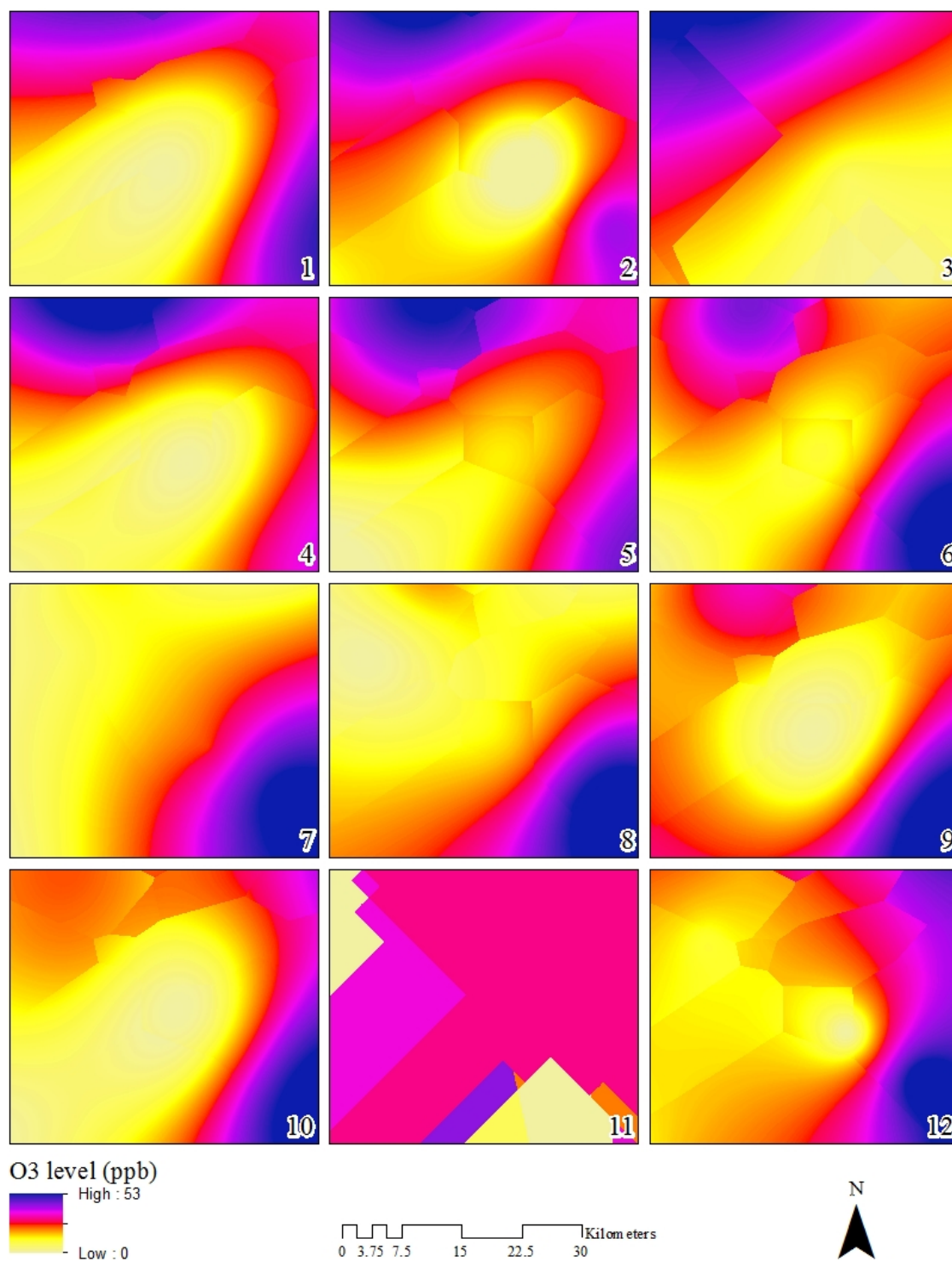
Figure 5.13. The Hourly Component Layers (Model #1 - Model #12) for Outdoor O_3 Prediction in the San Antonio Region on October 26th, 2010.

Indoor-Outdoor Microenvironment

2010 San Antonio land use data were obtained from the COSA web site. Parcels with land use codes 11** (Residential), 2*** (Commercial), 3*** (Industrial), and 40** / 4100 (Public Institutional) were assumed to be indoor microenvironment; other land was assumed to be outdoor microenvironment.

The indoor-outdoor microenvironment was acquired based on land use / land cover data, which had a spatial resolution of 30m (see Figure 5.14).
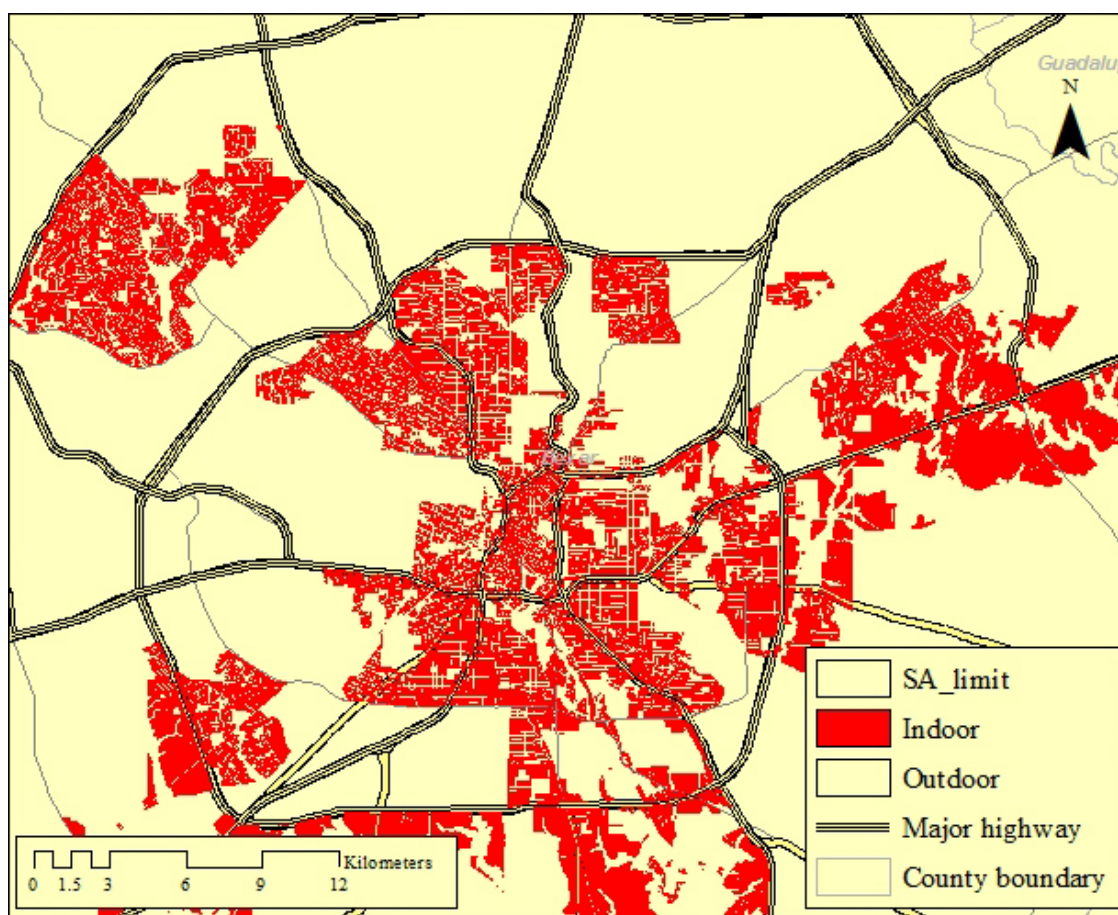
Figure 5.14. The Indoor-Outdoor Microenvironment in the San Antonio Region in 2010.

Constricting the Air Pollution Cube

Because the study period (i.e., October 26th, 2010) of the Austin air pollution cube constructing is in the fall season, Equation 2.12 was used to describe the indoor-outdoor O_3 relationship.

By integrating the hourly outdoor air pollution scenario layers and the indoor-outdoor microenvironment, the hourly near real-time space-time air pollution scenario layers were generated (see Figure 5.15).

O3 level (ppb)
High : 53
Low : 0

Figure 5.15. The Hourly Component Layers (Model #1 - Model #12) for O₃

Prediction in the San Antonio Region on October 26ᵗʰ, 2010.

By registering and stacking the hourly O_3 pollution component layers, the backbone for a near real-time space-time O_3 pollution scenario cube was built. Figure 5.16 illustrates the frame of the near real-time space-time O_3 pollution scenario cube for the San Antonio region. The between-layer pollution predictions were then generated using Equation 4.2.
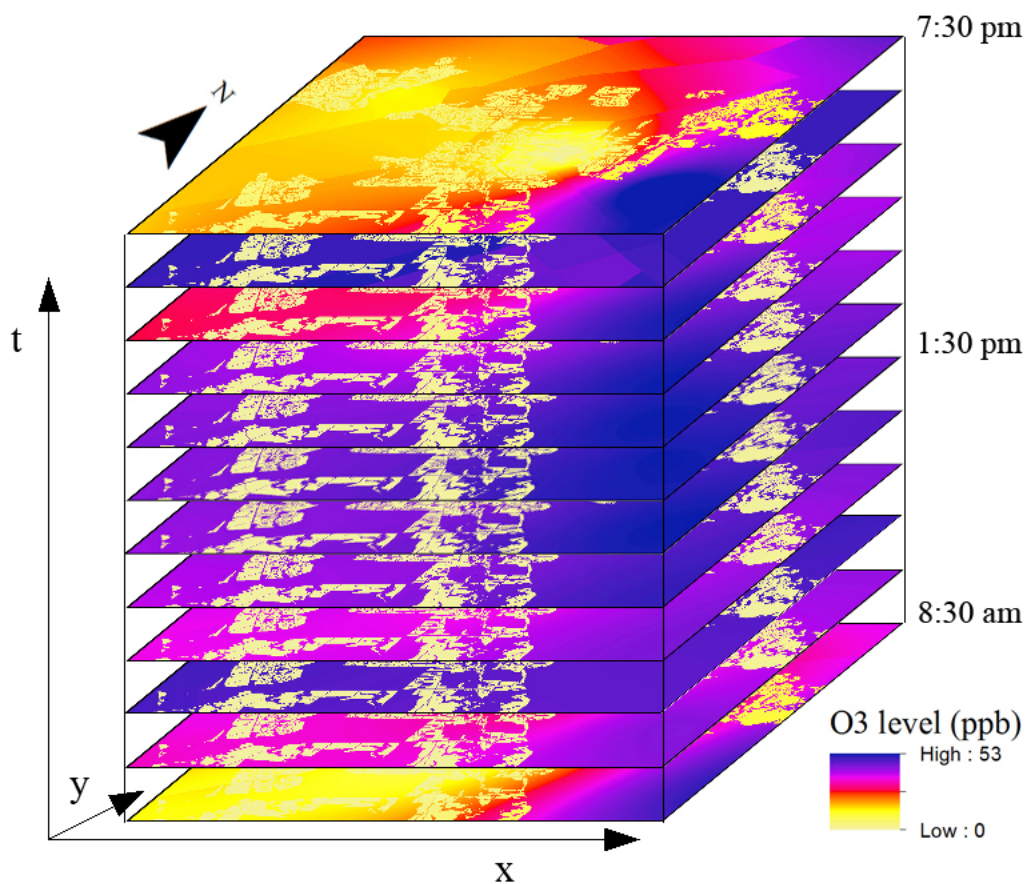
Figure 5.16. The Near Real-Time Space-Time O_3 Pollution Scenario Cube Constructed Using the Spatial Interpolation Methods in the San Antonio Region on October 26th, 2010.

CHAPTER VI

INDIVIDUAL REAL-TIME MONITORING

Individual Real-Time Monitoring in the Houston Region

Individual Real-Time Space-Time Behavior Monitoring

On December 27th & 28th, 2010, an adult male volunteer traveled in the Houston region and collected two data sets – the individual real-time space-time behavior data set and the individual real-time air pollution exposure ground truth data set.

The volunteer's two-day travel trajectory in the Houston region was shown on Figure 6.1. Figure 6.2 is a 3D visualization of the two-day trajectory of the volunteer. In the 3D space-time path map, the vertical dimension (z) represents the two-day travel time; the horizontal dimensions (x, y) represent the space of the Houston region.
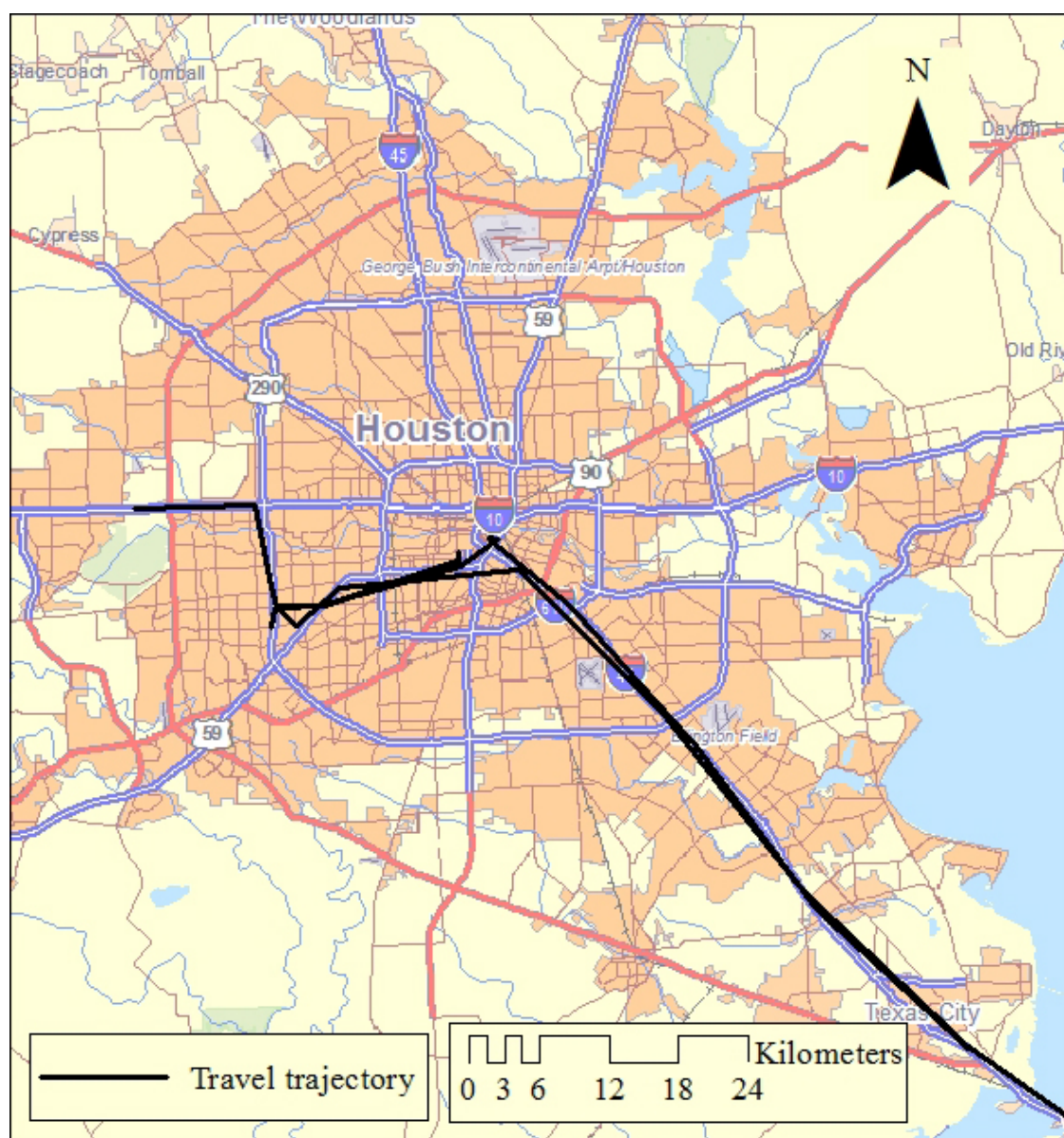
Figure 6.1. The Volunteer's 2D Travel Trajectory in the Houston Region on

December 27th & 28th, 2010.
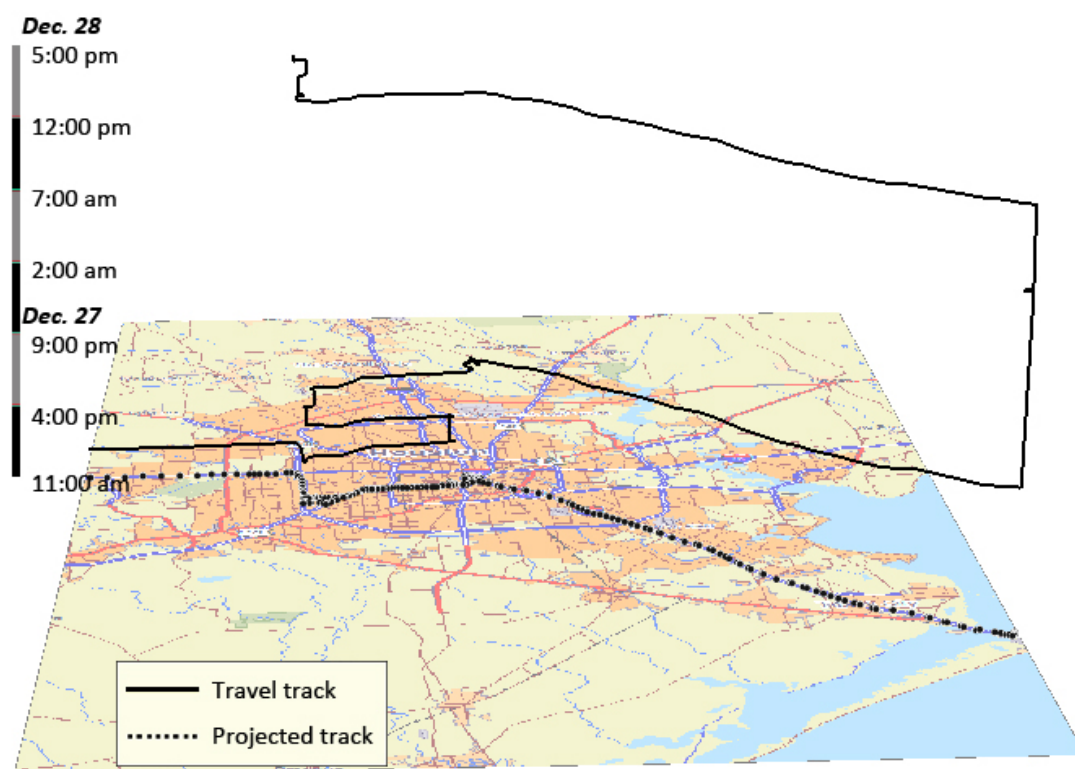
Figure 6.2. The Volunteer's Space-Time Path in the Houston Region on December 27th & 28th, 2010.

Individual Real-Time Air Pollution Exposure Monitoring

The volunteer's real-time individual O_3 exposure in the Houston region on December 27th & 28th, 2010, including ambient O_3 concentrations and real-time AQIs were recorded; real-time individual O_3 intake rates were calculated (see Figure 6.3).

$$Rate_{O_3} = C * Rate_{Air}$$ Equation 6.1.

where $Rate_{O_3}$ is the real-time individual O_3 intake rate, C is the real-time ambient O_3 concentration, and $Rate_{Air}$ is the real-time individual air intake volume per minute (see Table 2.2).

I found that the measured ambient O_3 concentrations (ground truth data) ranged from 20 ppb to 80 ppb on December 27th & 28th, 2010. During the afternoon of December 27th, the measured ambient O_3 concentrations varied a lot. According to GPS data and travel diary, the O_3 concentrations were medium when the volunteer traveled on major roads (e.g., Interstate 10, Interstate 45, and W Sam Houston Parkway S); the O_3 concentrations were low when the volunteer traveled on minor roads or stayed indoors for shopping and rest. This may be explained by the fact that the O_3 concentrations are closely related to traffic emissions in urban areas. During the night of December 27th and the morning of December 28th, the O_3 concentrations stayed low. During this period of time, the volunteer stayed in a hotel for most of time, except a 40-minute morning exercise, which included jogging and walking. Because the volunteer's travel range was limited at that time, ambient O_3 concentrations were stable. During the noon of December 28th, the O_3 concentrations were relative high. During this period of time, the volunteer traveled through the city of Houston along highways. During the afternoon of December 28th, the O_3 concentrations were low. During this period of time, the volunteer traveled in a small distance, but the space-time activities were complex, including staying, walking, and running.

The individual O_3 intake is more complex than individual O_3 exposure; the variation of the volunteer's real-time individual O_3 intake rates is quite different from that of the ambient O_3 concentrations in the Houston region during the two days. Generally speaking, the volunteer's individual O_3 intake rates were higher and more instable during the daytime. During the daytime, the volunteer visited different places and had many different daily activities, e.g., walking, running, and staying. These daily activities

affected the breathing rate, and resulted in a dramatic change in the individual O_3 intake. During the nighttime, the volunteer stayed inside. This explains the low and stable O_3 intake rates at that time. I found that the individual O_3 intake rate line had six peaks (i.e., O_3 intake rates $>10^{-6}$ L/min) – two peaks were occurred in the afternoon of December 27th, one peak in the morning of December 28th, one peak in the noon of December 28th, and two peaks in the afternoon of December 28th (see Figure 6.3).

Figure 6.3. The Volunteer's Real-Time Air Pollution Exposure and Intake in the Houston Region on December 27th & 28th, 2010.

Note: (a): O_3 Intake rates (10^{-8} L/min), (b): Portable air pollution sampler collected ambient O_3 concentrations (ppb), (c): Personal AQI values, which were converted from ambient O_3 concentrations using the AQI calculator.

Because AQIs are converted from O_3 concentrations directly, the variation of the volunteer's real-time personal AQIs is similar to that of the ambient O_3 concentrations. Following the U.S. AQI standard, I used different colors to visualize the volunteer's real-time personal AQIs – green color indicates good air quality (AQI range: 0-50), yellow color indicates moderate air quality (AQI range: 51-100), and orange color indicates that the air quality is unhealthy for sensitive groups (AQI range: 101-150) (see Figure 6.4).
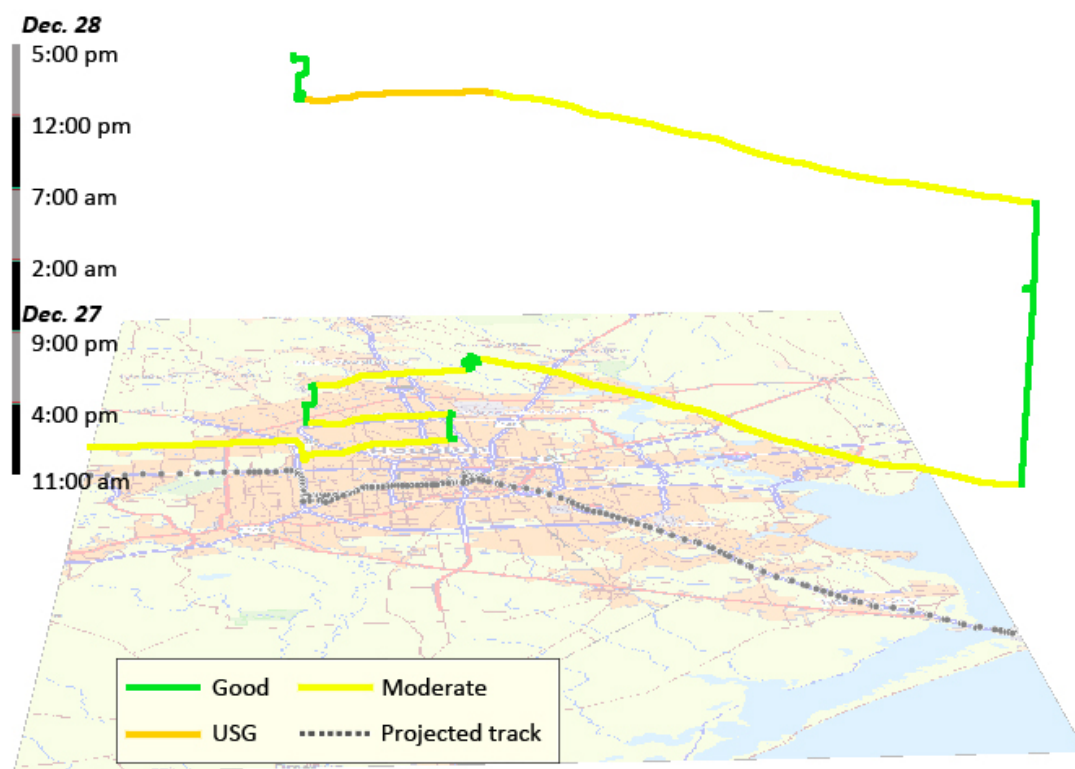
Figure 6.4. The Volunteer's Space-Time Path with Personal AQIs in the Houston Region on December 27th & 28th, 2010.

Individual Real-Time Monitoring in the Austin Region

Individual Real-Time Space-Time Behavior Monitoring

On November 2nd, 2010, an adult male volunteer traveled in the Austin region and collected two data sets – the individual real-time space-time behavior data set and the individual real-time air pollution exposure ground truth data set.

The volunteer's one-day travel trajectory in the Austin region was shown on Figure 6.5. Figure 6.6 is a 3D visualization of the one-day trajectory of the volunteer. In the 3D space-time path map, the vertical dimension (z) represents the one-day travel time; the horizontal dimensions (x, y) represent the space of the Austin region.

Figure 6.5. The Volunteer's 2D Travel Trajectory in the Austin Region on November 2nd, 2010.

Figure 6.6. The Volunteer's Space-Time Path in the Austin Region on November 2nd, 2010.

Individual Real-Time Air Pollution Exposure Monitoring

The volunteer's real-time individual O_3 exposure and intake in the Austin region on November 2nd, 2010, including ambient O_3 concentrations, real-time AQIs, and real-time O_3 intake rates were recorded / calculated (see Figure 6.7). The measured ambient O_3 concentrations (ground truth data) ranged from 0 ppb to 40 ppb in the daytime. According to GPS data and travel diary, during the morning of the day, the volunteer traveled on major roads (e.g., Interstate 35 and Highway 183); the O_3 concentrations were low (O_3 concentrations: 20-30ppb); traffic emissions were assumed to be the major air

pollution source during this period of time. Then the volunteer visited the friend's house for about 3 hours; the O_3 concentrations in this period of time were very low (O_3 concentrations: 0-10ppb); this may be explained by the fact that the volunteer stayed indoors, and indoor O_3 concentrations in the friend's house was very low. During the noon time, the volunteer traveled to the downtown area of Austin; the travel time was about half an hour. The O_3 concentrations increased to 30-40ppb, which indicated that outdoor O_3 concentrations during the noon time were higher than those during other time periods in the Austin region. Although outdoor O_3 concentrations during the noon time were relative high, the air quality was still not bad because AQIs were less than 50, which is a sign of good air quality. This aspect was also shown in Figure 6.10. The volunteer stayed in the downtown area for a long time (about 6-7 hours) for shopping and resting. Because the volunteer almost stayed indoors in this period of time, the measured O_3 concentrations were very low (O_3 concentrations: 0-10ppb). During the evening, the volunteer drove in the city of Austin; the measured O_3 concentrations rose to 20-30ppb.

Six O_3 intake peaks (i.e., O_3 intake rates$>2*10^{-7}$ L/min) were found in Figure 6.7. Two of them (i.e., the third peak and the fifth peak) were related to indoor microenvironment; physical activities, e.g., walk, were the major reason for high intake rates. The other peaks were related to outdoor O_3 concentrations.
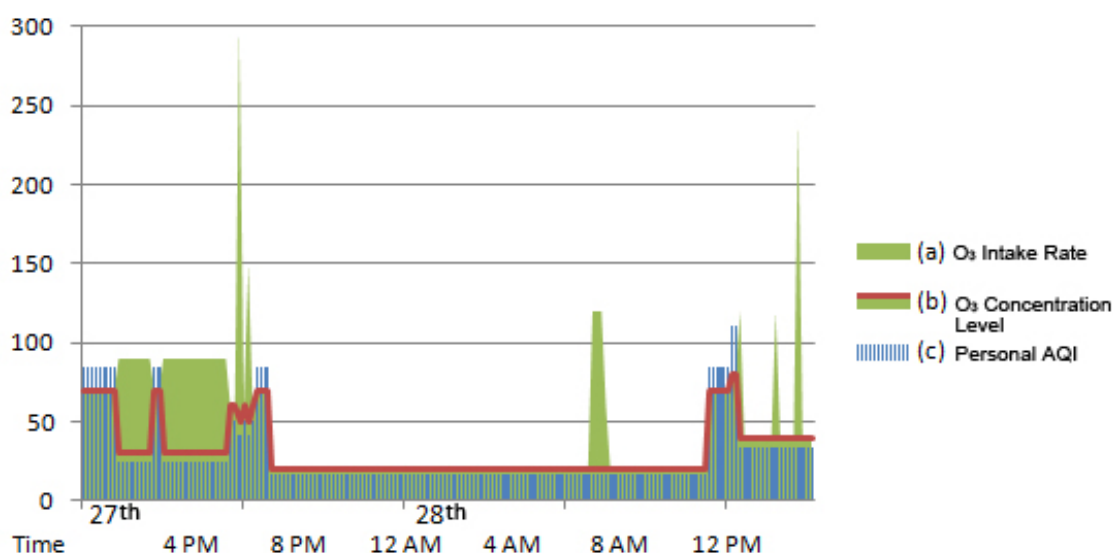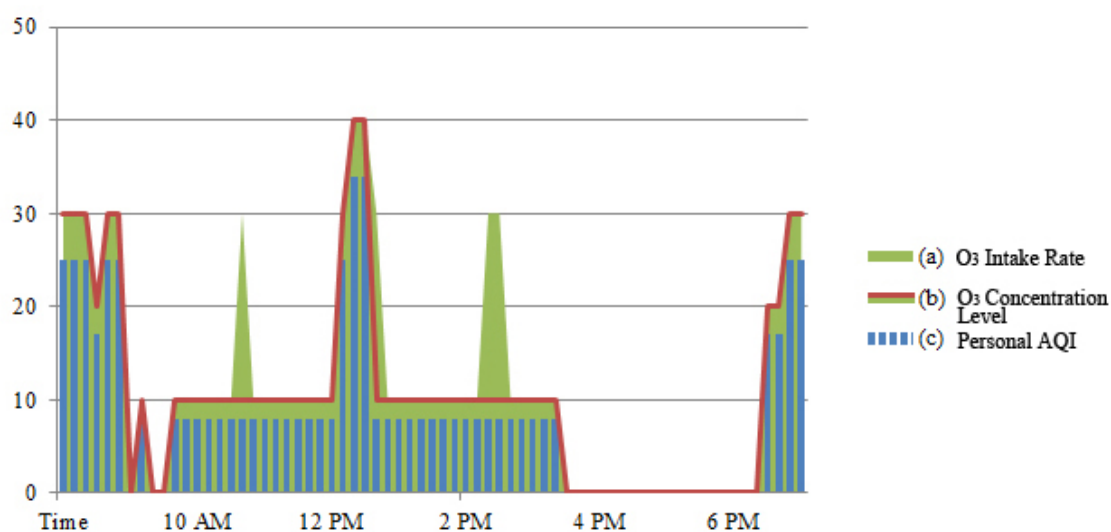
Figure 6.7. The Volunteer's Real-Time Air Pollution Exposure and Intake in the Austin Region on November 2nd, 2010.

Note: (a): O$_3$ Intake rates (10^{-8} L/min), (b): Portable air pollution sampler collected ambient O$_3$ concentrations (ppb), (c): Personal AQI values, which were converted from ambient O$_3$ concentrations using the AQI calculator.

Generally speaking, both O$_3$ concentrations and AQIs were low in the Austin Region on November 2nd, 2010. In other words, the diurnal air quality was good on that day. The variation of the volunteer's real-time personal AQIs is similar to that of the ambient O$_3$ concentrations. The ambient O$_3$ concentrations ranged from 0 ppb to 40 ppb; the AQIs ranged from 0 to 34. Based on the U.S. AQI color standard, i.e., green color indicates good air quality (AQI range: 0-50), yellow color indicates moderate air quality (AQI range: 51-100), and orange color indicates that the air quality is unhealthy for

sensitive groups (AQI range: 101-150), the volunteer's space-time path with personal

AQIs was mapped (see Figure 6.8). Only green color was found in the map.
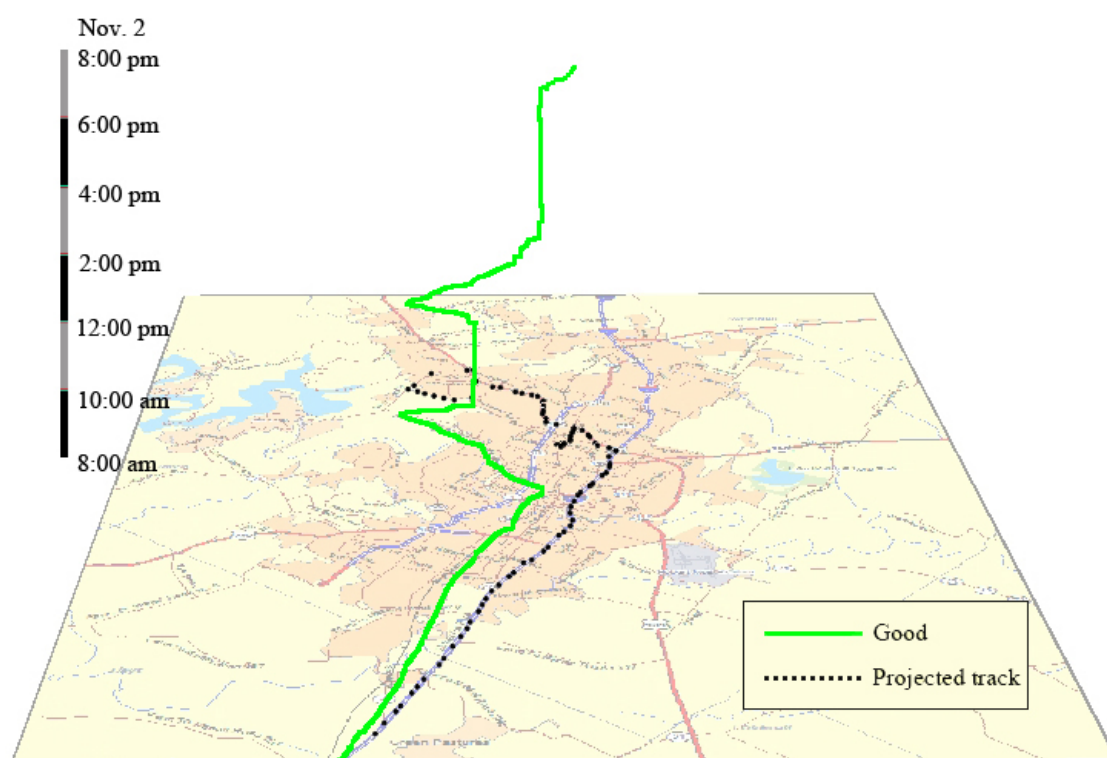
Figure 6.8. The Volunteer's Space-Time Path with Personal AQIs in the Austin

Region on November 2nd, 2010.

Individual Real-Time Monitoring in the San Antonio Region

Individual Real-Time Space-Time Behavior Monitoring

On October 26th, 2010, an adult male volunteer traveled in the San Antonio region and collected two data sets – the individual real-time space-time behavior data set and the individual real-time air pollution exposure ground truth data set.

The volunteer's one-day travel trajectory in the San Antonio region was shown on Figure 6.9. Figure 6.10 is a 3D visualization of the one-day trajectory of the volunteer. In the 3D space-time path map, the vertical dimension (z) represents the one-day travel time; the horizontal dimensions (x, y) represent the space of the San Antonio region.
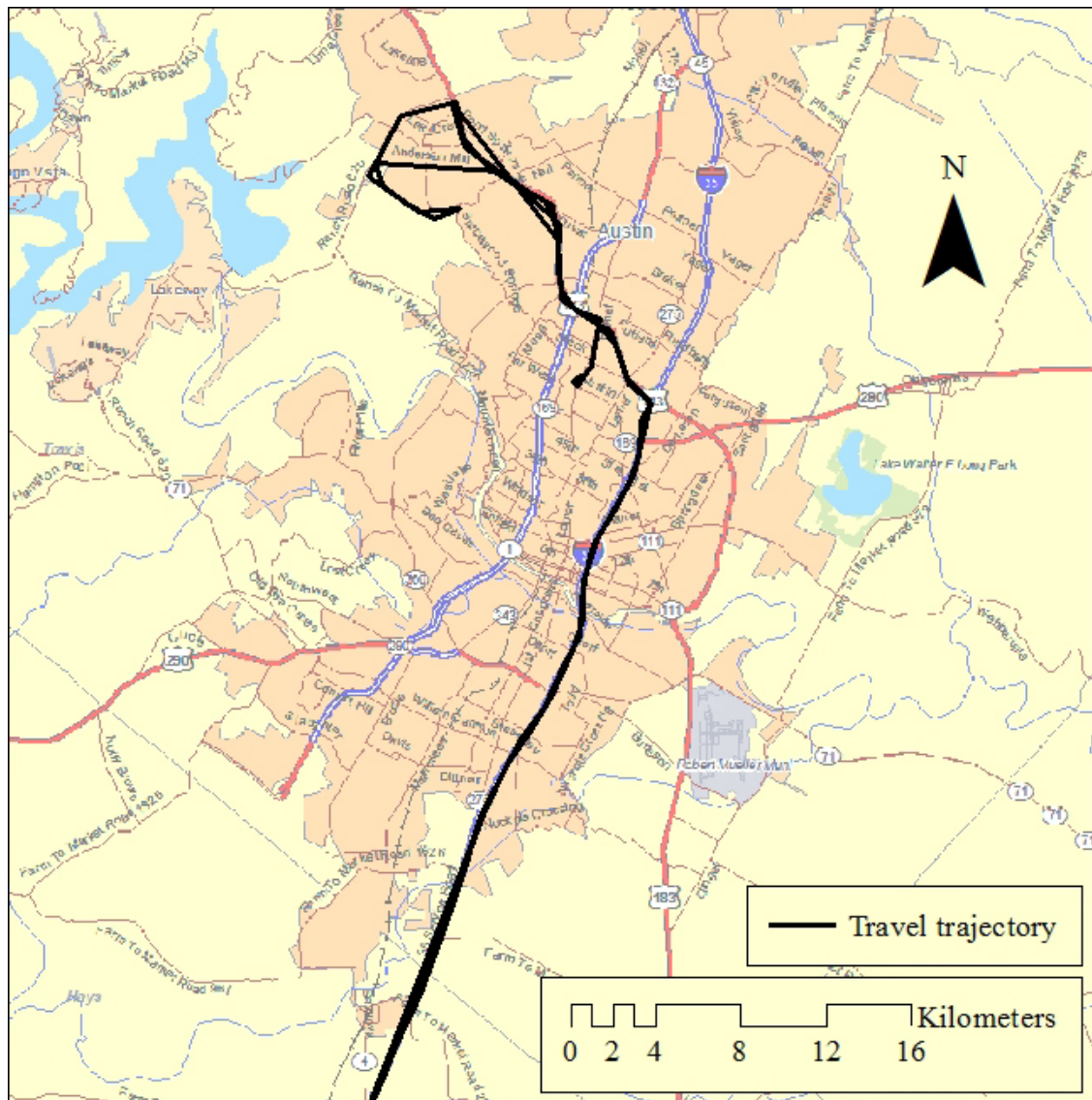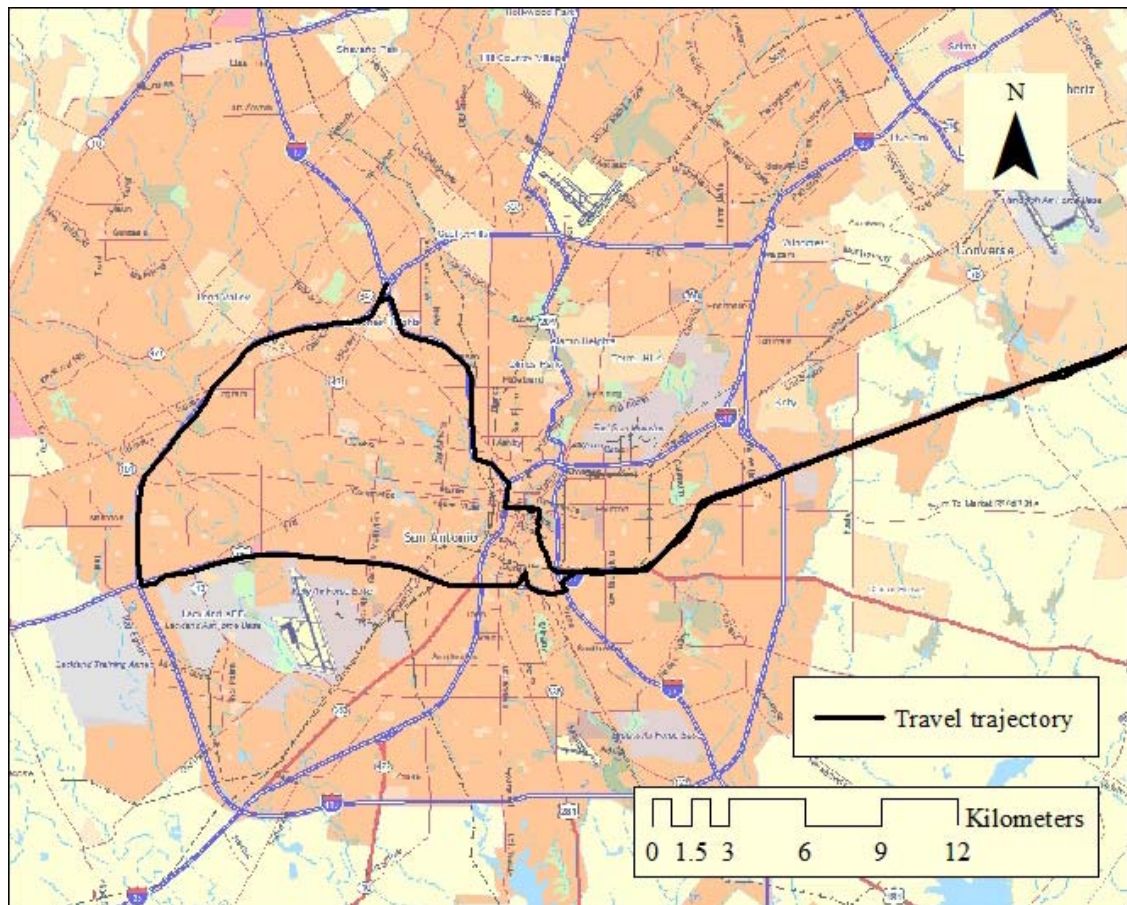
Figure 6.9. The Volunteer's 2D Travel Trajectory in the San Antonio Region on October 26th, 2010.
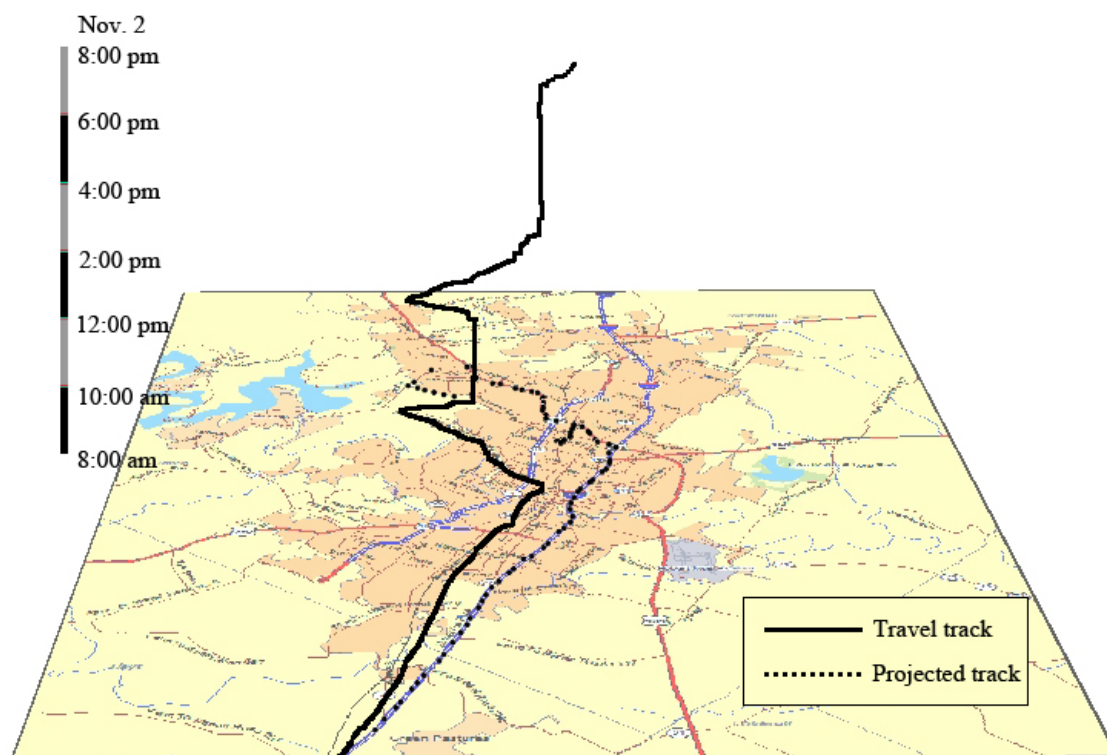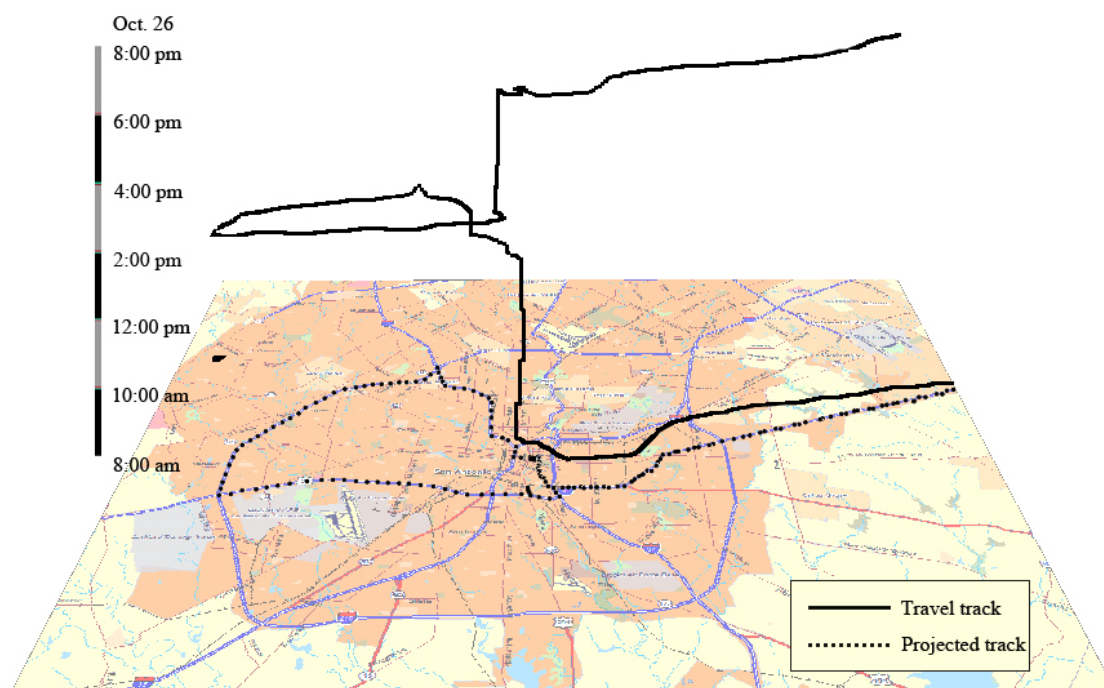
Figure 6.10. The Volunteer's Space-Time Path in the San Antonio Region on

October 26th, 2010.

Individual Real-Time Air Pollution Exposure Monitoring

The volunteer's real-time individual O_3 exposure and intake in the San Antonio

region on October 26th, 2010, including ambient O_3 concentrations, real-time AQIs, and

real-time O_3 intake rates were recorded / calculated (see Figure 6.11). The measured

ambient O_3 concentrations (ground truth data) ranged from 10 ppb to 60 ppb in the

daytime. According to GPS data and travel diary, during the morning of the day, the

volunteer drove on major roads (e.g., Interstate 10 and Interstate 37); the O_3

concentrations were very low (O_3 concentrations: 10ppb); air quality was good. The

volunteer stayed in the downtown area of San Antonio for about 5 hours (9:00am-

2:00pm). In the period of time, the main microenvironment was indoors. The O_3 concentrations were very low and constant (O_3 concentrations: 10ppb). During 2:00pm to 3:30pm on the same day, the volunteer drove across the city of San Antonio. The major roads he traveled included U.S. Highway 87, U.S. Highway 90, and Interstate 410. The O_3 concentrations ranged from 40 ppb to 60 ppb. Traffic emissions were the major air pollution source. Then the volunteer stayed in the downtown area for 3 hours and a half. GPS data showed that the main microenvironment was indoors; the O_3 concentrations were very low and constant (O_3 concentrations: 10ppb). In the evening, the volunteer drove back to home, Seguin, Texas, which is located in the east of San Antonio. In the period of time, the O_3 concentrations ranged from 10 ppb to 20 ppb.

Four O_3 intake peaks (i.e., O_3 intake rates$>2*10^{-7}$ L/min) were found in Figure 6.11. The first three peaks were related to indoor physical activities. Walking and running caused the increase of respiratory rates, so that O_3 intake rates were increased. The last peak was related to outdoor O_3 concentrations because the volunteer was driving and the respiratory rate was constant.
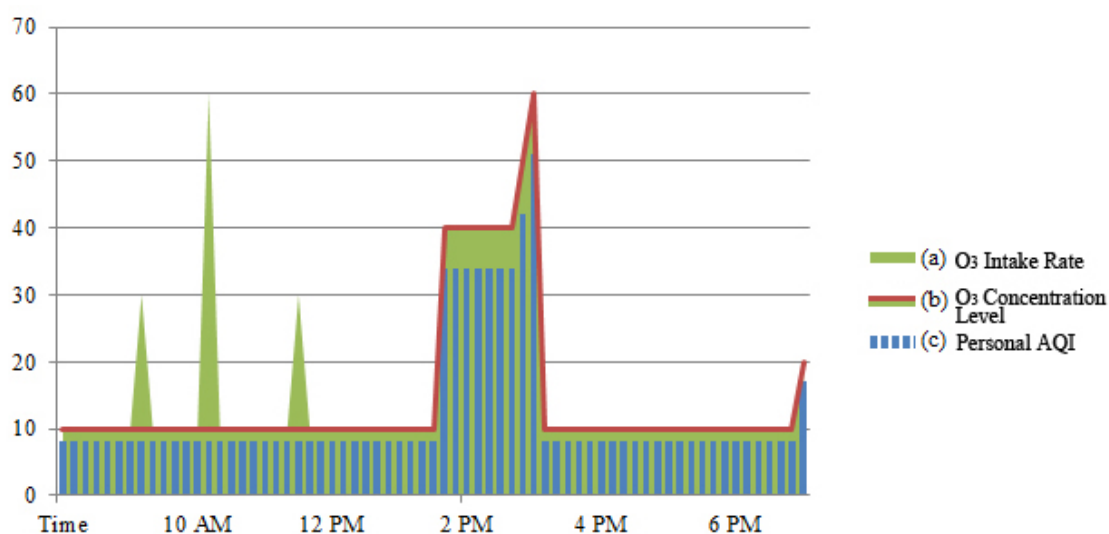
Figure 6.11. The Volunteer's Real-Time Air Pollution Exposure and Intake in the

San Antonio Region on October 26th, 2010.

Note: (a): O_3 Intake rates (10^{-8} L/min), (b): Portable air pollution sampler collected

ambient O_3 concentrations (ppb), (c): Personal AQI values, which were converted

from ambient O_3 concentrations using the AQI calculator.

Generally speaking, the air quality in the San Antonio on October 26th, 2010 was

good. In Figure 6.12, the volunteer's space-time path with personal AQIs showed a

majority of green color, which meant good air quality; the only yellow color (i.e.,

moderate air quality) was found located in the downtown area around 3:30pm.
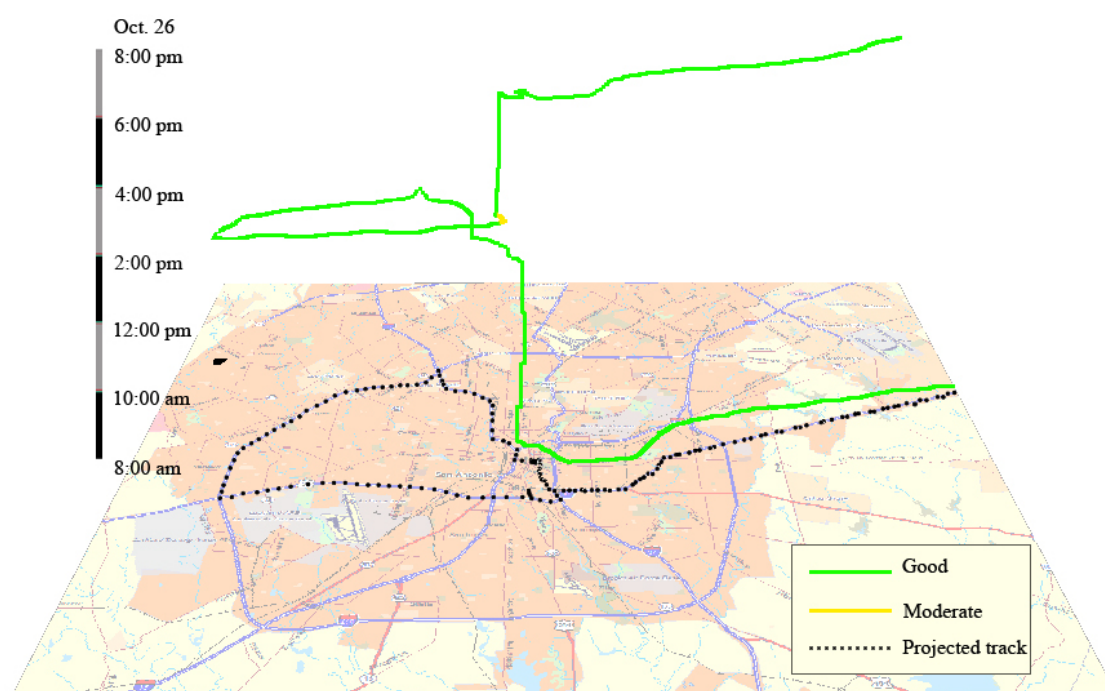
Figure 6.12. The Volunteer's Space-Time Path with Personal AQIs in the San Antonio Region on October 26th, 2010.

CHAPTER VII

INDIVIDUAL-BASED AIR POLLUTION EXPOSURE MODELING

Individual-Based Air Pollution Exposure Modeling in the Houston Region

The near real-time space-time O_3 pollution scenario cube constructed using LUR modeling method in the Houston region on December 27th & 28th, 2010 (see Figure 5.6) was used as the near real-time air pollution information platform for the individual air pollution exposure modeling in the Houston region. The volunteer's real-time space-time path in the Houston region on December 27th & 28th, 2010 (see Figure 6.2) was used as the individual real-time space-time behavior monitoring data for the individual air pollution exposure modeling in the Houston region. After ArcGIS operations such as raster calculation, raster extraction, and zonal statistics, PIRAM estimated individual O_3 exposure in the Houston region was calculated (see Figure 7.1). The curve of PIRAM estimated individual O_3 exposure fitted well with the result of portable air pollution sampler collected ambient O_3 concentrations (i.e., the observed ground truth data), which indicated that the PIRAM model can effectively assess individual's personal exposure to air pollution in the Houston region. This aspect was also verified through the paired-sample t-test for comparing PIRAM estimated individual O_3 exposure and portable air pollution sampler collected ambient O_3 concentrations in the Houston region on December 27th & 28th, 2010 using SPSS (see Table 7.1). Volunteer's individual O_3

exposure was sampled every ten minutes in the two days. Ninety-two paired-samples were analyzed. The *p*-value of the paired-sample t-test was 0.341. There was no significant difference between the two groups. Based on the result, hypothesis 1 in the Houston region was supported.

Figure 7.1. PIRAM Estimated Individual O$_3$ Exposure (a) vs. Portable Air Pollution Sampler Collected Ambient O$_3$ Concentrations (b) in the Houston Region on December 27th & 28th, 2010.

Note: Unit: (ppb).

Table 7.1. The Paired-Samples T-Test for Comparing PIRAM Estimated Individual

O_3 Exposure and Portable Air Pollution Sampler Collected Ambient O_3

Concentrations in the Houston Region on December 27th & 28th, 2010.

Paired Samples Test

					95% Confidence Interval of the Difference				
			Std. Deviation	Std. Error Mean					Sig. (2-tailed)
		Mean			Lower	Upper	t	df	
Pair 1	PIRAM estimated - Sampler collected	.3167210	3.1713639	.3306375	-.3400498	.9734919	.958	91	.341

AQIs have a segmented linear relationship with air pollutant concentrations (see Equation 2.15). Consequently the effectiveness of the PIRAQI model may be different from that of the PIRAM model.

PIRAM estimated individual O_3 AQIs and portable air pollution sampler collected ambient O_3 AQIs in the Houston region on December 27th & 28th, 2010 were converted using the AQI calculator (see Figure 7.2). The curve of PIRAM estimated individual O_3 AQIs fitted well with the result of portable air pollution sampler collected ambient O_3 AQIs, which indicated that PIRAQI can effectively assess individual AQIs in the Houston region. Through the paired-sample t-test for comparing PIRAM estimated individual O_3 AQIs and portable air pollution sampler collected ambient O_3 AQIs in the Houston region on December 27th & 28th, 2010 using SPSS, I found the *p*-value of the t-

test was 0.464, which meant that there was no significant difference between the two groups (see Table 7.2).

Figure 7.2. PIRAM Estimated Individual O$_3$ AQIs (a) vs. Portable Air Pollution Sampler Collected Ambient O$_3$ AQIs (b) in the Houston Region on December 27th & 28th, 2010.

Note: Unit: (ppb).

Table 7.2. The Paired-Samples T-Test for Comparing PIRAM Estimated Individual O$_3$ AQIs and Portable Air Pollution Sampler Collected Ambient O$_3$ AQIs in the Houston Region on December 27th & 28th, 2010.

Paired Samples Test

		Paired Differences							Sig. (2-tailed)
					95% Confidence Interval of the Difference				
		Mean	Std. Deviation	Std. Error Mean	Lower	Upper	t	df	
Pair 1	Estimated AQI – Observed AQI	-.457	5.951	.620	-1.689	.776	-.736	91	.464

Real-time individual O$_3$ intake rate is decided by the real-time ambient O$_3$ concentrations and real-time individual air intake volume per minute. In this dissertation research, real-time individual air intake volume per minute was estimated using Holmes's table of individual average air intake volume per minute, which is related to population groups (i.e., children, adult females, and adult males) and their physical activities (e.g., staying, walking, and running). Data needed for deciding individual average air intake volume per minute included questionnaire & travel diary, land use / land cover data, and GPS data. The ratio of PIRADS estimated individual O$_3$ intake to portable air pollution sampler collected ambient O$_3$ intake equals to the ratio of PIRADS estimated individual O$_3$ exposure to portable air pollution sampler collected ambient O$_3$ concentration.

$$\frac{I_{PIRADS}}{I_{Sampled}} = \frac{E_{PIRAM}*IR_{Air}}{C_{Sampled}*IR_{Air}} = \frac{E_{PIRAM}}{C_{Sampled}}$$
Equation 7.1.

where I_{PIRADS} is PIRADS estimated real-time individual O_3 intake, $I_{Sampled}$ is portable

air pollution sampler collected ambient O_3 intake, E_{PIRAM} is PIRAM estimated real-time

individual O_3 exposure, $C_{Sampled}$ is real-time ambient O_3 concentration, and IR_{Air} is real-

time individual air intake volume per minute.

Consequently the effectiveness of the PIRADS model is same as that of the

PIRAM model. The PIRADS model can effectively estimate individual's personal air

pollution intake in the Houston region.

Individual-Based Air Pollution Exposure Modeling in the Austin Region

The near real-time space-time O_3 pollution scenario cube constructed using the

spatial interpolation methods in the Austin region on November 2nd, 2010 (see Figure

5.11) was used as the near real-time air pollution information platform for the individual

air pollution exposure modeling in the Austin region. The volunteer's real-time space-

time path in the Austin region on November 2nd, 2010 (see Figure 6.6) was used as the

individual real-time space-time behavior monitoring data for the individual air pollution

exposure modeling in the Austin region. After ArcGIS operations such as raster

calculation, raster extraction, and zonal statistics, PIRAM estimated individual O_3

exposure in the Austin region was calculated (see Figure 7.3). The curve of PIRAM

estimated individual O_3 exposure did not fit well with the result of portable air pollution

sampler collected ambient O_3 concentrations (i.e., the observed ground truth data), which

indicated that the PIRAM model may not effectively assess individuals' personal

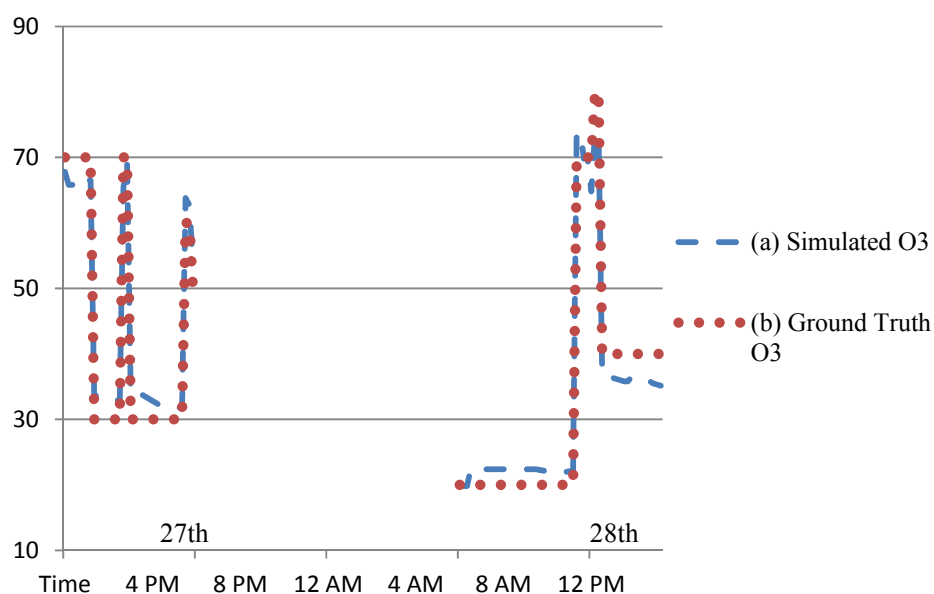exposure to air pollution in the Austin region. However, through the paired-sample t-test

for comparing PIRAM estimated individual O_3 exposure and portable air pollution

sampler collected ambient O_3 concentrations in the Austin region on November 2nd, 2010 using SPSS (volunteer's individual O_3 exposure was sampled every ten minutes in the day. Sixty-seven paired-samples were analyzed.), I found the *p*-value of the t-test was 0.087, which meant that there was significant difference between the two groups at the 90 percent confidence level (see Table 7.3). Based on the result, hypothesis 1 in the Austin region was not supported.

Figure 7.3. PIRAM Estimated Individual O_3 Exposure (a) vs. Portable Air Pollution Sampler Collected Ambient O_3 Concentrations (b) in the Austin Region on November 2nd, 2010.

Note: Unit: (ppb).

Table 7.3. The Paired-Samples T-Test for Comparing PIRAM Estimated Individual

O$_3$ Exposure and Portable Air Pollution Sampler Collected Ambient O$_3$

Concentrations in the Austin Region on November 2nd, 2010.

Paired Samples Test

| | | Paired Differences | | | | | | |
| | | | | | 95% Confidence Interval of the Difference | | | | Sig. (2-tailed) |
		Mean	Std. Deviation	Std. Error Mean	Lower	Upper	t	df	
Pair 1	PIRAM estimated - Sampler collected	.9741294	4.5893719	.5606810	-.1453064	2.0935651	1.737	66	.087

PIRAM estimated individual O$_3$ AQIs and portable air pollution sampler collected ambient O$_3$ AQIs in the Austin Region on November 2nd, 2010 were converted using the AQI calculator (see Figure 7.4). The curve of PIRAM estimated individual O$_3$ AQIs did not fit well with the result of portable air pollution sampler collected ambient O$_3$ AQIs, which indicated that PIRAQI may not effectively assess individual AQIs in the Austin region. Through the paired-sample t-test for comparing PIRAM estimated individual O$_3$ AQIs and portable air pollution sampler collected ambient O$_3$ AQIs in the Austin Region on November 2nd, 2010 using SPSS, I found the *p*-value of the t-test was 0.013, which meant that there was significant a difference between the two groups (see Table 7.4).
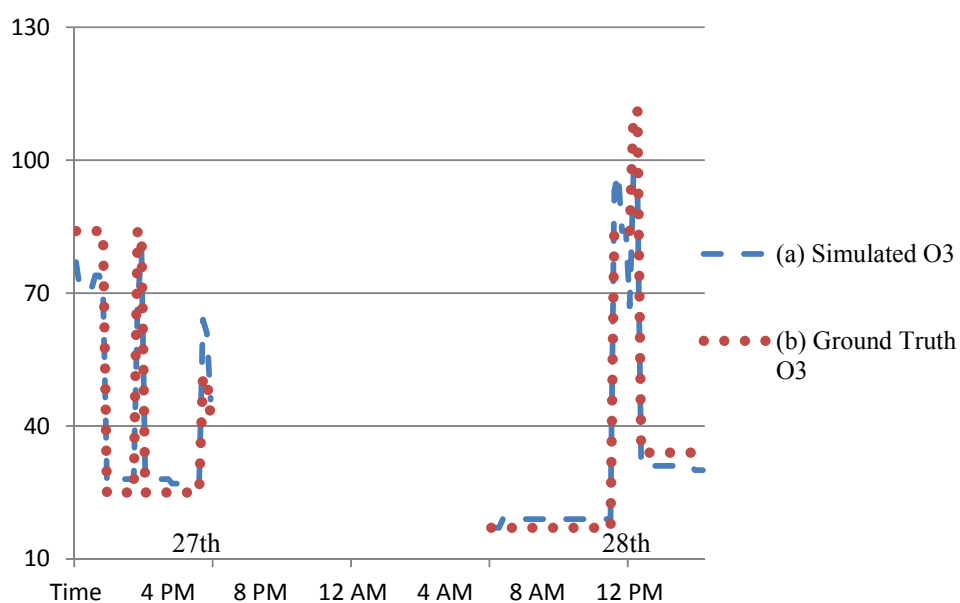
Figure 7.4. PIRAM Estimated Individual O$_3$ AQIs (a) vs. Portable Air Pollution

Sampler Collected Ambient O$_3$ AQIs (b) in the Austin Region on November 2nd,

2010.

Note: Unit: (ppb).

Table 7.4. The Paired-Samples T-Test for Comparing PIRAM Estimated Individual

O$_3$ AQIs and Portable Air Pollution Sampler Collected Ambient O$_3$ AQIs in the

Austin Region on November 2nd, 2010.

Paired Samples Test

					95% Confidence Interval of the Difference				
				Std.					**Sig. (2-**
			Std.	**Error**					
		Mean	**Deviation**	**Mean**	**Lower**	**Upper**	**t**	**df**	**tailed)**
Pair 1	Estimated AQI – Observed AQI	1.149	3.673	.449	.253	2.045	2.561	66	.013

Because the effectiveness of the PIRADS model is same as that of the PIRAM model, the PIRADS model can effectively estimate individual's personal air pollution intake in the Austin region.

Individual-Based Air Pollution Exposure Modeling in the San Antonio Region

The near real-time space-time O_3 pollution scenario cube constructed using the spatial interpolation methods in the San Antonio region on October 26th, 2010 (see Figure 5.16) was used as the near real-time air pollution information platform for the individual air pollution exposure modeling in the San Antonio region. The volunteer's real-time space-time path in the San Antonio region on October 26th, 2010 (see Figure 6.10) was used as the individual real-time space-time behavior monitoring data for the individual air pollution exposure modeling in the San Antonio region. After ArcGIS operations such as raster calculation, raster extraction, and zonal statistics, PIRAM estimated individual O_3 exposure in the San Antonio region was calculated (see Figure 7.5). The curve of PIRAM estimated individual O_3 exposure did not fit well with the result of portable air pollution sampler collected ambient O_3 concentrations (i.e., the observed ground truth data), which indicated that the PIRAM model may not effectively assess individuals' personal exposure to air pollution in the San Antonio region. However, through the paired-sample t-test for comparing PIRAM estimated individual O_3 exposure and portable air pollution sampler collected ambient O_3 concentrations in the San Antonio region on October 26th, 2010 using SPSS (volunteer's individual O_3 exposure was sampled every ten minutes in the day. Sixty-seven paired-samples were analyzed), I found the *p*-value of the t-test was 0.198, which meant that there was no significant difference between the two groups (see Table 7.5). Based on the result, hypothesis 1 in the San Antonio region was supported.
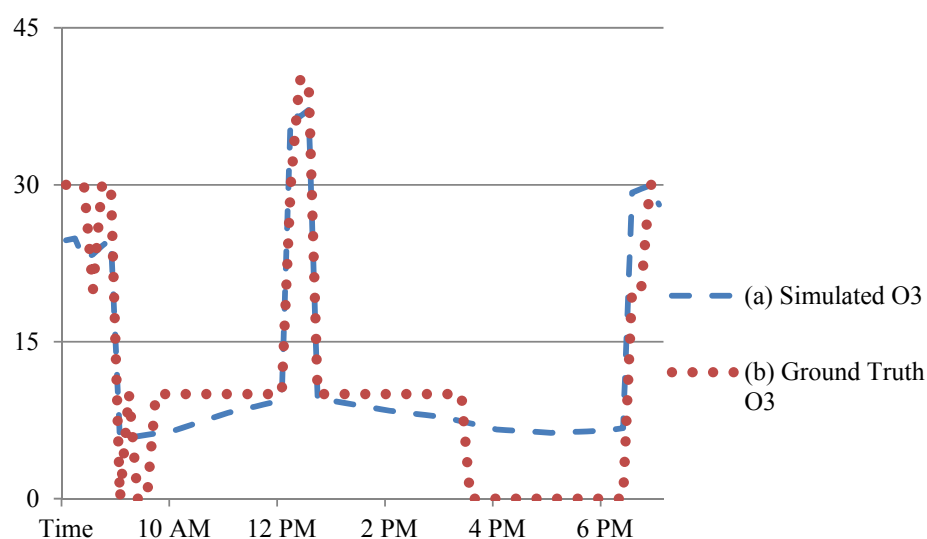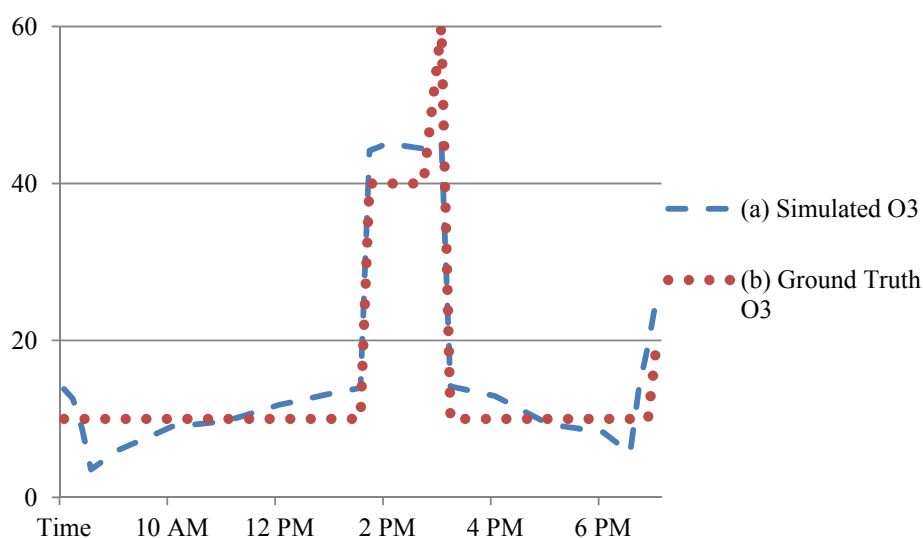
Figure 7.5. PIRAM Estimated Individual O$_3$ Exposure (a) vs. Portable Air Pollution Sampler Collected Ambient O$_3$ Concentrations (b) in the San Antonio Region on October 26th, 2010.

Note: Unit: (ppb).

Table 7.5. The Paired-Samples T-Test for Comparing PIRAM Estimated Individual O$_3$ Exposure and Portable Air Pollution Sampler Collected Ambient O$_3$ Concentrations in the San Antonio Region on October 26th, 2010.

			Paired Samples Test						
			Paired Differences						
					95% Confidence Interval of the Difference				
		Std. Deviation	**Std. Error Mean**						**Sig. (2-tailed)**
	Mean			**Lower**	**Upper**	**t**	**df**		
Pair 1 PIRAM estimated - Sampler collected	.5905473	3.7197922	.4544449	-.3167813	1.4978759	1.299	66		.198

PIRAM estimated individual O_3 AQIs and portable air pollution sampler collected ambient O_3 AQIs in the San Antonio Region on October 26th, 2010 were converted using the AQI calculator (see Figure 7.6). The curve of PIRAM estimated individual O_3 AQIs did not fit well with the result of portable air pollution sampler collected ambient O_3 AQIs, which indicated that PIRAQI may not effectively assess individual AQIs in the San Antonio region. Through the paired-sample t-test for comparing PIRAM estimated individual O_3 AQIs and portable air pollution sampler collected ambient O_3 AQIs in the San Antonio Region on October 26th, 2010 using SPSS, I found the *p*-value of the t-test was 0.020, which meant that there was significant a difference between the two groups (see Table 7.6).
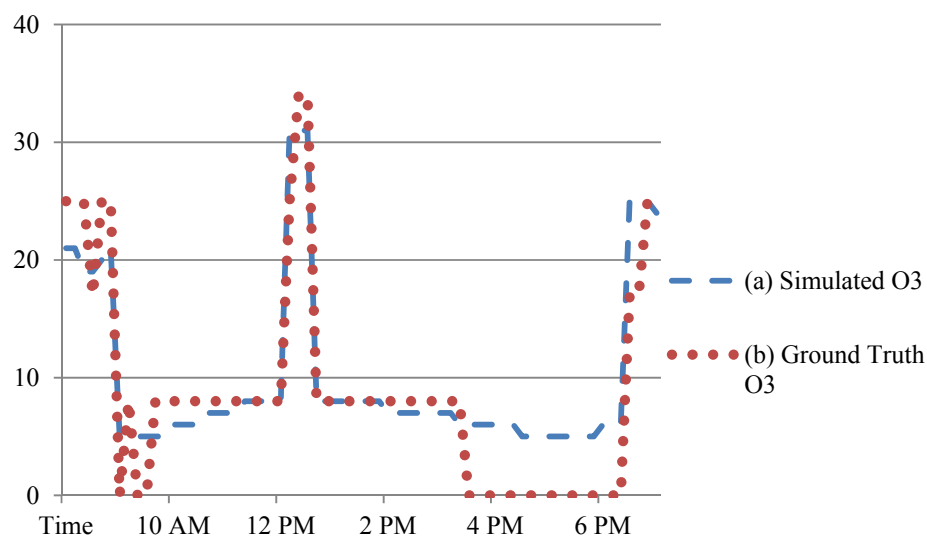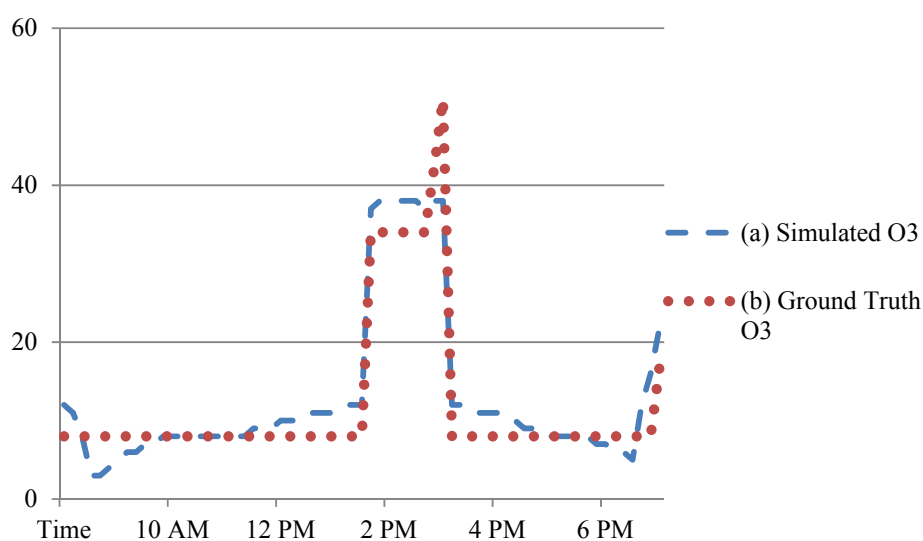

Figure 7.6. PIRAM Estimated Individual O_3 AQIs (a) vs. Portable Air Pollution Sampler Collected Ambient O_3 AQIs (b) in the San Antonio Region on October 26th, 2010.

Note: Unit: (ppb).

Table 7.6. The Paired-Samples T-Test for Comparing PIRAM Estimated Individual O₃ AQIs and Portable Air Pollution Sampler Collected Ambient O₃ AQIs in the San Antonio Region on October 26ᵗʰ, 2010.

<div align="center">Paired Samples Test</div>

		Paired Differences						
					95% Confidence Interval of the Difference				
		Mean	Std. Deviation	Std. Error Mean	Lower	Upper	t	df	Sig. (2-tailed)
Pair 1	Estimated AQI - Observed AQI	.910	3.127	.382	.148	1.673	2.383	66	.020

Because the effectiveness of the PIRADS model is same as that of the PIRAM model, the PIRADS model can effectively estimate individual's personal air pollution intake in the San Antonio region.

Summary

The effectiveness of the pseudo individual near real-time air pollution monitoring (PIRAM) models in the Houston region, the Austin region, and the San Antonio region was examined using the paired-sample t-test. T-test results showed that the PIRAM models in the Houston region and the San Antonio region were effective (the *p*-values of the two models were greater than 0.10). Hypothesis 1 for Houston and San Antonio was accepted. However, the PIRAM model in the Austin region was not effective at the 90 percent confidence level. Hypothesis 1 for Austin was not rejected.

Furthermore, the effectiveness of the PIRAM models in different cities was different. T-test results showed that the effectiveness of the PIRAM model in the Houston region was highest, in the San Antonio region was medium, and in the Austin region was lowest. Hypothesis 2 was rejected.

The effectiveness of the pseudo individual near real-time air quality index (PIRAQI) models in the Houston region, the Austin region, and the San Antonio region was examined using the paired-sample t-test too. Among the PIRAQI models in the three regions, only the PIRAQI model in the Houston region was effective at the 90 percent confidence level.

The effectiveness of the pseudo individual near real-time air pollution dose simulation (PIRADS) models was similar to that of the PIRAM models. Consequently, the PIRADS models in the Houston region and the San Antonio region were effective; the PIRADS model in the Austin region was not effective.

CHAPTER VIII

CONCLUSION AND DISCUSSION

Summary of Research and Findings

Through a series of spatial analysis and modeling approaches, this dissertation research enhances the knowledge regarding individual near real-time measurement for air pollution exposure and intake in three selected Texas cities – Houston, Austin, and San Antonio. This research builds upon individual-based air pollution exposure measures and offers a new method to assess individual air pollution exposure. The main purpose of this research was to build models to estimate individual near real-time air pollution exposure and intake. Three innovative aspects of the study included: development of near real-time space-time air pollution scenario cubes, individual real-time space-time behavior 3D mapping, and integrating space-time cubes and space-time behaviors to develop the pseudo individual near real-time air pollution monitoring models.

First, this study adopted a near real-time space-time air pollution scenario cube approach to portray a dynamic urban air pollution scenario across space and time. Originating from time geography, space-time cubes provide an approach to integrate spatial and temporal air pollution information into a 3D space. The base of the cube represents the variation of air pollution in a 2D geographical space while the height represents time. This way, the changes of pollution over time can be described by the

different component layers of the cube from the base up. The diurnal ambient ozone (O_3) pollution conditions in Houston, Austin, and San Antonio, Texas were modeled using the space-time air pollution cube approach. Two methods, i.e., the LUR modeling and the spatial interpolation methods, were applied to build the hourly component layers for the air pollution cube in the Houston region. It was found that the LUR modeling performed better than the spatial interpolation methods in predicting air pollution level. The spatial interpolation methods were applied in the Austin region and the San Antonio region. With the availability of real-time air pollution data, this approach can be extended to produce real-time air pollution cube for more accurate air pollution measurement across space and time, which can provide important support to studies in epidemiology, health geography, and environmental regulation.

Second, volunteers' individual real-time space-time travel behavior data in the three study areas were geovisualized using 3D space-time path maps. Comparing with conventional 2D maps, 3D maps can show individual travel behavior without losing temporal information and make individual travel path more readable. The volunteer's space-time travel data were processed in ArcScene. In the 3D space-time path maps, the vertical dimension (z) represents travel time; the horizontal dimensions (x, y) represent the horizontal space of study areas.

Third, the integrated pseudo individual near real-time air pollution monitoring (PIRAM) models, the integrated pseudo individual near real-time air quality index (PIRAQI) models, and the integrated pseudo individual near real-time air pollution dose simulation (PIRADS) models were developed on the base of the near real-time space-

time cubes, the individual real-time space-time travel paths, the AQI calculator, and individual real-time air intake volume per minute.

Consequently, this study was carried out through developing models and answering the two major research questions about the models:

- Does the pseudo individual near real-time air pollution monitoring model effectively assess individuals' personal exposure to air pollution?

- Is the monitoring model equally effective in different cities and regions?

Results of paired-sample t-tests for comparing PIRAM estimated individual O_3 exposure and portable air pollution sampler collected ambient O_3 concentrations showed the PIRAM models in the Houston region and the San Antonio region were effective (*p*-values were 0.341 and 0.198 in the Houston region and the San Antonio region, respectively). However, the PIRAM model in the Austin region was not effective at the 90 percent confidence level (p-value was 0.087). The effectiveness order of the PIRAM models is Houston greater than San Antonio greater than Austin. The effectiveness order is similar to the order of the numbers of EPA air monitoring sites in each region, which largely impacts the accuracy of the near real-time space-time air pollution scenario cube. In other words, the effectiveness of the PIRAM model is related to the number of EPA air monitoring sites in the region.

The effectiveness of the PIRADS models was similar to that of the PIRAM models (see Equation 7.1). Consequently, the PIRADS models in the Houston region and the San Antonio region were effective; the PIRADS model in the Austin region was not effective.

AQIs have a segmented linear relationship with air pollutant concentrations (see Equation 2.15). Consequently the effectiveness of the PIRAQI model may be different from that of the PIRAM model. Results of paired-sample t-tests for comparing PIRAM estimated individual O_3 AQIs and portable air pollution sampler collected ambient O_3 AQIs were different. The PIRAQI model in the Houston region was effective (*p*-value was 0.464); the PIRAQI models in the Austin region and the San Antonio region were not effective (*p*-values were 0.013 and 0.020, respectively). Given the limited numbers of EPA air monitoring sites in the Austin region and the San Antonio region, the PIRAQI model is suitable for cities with a large number of EPA air monitoring sites.

Comparing results of the PIRAM models and the PIRAQI models in the study area, I found that both models were effective in the Houston region; the PIRAM model was effective and the PIRAQI model was not effective in the San Antonio region; both models were not effective in the Austin region. The results show that the practical application of the dissertation research needs to consider the actual condition of the study area.

The severity of O_3 pollution in the three selected Texas cities is Houston greater than San Antonio greater than Austin. The different air pollution scenarios in these regions cause the variations of the degree of concerns about air pollution and adverse health effect, and influence government decision-making for air monitoring, which is related to the numbers of regional EPA air monitoring sites. Consequently, in heavily polluted cities, near real-time space-time urban ambient air pollution scenario cubes are more accurate, and then pseudo individual near real-time air pollution monitoring models are more effective. The second research question can be answered as: the pseudo

individual near real-time air pollution monitoring model is not equally effective in different cities and regions; the effectiveness of the model is positively correlated to the degree of air pollution in the region.

It should be noted that the PIRAM model has very flexible structures because individual position monitoring and the air pollution monitoring are allowed to operate separately. This approach is not unfamiliar to the public considering that numerous mobile phone users are already recording real-time location through the embedded GPS units and that thousands public air monitoring sites (including EPA sites) in the U.S. have been recording real-time air pollution concentration. With proper integration mechanism designed, the application of the PIRAM model could be accepted by the general population relatively easily. Citizens do not need to carry any additional air pollution sampler; a regular smart phone is the only personal equipment needed. The whole monitoring process is automatic; personal daily activities are not affected.

Limitations

Several limitations may impact the accuracy of the pseudo individual near real-time measurement for assessing air pollution exposure. First, the accuracy of the PIRAM models may be influenced by the outdoor air pollution assessment method. Because when constructing the near real-time space-time air pollution scenario cube, the outdoor air pollution maps were generated by either the LUR model or the interpolation of the EPA air monitoring site report data, the accuracy of the hourly outdoor air pollution maps were affected by the number and the distribution of the monitoring sites and the modeling method applied. Consequently, in the lightly polluted cities such as the Austin region,

where the EPA air monitoring site report data is very limited, the hourly outdoor air pollution maps may not depict the spatial variation of pollution actually. Nevertheless, because the air pollution spatial heterogeneity in the lightly polluted cities is not as obvious as that in the heavily polluted cities, the insufficiency of EPA air monitoring sites is not a critical limitation. Second, the accuracy of the PIRAM models may be influenced by the indoor air pollution assessment method. In this dissertation research, indoor air pollution was calculated by the indoor-generated and the outdoor-penetrated air pollution. Indoor-generated O_3 and ventilation-filter-removed O_3 were not considered because of their small proportion. The outdoor-penetrated air pollution was decided by the outdoor air pollution concentration and the ACH, which is season-specific instead of building-specific. Third, the integration of the indoor-outdoor microenvironments and the individual space-time travel trajectories may not be accurate enough. In this dissertation research, the indoor-outdoor microenvironments were defined on the basis of land use / land cover data instead of on site measurement. The individual space-time travel trajectories were collected by GPS units. Because the GPS units have system errors and multipath errors, it is possible that the GPS records show the individual is in a building (i.e., indoor) but in fact the individual is on the side of the road (i.e., outdoor). Besides, the GPS units may lose signal inside buildings. The volunteer's travel diaries were used to help mitigate the GPS system error and signal problem. Fourth, real-time individual air intake volume per minute was estimated instead of measured. Because it is very hard to measure volunteer's real-time individual air intake volume per minute directly, this study applied Holmes's table of individual average air intake volume per minute and used questionnaire, travel diary, land use / land cover data, and GPS data to estimate

volunteer's real-time individual air intake volume per minute. This approach may affect the effectiveness of the PIRADS models. Fifth, only one volunteer was used in each region. The PIRAM models may suffer from problems such as sample representativeness.

Given these limitations, this dissertation research is not free from uncertainties for the individual-based air pollution exposure modeling.

Future Research

This dissertation research is motivated by the needs to assess individual air pollution exposure. It is grounded by the theory of time geography, spatial analysis and statistical analysis, geographic information technologies, information technologies, and health and epidemiology. This dissertation research tries to depict an individual-based air pollution exposure and dose accumulation scenario. This dissertation research is an exploratory study that provides a quick-response and low-cost individual near real-time air pollution exposure assessment solution.

Due to the limitations in the individual-based air pollution exposure modeling approach as discussed above, future research may focus on three aspects. First, efforts will be made to enhance the accuracy of the individual-based air pollution exposure modeling. As one important module of the individual-based air pollution exposure modeling, the space-time air pollution scenario cube needs to be improved. In cities with limited numbers of EPA air monitoring sites (e.g., Austin), other sampling methods, such as local government and private ambient air sampling network, are good supplementary approaches. Indoor air pollution assessment method needs to be refined. Besides outdoor-penetrated O_3, O_3 from other sources should be estimated appropriately. Second, the

representativeness and effectiveness of the individual-based air pollution exposure modeling will be further examined by recruiting more volunteers in similar age groups and/or from similar backgrounds. For example, it would be interesting to modeling near real-time air pollution exposure for specific population groups (e.g., housewives and school-age children). The individual-based air pollution exposure modeling will be applied in other regions to evaluate its adaptability. Third, other air pollutants (e.g., $PM_{2.5}$ and SO_2) will be included to widen the application of the model and improve the model as a near real-time personal air monitoring platform.

The major focus of this dissertation research was the development of the PIRAM model. Two derivatives of the PIRAM model (i.e., the PIRAQI model and the PIRADS model) are not investigated intensively. They are important models – the PIRAQI model can concisely indicate individual's personal air pollution exposure level and personal air pollution health concern; the PIRADS can provide the detailed inhaled air pollutant dose, it is suitable to profile individual real-time air pollution health risk. Further study on the PIRAQI model and the PIRADS model will be undertaken to support the study of human health effect of air pollution.

LITERATURE CITED

Abrahamowicz, M., et al. 2003. Flexible modeling of exposure-response relationship between long-term average levels of particulate air pollution and mortality in the American Cancer Society Study. *Journal of Toxicology and Environmental Health - Part A,* 66(16-19)**:** 1625-53.

AbuJayyab, M., et al. 2006. PolluMap: A pollution mapper for cities. In *proceedings of the Innovations in Information Technology*, 491-95, 541. Dubai, the United Arab Emirates: IEEE.

ACE. 2010. Natural air pollution. http://www.ace.mmu.ac.uk/eae/air_quality/older/Natural_Air_Pollution.html (last accessed 17 September 2010).

Adams, C., P. Riggs & J. Volckens. 2009. Development of a method for personal, spatiotemporal exposure assessment. *Journal of Environmental Monitoring,* 11(7)**:** 1331-39.

AIR. 2010. AIR preemptive media project. http://www.pm-air.net/index.php (last accessed 23 April 2010).

AIRNow. 2010a. AQI calculator: Concentration to AQI. http://www.airnow.gov/index.cfm?action=resources.conc_aqi_calc (last accessed 17 September 2010).

_____. 2010b. Local air quality conditions and forecasts. http://www.airnow.gov/index.cfm?action=airnow.main (last accessed 17 September 2010).

ALA. 2010. The state of the air. http://www.stateoftheair.org/2010/assets/SOTA2010.pdf (last accessed 17 October 2010).

Andersen, Z. J., et al. 2008. Ambient air pollution triggers wheezing symptoms in infants. *Thorax,* 63(8)**:** 710-16.

Arain, M. A., et al. 2009. Meteorological influences on the spatial and temporal variability of NO2 in Toronto and Hamilton. *Canadian Geographer / Le Géographe canadien,* 53(2)**:** 165-90.

Arain, M. A., et al. 2007. The use of wind fields in a land use regression model to predict air pollution concentrations for health exposure studies. *Atmospheric Environment,* 41(16)**:** 3453-64.

Arshad, M. J., A. Farooq & A. Shah. 2010. Evolution and development towards 4 th generation (4G) mobile communication systems. *Journal of American Science,* 6(12)**:** 63-68.

Avruskin, G. A., et al. 2004. Visualization and exploratory analysis of epidemiologic data using a novel space time information system. *International Journal of Health Geographics,* 3(1)**:** 26.

Ballesta, P. P., et al. 2008. An approach for the evaluation of exposure patterns of urban populations to air pollution. *Atmospheric Environment,* 42(21)**:** 5350-64.

Barzyk, T. M., et al. 2009. Development of a distance-to-roadway proximity metric to compare near-road pollutant levels to a central site monitor. *Atmospheric Environment,* 43(4)**:** 787-97.

Bell, M., et al. 2007. Climate change, ambient ozone, and health in 50 US cities. *Climatic Change,* 82(1)**:** 61-76.

Bell, M. L., D. L. Davis & T. Fletcher. 2004a. A retrospective assessment of mortality from the London smog episode of 1952: The role of influenza and pollution. *Environmental Health Perspectives,* 112(1)**:** 6-8.

Bell, M. L., et al. 2004b. Ozone and short-term mortality in 95 US urban communities, 1987-2000. *Journal of the American Medical Association,* 292(19)**:** 2372-78.

Bell, M. L., J. M. Samet & F. Dominici. 2004c. Time-series studies of particulate matter. *Annual Review of Public Health,* 25: 247-80.

Belleudi, V., et al. 2010. Impact of fine and ultrafine particles on emergency hospital admissions for cardiac and respiratory diseases. *Epidemiology,* 21(3)**:** 414-23.

Benenson, I. & P. M. Torrens. 2004. *Geosimulation: Automata-based Modeling of Urban Phenomena*. Chichester, West Sussex, England: John Wiley & Sons.

Bian, L. 2007. Object-oriented representation of environmental phenomena: Is everything best represented as an object? *Annals of the Association of American Geographers,* 97(2)**:** 267-81.

Bonabeau, E. 2002. Agent-based modeling: Methods and techniques for simulating human systems. *Proceedings of the National Academy of Sciences of the United States of America,* 99: 7280-87.

Boogaard, H., et al. 2009. Exposure to ultrafine and fine particles and noise during cycling and driving in 11 Dutch cities. *Atmospheric Environment,* 43(27)**:** 4234-42.

Briggs, D. J., et al. 1997. Mapping urban air pollution using GIS: A regression-based approach. *International Journal of Geographical Information Science,* 11(7)**:** 699-718.

Brunekreef, B. & S. T. Holgate. 2002. Air pollution and health. *Lancet,* 360(9341)**:** 1233-42.

Butz, W. P. & B. B. Torrey. 2006. Some frontiers in social science. *Science,* 312(5782)**:** 1898-900.

Butzer, K. W. 2002. Commentary/response: Turner's "contested identities". *Annals of the Association of American Geographers,* 92(1)**:** 75-86.

Canova, C., et al. 2010. Carbon monoxide pollution is associated with decreased lung function in asthmatic adults. *European Respiratory Journal,* 35(2)**:** 266-72.

CAPCOG. 2010. Capital area council of governments' information clearinghouse. http://www.capcog.org/information-clearinghouse/geospatial-data/ (last accessed 17 September 2010).

Cape, J. N. 2008. Interactions of forests with secondary air pollutants: some challenges for future research. *Environmental Pollution,* 155(3)**:** 391-97.

Chiang, K., et al. 2008. In the direction of a sensor mapping platform based on cellular phone networks. In *proceedings of the Wireless Telecommunications Symposium, 2008*, 348-53. Pomona, CA: IEEE.

Clougherty, J., et al. 2008. Land use regression modeling of intra-urban residential variability in multiple traffic-related air pollutants. *Environmental Health,* 7(1)**:** 17.

Clougherty, J. E., et al. 2007. Synergistic effects of traffic-related air pollution and exposure to violence on urban asthma etiology. *Environmental Health Perspectives,* 115(8)**:** 1140-46.

CoCoRaHS. 2010. Community collaborative rain, hail & snow network. http://www.cocorahs.org/ (last accessed April 23 2010).

Cohen, A., et al. 2004. Urban air pollution. In *Comparative Quantification of Health Risks,* eds. M. Ezzati, A. Lopez, A. Rodgers & C. Murray, 1353-434. Geneva: World Health Organization.

COHGIS. 2010. City Of Houston geographic information system release. http://cohgis.houstontx.gov/cohgis2009/index.htm (last accessed 17 September 2010).

Cook, R., et al. 2008. Resolving local-scale emissions for modeling air quality near roadways. *Journal of the Air & Waste Management Association,* 58(3)**:** 451-61.

COSA. 2010. City of San Antonio - Geographic information systems. https://gis.sanantonio.gov/GIS/default.aspx (last accessed 17 September 2010).

Coulibaly, M. & S. Becker. 2007. Spatial interpolation of annual precipitation in South Africa - Comparison and evaluation of methods. *Water International,* 32(3)**:** 494-502.

CreativeMethods. 2010. United States air quality. http://www.creativemethods.com/airquality/maps/united_states.htm (last accessed 17 September 2010).

Croner, C. M., J. Sperling & F. R. Broome. 1996. Geographic information systems (GIS): New perspectives in understanding human health and environmental relationships. *Statistics in Medicine,* 15(17-18)**:** 1961-77.

Cullinan, P., S. D. Acquilla & V. R. Dhara. 1996. Long term morbidity in survivors of the 1984 Bhopal gas leak. *National Medical Journal of India,* 9(1)**:** 5-10.

Curtis, L., et al. 2006. Adverse health effects of outdoor air pollutants. *Environment International,* 32(6)**:** 815-30.

de Bilderling, G., et al. 2005. Gas cooking and smoking habits and the risk of childhood and adolescent wheeze. *American Journal of Epidemiology,* 162(6)**:** 513-22.

Delfino, R. J., et al. 2009. Air pollution exposures and circulating biomarkers of effect in a susceptible population: Clues to potential causal component mixtures and mechanisms. *Environmental Health Perspectives,* 117(8)**:** 1232-38.

Delfino, R. J., et al. 2008. Circulating biomarkers of inflammation, antioxidant activity, and platelet activation are associated with primary combustion aerosols in subjects with coronary artery disease. *Environmental Health Perspectives,* 116(7)**:** 898-906.

Delgado-Saborit, J. M., et al. 2009. Model development and validation of personal exposure to volatile organic compound concentrations. *Environmental Health Perspectives,* 117(10)**:** 1571-79.

Demšar, U. & K. Virrantaus. 2010. Space-time density of trajectories: Exploring spatio-temporal patterns in movement data. *International Journal of Geographical Information Science,* 24(10)**:** 1527-42.

DiNucci, D. 1999. Fragmented future. *Print,* 53(4)**:** 32.

Dockery, D. W., et al. 1996. Health effects of acid aerosols on North American children: Respiratory symptoms. *Environmental Health Perspectives,* 104(5)**:** 500-05.

Dominici, F., et al. 2006. Fine particulate air pollution and hospital admission for cardiovascular and respiratory diseases. *Journal of the American Medical Association,* 295(10)**:** 1127-34.

Doyle, M. W. & S. H. Ensign. 2009. Alternative reference frames in river system science. *Bioscience,* 59(6)**:** 499-510.

Du, X. & J. Liu. 2009. Relationship between outdoor and indoor ozone pollution concentration. *Transactions of Tianjin University,* 15(5)**:** 330-35.

Duan, N. 1982. Models for human exposure to air pollution. *Environment International,* 8: 305-09.

Duncan, M. J., H. M. Badland & W. K. Mummery. 2009. Applying GPS to enhance understanding of transport-related physical activity. *Journal of Science and Medicine in Sport,* 12(5)**:** 549-56.

Dutta, P., et al. 2009. Common sense: Participatory urban sensing using a network of handheld air quality monitors. In *proceedings of the 7th ACM Conference on Embedded Networked Sensor Systems*, 349-50. Berkeley, CA: ACM.

Edwards, R. & M. Jantunen. 2009. Subgroups exposed to systematically different elemental compositions of PM2.5. *Atmospheric Environment,* 43(22-23)**:** 3571-78.

Edwards, R., et al. 2006. Does living near heavy industry cause lung cancer in women? A case-control study using life grid interviews. *Thorax,* 61(12)**:** 1076-82.

Edwards, R. D., et al. 2001. VOC source identification from personal and residential indoor, outdoor and workplace microenvironment samples in EXPOLIS-Helsinki, Finland. *Atmospheric Environment,* 35(28)**:** 4829-41.

Edwards, R. D., et al. 2005. Personal exposures to VOC in the upper end of the distribution - Relationships to indoor, outdoor and workplace concentrations. *Atmospheric Environment,* 39(12)**:** 2299-307.

EPA. 2008a. About the national emission inventory database. http://www.epa.gov/oar/data/neidb.html (last accessed 15 August 2010).

_____. 2008b. History of the Clean Air Act. http://www.epa.gov/air/caa/caa_history.html (last accessed 17 September 2010).

_____. 2008c. Total risk integrated methodology (TRIM) air pollutants exposure model documentation (TRIM.Expo/APEX, version 4.3) volume I: User's guide. http://www.epa.gov/ttn/fera/data/apex/APEX_UsersGuide_Vol1_Oct08.pdf (last accessed 22 September 2012).

_____. 2009a. Air pollutants. http://www.epa.gov/ebtpages/airairpollutants.html (last accessed 6 December 2009).

_____. 2009b. Technical assistance document for the reporting of daily air quality: The air quality index (AQI). Research Triangle Park, North Carolina: Environmental Protection Agency. EPA-454/B-09-001.

_____. 2010a. Air quality index report. http://iaspub.epa.gov/airsdata/adaqs.aqi?geotype=st&geocode=TX&geoinfo=st~TX~Texas&year=2008&sumtype=co&fld=gname&fld=gcode&fld=stabbr&fld=regn&rpp=25 (last accessed 17 September 2010).

_____. 2010b. National ambient air quality standards (NAAQS).
http://www.epa.gov/air/criteria.html (last accessed 17 September 2010).

_____. 2010c. What is air pollution? http://www.epa.gov/airnow/airaware/day1.html (last accessed 17 September 2010).

Ezzati, M. 2005. Indoor air pollution and health in developing countries. *Lancet,* 366(9480)**:** 104-06.

Fang, T. B. & Y. Lu. 2011. Constructing a near real-time space-time cube to depict urban ambient air pollution scenario. *Transactions in GIS,* 15(5)**:** 635-49.

_____. 2012. Personal real-time air pollution exposure assessment methods promoted by information technological advances. *Annals of GIS,* in press. DOI: 10.1080/19475683.2012.727866.

Filleul, L., et al. 2006. The relation between temperature, ozone, and mortality in nine French cities during the heat wave of 2003. *Environmental Health Perspectives,* 114(9)**:** 1344-47.

Fruin, S., et al. 2008. Measurements and predictors of on-road ultrafine particle concentrations and associated pollutants in Los Angeles. *Atmospheric Environment,* 42(2)**:** 207-19.

Fuentes, M. 2002. Interpolation of nonstationary air pollution processes: A spatial spectral approach. *Statistical Modelling,* 2(4)**:** 281-98.

Gaffin, J. M. & W. Phipatanakul. 2009. The role of indoor allergens in the development of asthma. *Current Opinion in Allergy and Clinical Immunology,* 9(2)**:** 128-35.

Garcia-Alegre, M. C., et al. 2001. Fuzzy diagnose microcontroller based system for air quality surveillance. In *proceedings of the 10th International Conference on Fuzzy Systems*, 1092-95, 597. Melbourne, Australia: IEEE.

Gatalsky, P., N. Andrienko & G. Andrienko. 2004. Interactive analysis of event data using space-time cube. In *proceedings of the 8th International Conference on Information Visualization*, 145-52. London, UK: IEEE.

Gauderman, W. J., et al. 2007. Effect of exposure to traffic on lung development from 10 to 18 years of age: A cohort study. *Lancet,* 369(9561)**:** 571-77.

Georgopoulos, P. G. & P. J. Lioy. 1994. Conceptual and theoretical aspects of human exposure and dose assessment. *Journal of Exposure Analysis and Environmental Epidemiology,* 4(3)**:** 253-85.

Gerharz, L. E., A. Kruger & O. Klemm. 2009. Applying indoor and outdoor modeling techniques to estimate individual exposure to PM2.5 from personal GPS profiles and diaries: A pilot study. *Science of the Total Environment,* 407(18)**:** 5184-93.

Gimbutaite, I. & Z. Venckus. 2008. Air pollution burning different kinds of wood in small power boilers. *Journal of Environmental Engineering and Landscape Management,* 16(2)**:** 97-103.

Goodchild, M. F. 2007a. Citizens as sensors: The world of volunteered geography. *GeoJournal,* 69(4)**:** 211-21.

_____. 2007b. Citizens as voluntary sensors: Spatial data infrastructurein the world of Web 2.0. *International Journal of Spatial Data Infrastructures Research,* 2: 24-32.

GranÖ, O. 2008. The history of geography in Sweden. *Geographical Review,* 98(3)**:** 416-21.

Greaves, S., T. Issarayangyun & Q. Liu. 2008. Exploring variability in pedestrian exposure to fine particulates (PM2.5) along a busy road. *Atmospheric Environment,* 42(8)**:** 1665-76.

H-GAC. 2010. Houston-Galveston area council http://www.h-gac.com/community/socioeconomic/land_use/default.aspx (last accessed 17 September 2010).

Hägerstrand, T. 1970. What about people in regional science. *Papers in Regional Science Association,* 24: 1-12.

Haynes, R., et al. 2007. Modifiable neighbourhood units, zone design and residents' perceptions. *Health & Place,* 13(4)**:** 812-25.

He, Q. Q., et al. 2010. Effects of ambient air pollution on lung function growth in Chinese schoolchildren. *Respiratory Medicine,* 104(10)**:** 1512-20.

Helfand, W. H., J. Lazarus & P. Theerman. 2001. Donora, Pennsylvania: An environmental disaster of the 20th century. *American Journal of Public Health,* 91(4)**:** 553.

Hertel, O., et al. 2006. Exposure modeling - Using operational air pollution models. *Toxicology Letters,* 164: 15-15.

Hoek, G., et al. 2008. A review of land-use regression models to assess spatial variation of outdoor air pollution. *Atmospheric Environment,* 42(33)**:** 7561-78.

Hoek, G., et al. 2001. Estimation of long-term average exposure to outdoor air pollution for a cohort study on mortality. *Epidemiology,* 12(4)**:** S92-S92.

Hoek, G., et al. 2002. Spatial variability of fine particle concentrations in three European areas. *Atmospheric Environment,* 36(25)**:** 4077-88.

Holmes, J. R. 1994. How much air do we breathe? (Measurement of breathing rate and volume in routinely performed activites). Springfield, VA: National Technical Information Service. No. 94-11.

Honicky, R., et al. 2008. N-smarts: Networked suite of mobile atmospheric real-time sensors. In *proceedings of the 2nd ACM SIGCOMM workshop on Networked systems for developing regions*, 25-30. Seattle, WA: ACM.

Honicky, R. E., C. A. Akpom & J. S. Osborne. 1983. Infant respiratory illness and indoor air-pollution from a woodburning stove. *Pediatrics,* 71(1)**:** 126-28.

IGS. 2009. International GNSS service, formerly the international GPS service. http://igscb.jpl.nasa.gov/ (last accessed Dec. 09 2009).

Ilgen, E., et al. 2001. Aromatic hydrocarbons in the atmospheric environment. Part III: Personal monitoring. *Atmospheric Environment,* 35(7)**:** 1265-79.

ITU. 2010. The world in 2010: ICT facts and figures. http://www.itu.int/ITU-D/ict/material/FactsFigures2010.pdf (last accessed 01 April 2011).

Janelle, D. G. 1969. Spatial organization: A model and concept. *Annals of the Association of American Geographers,* 59: 348-64.

Janssen, S., et al. 2008. Spatial interpolation of air pollution measurements using CORINE land cover data. *Atmospheric Environment,* 42(20)**:** 4884-903.

Jensen, S. S. 2006. A GIS-GPS modeling system for personal exposure to traffic air pollution. *Epidemiology,* 17(6)**:** S38-S38.

Johanson, G., et al. 1986. Toxicokinetics of inhaled 2-butoxyethanol (ethylene-glycol monobutyl ether) in man. *Scandinavian Journal of Work Environment & Health,* 12(6)**:** 594-602.

Juda-Rezler, K. 2010. New challenges in air quality and climate modeling. *Archives of Environmental Protection,* 36(1)**:** 3-28.

Kalapanidas, E. & N. Avouris. 2002. Air quality management using a multi-agent system. *Computer-Aided Civil and Infrastructure Engineering,* 17(2)**:** 119-30.

Kampa, M. & E. Castanas. 2008. Human health effects of air pollution. *Environmental Pollution,* 151(2)**:** 362-67.

Kan, H., et al. 2010. Short-term association between sulfur dioxide and daily mortality: The public health and air pollution in Asia (PAPA) study. *Environmental Research,* 110(3)**:** 258-64.

Kang, S. C., et al. 2009. Total suspended particulate matter and toxic elements indoors during cooking with yak dung. *Atmospheric Environment,* 43(27)**:** 4243-46.

Kattan, M., et al. 2007. Health effects of indoor nitrogen dioxide and passive smoking on urban asthmatic children. *Journal of Allergy and Clinical Immunology,* 120(3)**:** 618-24.

Keita, N., E. Carfagna & G. Mu'Ammar. 2010. Issues and guidelines for the emerging use of GPS and PDAs in agricultural statistics in developing countries. In *proceedings of the 5th International Conference on Agricultural Statistics (ICAS-V),* 12-15. Kampala, Uganda: FAO.

Khoder, M. I. 2009. Diurnal, seasonal and weekdays-weekends variations of ground level ozone concentrations in an urban area in greater Cairo. *Environmental Monitoring and Assessment,* 149(1-4)**:** 349-62.

Kim, E., et al. 2005. Spatial variability of fine particle mass, components, and source contributions during the regional air pollution study in St. Louis. *Environmental Science & Technology,* 39(11)**:** 4172-79.

Kim, S., E. Paulos & M. D. Gross. 2010. WearAir: Expressive t-shirts for air quality sensing. In *proceedings of the 4th International Conference on Tangible, Embedded, and Embodied Interaction,* 295-96. Cambridge, MA: ACM.

Korpi, A., J. Jarnberg & A. L. Pasanen. 2009. Microbial volatile organic compounds. *Critical Reviews in Toxicology,* 39(2)**:** 139-93.

Kostiainen, R. 1995. Volatile organic-compounds in the indoor air of normal and sick houses. *Atmospheric Environment,* 29(6)**:** 693-702.

Kraak, M. J. 2003. The space-time-cube revisited from a geovisualization perspective. In *proceedings of the 21st International Cartographic Conference (ICC),* 1988-96. Durban, South Africa:

Kramer, C. B., A. C. Cullen & E. M. Faustman. 2006. Policy implications of genetic information on regulation under the Clean Air Act: The case of particulate matter and asthmatics. *Environmental Health Perspectives,* 114(3)**:** 313-19.

Kwan, M.-P. 2002. Time, information technologies and the geographies of everyday life. *Urban Geography,* 23(5)**:** 471-82.

_____. 2009. From place-based to people-based exposure measures. *Social Science & Medicine,* 69(9)**:** 1311-13.

Kwan, M.-P., et al. 2003. Recent advances in accessibility research: Representation, methodology and applications. *Journal of Geographical Systems,* 5(1)**:** 129-38.

Kwan, M.-P. & J. Weber. 2003. Individual accessibility revisited: Implications for geographical analysis in the twenty-first century. *Geographical Analysis,* 35(4)**:** 341-53.

_____. 2008. Scale and accessibility: Implications for the analysis of land use-travel interaction. *Applied Geography,* 28(2)**:** 110-23.

Lam, N. S. N. 1983. Spatial interpolation methods: A review. *American Cartographer,* 10(2)**:** 129-49.

LaMance, J., J. DeSalas & J. Jarvinen. 2002. Assisted GPS: A low-infrastructure approach. *GPS World,* 13(3)**:** 46-51.

Latza, U., S. Gerdes & X. Baur. 2009. Effects of nitrogen dioxide on human health: Systematic review of experimental and epidemiological studies conducted between 2002 and 2006. *International Journal of Hygiene and Environmental Health,* 212(3)**:** 271-87.

Lewtas, J. 2007. Air pollution combustion emissions: Characterization of causative agents and mechanisms associated with cancer, reproductive, and cardiovascular effects. *Mutation Research/Reviews in Mutation Research,* 636(1-3)**:** 95-133.

Li, H. C., et al. 2010. Meteorologically adjusted long-term trend of ground-level ozone concentrations in Kaohsiung County, southern Taiwan. *Atmospheric Environment,* 44(29)**:** 3605-08.

Lin, H. H., M. Ezzati & M. Murray. 2007. Tobacco smoke, indoor air pollution and tuberculosis: A systematic review and meta-analysis. *PLoS Medicine,* 4(1)**:** 173-89.

Lin, S., et al. 2008. Chronic exposure to ambient ozone and asthma hospital admissions among children. *Environmental Health Perspectives,* 116(12)**:** 1725-30.

Lin, S. & Y. Lu. 2009. The spatial patterns of adverse health effects of ozone pollution on childhood respiratory diseases in urban Houston. *Annals of GIS,* 15(2)**:** 127-40.

Lioy, P. J. 1990. Assessing total human exposure to contaminants. *Environmental Science & Technology,* 24(7)**:** 938-45.

Liu, L. J. S., et al. 2007. Characterization of source-specific air pollution exposure for a large population-based Swiss Cohort (SAPALDIA). *Environmental Health Perspectives,* 115(11)**:** 1638-45.

Liu, L. J. S., et al. 1993. Use of personal measurements for ozone exposure assessment - A pilot-study. *Environmental Health Perspectives,* 101(4)**:** 318-24.

Lu, Y. & Y. Liu. 2012. Pervasive location acquisition technologies: Opportunities and challenges for geospatial studies. *Computers, Environment and Urban Systems,* 36(2)**:** 105-08.

Maisonneuve, N., et al. 2009. Noisetube: Measuring and mapping noise pollution with mobile phones. *Information Technologies in Environmental Engineering***:** 215-28.

Marshall, J. D., et al. 2006. Inhalation intake of ambient air pollution in California's south coast air basin. *Atmospheric Environment,* 40(23)**:** 4381-92.

Martin, S., et al. 2008. Guidance for exposure and risk evaluation for bystanders and residents exposed to plant protection products during and after application. *Journal of Consumer Protection and Food Safety,* 3(3)**:** 272-81.

Massey, D. 1997. A global sense of place. In *Studying Culture,* eds. A. Gray & J. McGuigan, 232-40. London: Edward Arnold.

Massey, D., et al. 2009. Indoor/outdoor relationship of fine particles less than 2.5 μm (PM2.5) in residential homes locations in central Indian region. *Building and Environment,* 44(10)**:** 2037-45.

Massolo, L., et al. 2010. Indoor-outdoor distribution and risk assessment of volatile organic compounds in the atmosphere of industrial and urban areas. *Environmental Toxicology,* 25(4)**:** 339-49.

Matejicek, L., P. Engst & Z. Janour. 2006. A GIS-based approach to spatio-temporal analysis of environmental pollution in urban areas: A case study of Prague's environment extended by LIDAR data. *Ecological Modelling,* 199(3)**:** 261-77.

Matthews, S. A. 2008. The salience of neighborhood: Some lessons from sociology. *American Journal of Preventive Medicine,* 34(3)**:** 257-59.

Mauderly, J. L. & J. M. Samet. 2009. Is there evidence for synergy among air pollutants in causing health effects? *Environmental Health Perspectives,* 117(1)**:** 1-6.

McCune, B. & D. Keon. 2002. Equations for potential annual direct incident radiation and heat load. *Journal of Vegetation Science,* 13(4)**:** 603-06.

Melia, R. J. W., et al. 1977. Association between gas cooking and respiratory-disease in children. *British Medical Journal,* 2(6080)**:** 149-52.

Metcalf, S. W. & K. G. Orloff. 2004. Biomarkers of exposure in community settings. *Journal of Toxicology and Environmental Health, Part A: Current Issues,* 67(8-10)**:** 715-26.

Mikhailuta, S. V., et al. 2009. Seasonal variations of air pollutant concentrations within Krasnoyarsk City. *Environmental Monitoring and Assessment,* 149(1-4)**:** 329-41.

Miller, H. J. 1991. Modelling accessibility using space-time prism concepts within geographical information systems. *International Journal of Geographical Information Systems,* 5(3)**:** 287-301.

Miller, H. J. 1999. Measuring space-time accessibility benefits within transportation networks: Basic theory and computational procedures. *Geographical Analysis,* 31(2)**:** 187-212.

_____. 2007. Place-based versus people-based geographic information science. *Geography Compass,* 1(3)**:** 503-35.

Miller, H. J. & S. A. Bridwell. 2009. A field-based theory for time geography. *Annals of the Association of American Geographers,* 99(1)**:** 49-75.

Mölter, A., et al. 2010. Modelling air pollution for epidemiologic research - Part II: Predicting temporal variation through land use regression. *Science of the Total Environment,* 409(1)**:** 211-17.

Monn, C. 2001. Exposure assessment of air pollutants: A review on spatial heterogeneity and indoor/outdoor/personal exposure to suspended particulate matter, nitrogen dioxide and ozone. *Atmospheric Environment,* 35(1)**:** 1-32.

Moore, D. K., et al. 2007. A land use regression model for predicting ambient fine particulate matter across Los Angeles, CA. *Journal of Environmental Monitoring,* 9(3)**:** 246-52.

Moore, K., et al. 2009. Intra-community variability in total particle number concentrations in the San Pedro harbor area (Los Angeles, California). *Aerosol Science and Technology,* 43(6)**:** 587-603.

Moore, K., et al. 2008. Ambient ozone concentrations cause increased hospitalizations for asthma in children: An 18-year study in Southern California. *Environmental Health Perspectives,* 116(8)**:** 1063-70.

Morabia, A., et al. 2009. Air pollution and activity during transportation by car, subway, and walking. *American Journal of Preventive Medicine,* 37(1)**:** 72-77.

Mu, L. & F. H. Wang. 2008. A scale-space clustering method: Mitigating the effect of scale in the analysis of zone-based data. *Annals of the Association of American Geographers,* 98(1)**:** 85-101.

Muller, N. Z. & R. Mendelsohn. 2007. Measuring the damages of air pollution in the United States. *Journal of Environmental Economics and Management,* 54(1)**:** 1-14.

Naess, O., et al. 2007. Relation between concentration of air pollution and cause-specific mortality: Four-year exposures to nitrogen dioxide and particulate matter pollutants in 470 neighborhoods in Oslo, Norway. *American Journal of Epidemiology,* 165(4)**:** 435-43.

NationalResearchCouncil. 2002. *Community and Quality of Life: Data Needs for Informed Decision Making* Washington, DC: National Academy Press.

Nemery, B., P. H. Hoet & A. Nemmar. 2001. The Meuse Valley fog of 1930: An air pollution disaster. *Lancet,* 357(9257)**:** 704-08.

Nerriere, E., et al. 2007. Spatial heterogeneity of personal exposure to airborne metals in French urban areas. *Science of the Total Environment,* 373(1)**:** 49-56.

Nethery, E., et al. 2008. From measures to models: An evaluation of air pollution exposure assessment for epidemiological studies of pregnant women. *Occupational and Environmental Medicine,* 65(9)**:** 579-86.

Neupane, B., et al. 2010. Long-term exposure to ambient air pollution and risk of hospitalization with community-acquired pneumonia in older adults. *American Journal of Respiratory and Critical Care Medicine,* 181(1)**:** 47-53.

Nieuwenhuijsen, M., D. Paustenbach & R. Duarte-Davidson. 2006. New developments in exposure assessment: The impact on the practice of health risk assessment and epidemiological studies. *Environment International,* 32(8)**:** 996-1009.

O'Neill, M. S., et al. 2003. Health, wealth, and air pollution: Advancing theory and methods. *Environmental Health Perspectives,* 111(16)**:** 1861-70.

O'Reilly, T. 2005. What is Web 2.0. http://oreilly.com/web2/archive/what-is-web-20.html (last accessed 01 April 2011).

Okabe, A. & M. Kitamura. 1996. A computational method for market area analysis on a network. *Geographical Analysis,* 28(4)**:** 330-49.

Ostro, B., et al. 2010. Long-term exposure to constituents of fine particulate air pollution and mortality: Results from the California teachers study. *Environmental Health Perspectives,* 118(3)**:** 363-69.

Ott, W. R. 1982. Concepts of human exposure to air pollution. *Environment International,* 7(3)**:** 179-96.

Pattison, W. D. 1990. The four traditions of geography. *Journal of Geography,* 89(5)**:** 202-06.

Peuquet, D. J. 1994. It's about time: A conceptual framework for the representation of temporal dynamics in geographic information systems. *Annals of the Association of American Geographers,* 84(3)**:** 441-61.

Pope, C. A., 3rd, M. Ezzati & D. W. Dockery. 2009. Fine-particulate air pollution and life expectancy in the United States. *New England Journal of Medicine,* 360(4)**:** 376-86.

Pope, C. A. & D. W. Dockery. 2006. Health effects of fine particulate air pollution: Lines that connect. *Journal of the Air & Waste Management Association,* 56(6)**:** 709-42.

Pudasainee, D., et al. 2006. Ground level ozone concentrations and its association with NOx and meteorological parameters in Kathmandu Valley, Nepal. *Atmospheric Environment,* 40(40)**:** 8081-87.

Puett, R. C., et al. 2009. Chronic fine and coarse particulate exposure, mortality, and coronary heart disease in the Nurses' health study. *Environmental Health Perspectives,* 117(11)**:** 1697-701.

Raftery, T. 2009. Mobile phones - Distributed air quality sensor network? http://greenmonk.net/mobile-phones-distributed-air-quality-sensor-network/ (last accessed 8 April 2010).

Rage, E., et al. 2009. Air pollution and asthma severity in adults. *Occupational and Environmental Medicine,* 66(3)**:** 182-88.

Riva, M., et al. 2009. Disentangling the relative influence of built and socioeconomic environments on walking: The contribution of areas homogenous along exposures of interest. *Social Science & Medicine,* 69(9)**:** 1296-305.

Romieu, I., et al. 1998. Evaluation of indoor ozone concentration and predictors of indoor-outdoor ratio in Mexico City. *Journal of the Air & Waste Management Association,* 48(4)**:** 327-35.

Rosenbaum, A., et al. 2008. Nitrogen dioxide (NO2) exposure assessment in support of U.S. EPA's NAAQS review: application of AERMOD and APEX to Philadelphia County. *Epidemiology,* 19(6)**:** S344-S45.

Rosenlund, M., et al. 2007. Comparison of regression models with land-use and emissions data to predict the spatial distribution of traffic-related air pollution in Rome. *Journal of Exposure Science and Environmental Epidemiology,* 18(2)**:** 192-99.

Ross, Z., et al. 2007. A land use regression for predicting fine particulate matter concentrations in the New York City region. *Atmospheric Environment,* 41(11)**:** 2255-69.

Ruangdej, K. & P. Chaosuansreecharoen. 2008. Short term effects of ground-level ozone on mortality in Bangkok, Thailand. *Journal of Public Health,* Special issue on 60th anniversary)**:** 21-35.

Ryan, P. B., et al. 2007a. Using biomarkers to inform cumulative risk assessment. *Environmental Health Perspectives,* 115(5)**:** 833-40.

Ryan, P. H. & G. K. LeMasters. 2007. A review of land-use regression models for characterizing intraurban air pollution exposure. *Inhalation Toxicology,* 19(Suppl 1)**:** 127-33.

Ryan, P. H., et al. 2007b. A comparison of proximity and land use regression traffic exposure models and wheezing in infants. *Environmental Health Perspectives,* 115(2)**:** 278-84.

Sahsuvaroglu, T. & M. Jerrett. 2007. Sources of uncertainty in calculating mortality and morbidity attributable to air pollution. *Journal of Toxicology and Environmental Health, Part A: Current Issues,* 70(3-4)**:** 243-60.

Samet, J. M., et al. 2000. Fine particulate air pollution and mortality in 20 US Cities, 1987-1994. *New England Journal of Medicine,* 343(24)**:** 1742-49.

Samoli, E., et al. 2007. Short-term effects of carbon monoxide on mortality: An analysis within the APHEA project. *Environmental Health Perspectives,* 115(11)**:** 1578-83.

Samoli, E., et al. 2009. The temporal pattern of mortality responses to ambient ozone in the APHEA project. *Journal of Epidemiology & Community Health,* 63(12)**:** 960-66.

Schaefer-McDaniel, N., et al. 2009. Examining methodological details of neighbourhood observations and the relationship to health: A literature review. *Social Science & Medicine,* 70(2)**:** 277-92.

Schelling, T. C. 1971. Dynamic models of segregation. *Journal of Mathematical Sociology,* 1(2)**:** 143-86.

See, S. W. & R. Balasubramanian. 2006. Risk assessment of exposure to indoor aerosols associated with Chinese cooking. *Environmental Research,* 102(2)**:** 197-204.

Sensaris. 2010. Senspods. http://www.sensaris.com (last accessed 23 April 2010).

Setton, E. M., et al. 2011. Outdoor air pollution and health - A review of the contributions of geotechnologies to exposure assessment. In *Geospatial Analysis of Environmental Health,* eds. J. A. Maantay & S. McLafferty, 67-91. Springer Netherlands.

Shah, A. P., et al. 2008. Effect of inhaled carbon ultrafine particles on reactive hyperemia in healthy human subjects. *Environmental Health Perspectives,* 116(3)**:** 375-80.

Sheppard, D., et al. 1981. Exercise increases sulfur dioxide-induced bronchoconstriction in asthmatic subjects. *American Review of Respiratory Disease,* 123(5)**:** 486-91.

Silverman, R. A. & K. Ito. 2010. Age-related association of fine particles and ozone with severe acute asthma in New York City. *Journal of Allergy and Clinical Immunology,* 125(2)**:** 367-73, e5.

Sokolova, M. V. & A. Fernandez-Caballero. 2009. Modeling and implementing an agent-based environmental health impact decision support system. *Expert Systems with Applications,* 36(2)**:** 2603-14.

Somers, C. M. & D. N. Cooper. 2009. Air pollution and mutations in the germline: Are humans at risk? *Human Genetics,* 125(2)**:** 119-30.

Song, W. & G. Sun. 2010. The role of mobile volunteered geographic information in urban management. In *proceedings of the 18th International Conference on Geoinformatics*, 1-5. Beijing, China: IEEE.

Spengler, J. D., et al. 1981. Long-term measurements of respirable sulfates and particles inside and outside homes. *Atmospheric Environment,* 15(1)**:** 23-30.

Sram, R. J., et al. 2005. Ambient air pollution and pregnancy outcomes: a review of the literature. *Environmental Health Perspectives,* 113(4)**:** 375-82.

Srivastava, A. 2005. Variability in VOC concentrations in an urban area of Delhi. *Environmental Monitoring and Assessment,* 107(1-3)**:** 363-73.

Sun, Z. M. 2007. Multi-agent based modeling: Methods and techniques for investigating human behaviors. In *proceedings of the International Conference on Mechatronics and Automation*, 779-83. Harbin, China: IEEE.

Swenberg, J. A., et al. 2008. Biomarkers in toxicology and risk assessment: Informing critical dose-response relationships. *Chemical Research in Toxicology,* 21(1)**:** 253-65.

TCEQ. 2010. Air monitoring sites monthly summary report. http://www.tceq.state.tx.us/cgi-bin/compliance/monops/monitors.pl (last accessed 17 September 2010).

Thatcher, T. L., et al. 2001. Factors affecting the concentration of outdoor particles indoors (COPI): Identification of data needs and existing data. Berkeley, CA: Lawrence Berkeley National Laboratory. LBNL-49321.

Tian, F. L., et al. 2009. Sources and seasonal variation of atmospheric polycyclic aromatic hydrocarbons in Dalian, China: Factor analysis with non-negative constraints combined with local source fingerprints. *Atmospheric Environment,* 43(17)**:** 2747-53.

Tobler, W. R. 1989. Frame independent spatial analysis. In *The Accuracy of Spatial Databases,* eds. M. Goodchild & S. Gopa, 115-22. London: Taylor & Francis.

Tomlin, A. S., et al. 2009. A field study of factors influencing the concentrations of a traffic-related pollutant in the vicinity of a complex urban junction. *Atmospheric Environment,* 43(32)**:** 5027-37.

Trandabat, A., et al. 2007. Using GPS technology and distributed measurement system for air quality maping of rezidential area. *Environmental Engineering and Management Journal,* 6(6)**:** 545-48.

Trandabat, A., et al. 2005. High altitude air quality mapping system for large area using GPS technology and distributed measurement system. *Management of Technological Changes, Book 1***:** 431-34, 40.

Turner, B. L. 2002. Contested identities: Human-environment geography and disciplinary implications in a restructuring academy. *Annals of the Association of American Geographers,* 92(1)**:** 52-74.

U.S. Census. 2010. Population Finder: Texas. http://factfinder.census.gov/servlet/GCTTable?_bm=y&-geo_id=04000US48&-_box_head_nbr=GCT-T1-R&-ds_name=PEP_2009_EST&-_lang=en&-redoLog=false&-mt_name=PEP_2009_EST_GCTT1R_ST2S&-format=ST-9S&-_sse=on (last accessed 19 September 2010).

Wallace, L. 1996. Indoor particles: A review. *Journal of the Air & Waste Management Association,* 46(2)**:** 98-126.

_____. 2006. Indoor sources of ultrafine and accumulation mode particles: Size distributions, size-resolved concentrations, and source strengths. *Aerosol Science and Technology,* 40(5)**:** 348-60.

Warren, T. 2006. Information and communication technologies and real-life learning: New education for the knowledge society. *Technical Communication,* 53(4)**:** 482-83.

Weber, J. & M.-P. Kwan. 2003. Evaluating the effects of geographic contexts on individual accessibility: A multilevel approach. *Urban Geography,* 24(8)**:** 647-71.

Weinhold, B. 2010. Policy: EPA's ground-level ozone standard redux. *Environmental Health Perspectives,* 118(3)**:** A115.

Weisel, C. P. 2002. Assessing exposure to air toxics relative to asthma. *Environmental Health Perspectives,* 110(Suppl 4):527-37.

WHO. 1993. Biomarkers and risk assessment: Concepts and principles. Geneva, Switzerland: World Health Organization. 22 September.

_____. 2007. Estimated deaths & DALYs attributable to selected environmental risk factors, by WHO Member State, 2002. Geneva, Switzerland: World Health Organization.

_____. 2009. Global health risks: Burden of disease attributable to selected major risks. Geneva, Switzerland: World Health Organization.

Wilhelm, M., L. Qian & B. Ritz. 2009. Outdoor air pollution, family and neighborhood environment, and asthma in LA FANS children. *Health & Place,* 15(1)**:** 25-36.

Wong, D. W., L. Yuan & S. A. Perlin. 2004. Comparison of spatial interpolation methods for the estimation of air quality data. *Journal of Exposure Analysis and Environmental Epidemiology,* 14(5)**:** 404-15.

Wu, Y.-H. & H. J. Miller. 2001. Computational tools for measuring space-time accessibility within dynamic flow transportation networks. *Journal of Transportation and Statistics,* 4(2/3)**:** 1-14.

Xin, S., C. S. Li & T. Di. 2005. Data transmission reliability in short message integrated distributed monitoring systems. In *proceedings of the International Enformatika Conference*, 362-67, 446. Prague, Czech Republic:

Yamamoto, N., et al. 2010. Residential air exchange rates in three major US metropolitan areas: Results from the relationship among indoor, outdoor, and personal air study 1999-2001. *Indoor Air,* 20(1)**:** 85-90.

Yang, D. X., Z. Q. Wang & R. J. Zhang. 2008. Estimating air quality impacts of elevated point source emissions in Chongqing, China. *Aerosol and Air Quality Research,* 8(3)**:** 279-94.

Yu, H. 2006. Spatio-temporal GIS design for exploring interactions of human activities. *Cartography and Geographic Information Science,* 33(1):3-19.

Zhan, F. B., et al. 2006. Match rate and positional accuracy of two geocoding methods for epidemiologic research. *Annals of Epidemiology,* 16(11)**:** 842-49.

Zhou, Z., et al. 2006. Community effectiveness of stove and health education interventions for reducing exposure to indoor air pollution from solid fuels in four Chinese provinces. *Environmental Research Letters,* 1(1)**:** 014010.

Zou, B., et al. 2009a. Air pollution exposure assessment methods utilized in epidemiological studies. *Journal of Environmental Monitoring,* 11(3)**:** 475-90.

_____. 2009b. Spatially differentiated and source-specific population exposure to ambient urban air pollution. *Atmospheric Environment,* 43(26)**:** 3981-88.

VITA

Tianfang Bernie Fang was born in Hegang, China on May 24, 1981, the son of G. Fang and Y. Yang. Bernie grew up in Northeast China where he attended Northeast Agricultural University. After earning his bachelor's degree in Land Use Planning in July 2002 and then his Master's degree in Land Resource Management in January 2006, Bernie entered the doctoral program at Texas State University-San Marcos in August 2007 and researched environmental and socioeconomic applications of Geographic Information Science.

Permanent Address: 10301 Ranch Rd 2222 Apt 537

                      Austin, Texas 78730

Permanent Email Address: tianfang.fang@hotmail.com

This dissertation was typed by Tianfang Bernie Fang.